

Energy Efficient Geographic Routing Resilient to Location Errors

by

Ana Maria Popescu

Submitted in accordance with the requirements for the degree of
Doctor of Philosophy

University of Leeds

School of Electronic and Electrical Engineering

September 2013

The candidate confirms that the work submitted is her own, except where work which has formed part of jointly authored publications has been included. The contribution of the candidate and the other authors to this work has been explicitly indicated below. The candidate confirms that appropriate credit has been given within the thesis where reference has been made to the work of others.

- a. All chapters in the thesis are based on work from jointly authored publications, whose main author is A. M. Popescu.
- b. Details of the publications which have been used (e.g. titles, journals, dates, names of authors):

In Chapter 2: “Surveying Position Based Routing Protocols for Wireless Sensor and Ad-hoc Networks”, *International Journal of Communication Networks and Information Security* 4 (1), 2012. Co-authors: G. I. Tudorache, Dr. B. Peng and Dr. A. H. Kemp.

In Chapter 3:

1. “Surveying Position Based Routing Protocols for Wireless Sensor and Ad-hoc Networks”, *International Journal of Communication Networks and Information Security* 4 (1), 2012. Co-authors: G. I. Tudorache, Dr. B. Peng and Dr. A. H. Kemp.

2. “Performance study of node placement for geographic routing in WSNs”, *IEEE Swedish Communication Technologies Workshop (Swe-CTW)*, Stockholm, Sweden, pp. 13-18, Oct. 2011. Co-authors: G. I. Tudorache and Dr. A. H. Kemp.

In Chapter 4:

1. “Energy consumption analysis of geographic routing in WSNs with location error”, *18th European Wireless Conference*, Manchester, pp. 1-8, April 2012

2. “Energy consumption of geographic routing with realistic localisation”, *IET Networks*, vol. 1, no. 3, pp. 126-135, Sept. 2012

Co-authors for both: N. Salman and Dr. A. H. Kemp

In Chapter 5:

1. “Geographic Routing Resilient to Location Errors”, *IEEE Wireless Communications Letters*, vol. 2, no. 2, pp. 203-206, April 2013.

2. “Energy Efficient Geographic Routing Robust Against Location Errors”, Accepted for publication in *IEEE Sensors Journal*, February 2014

Co-authors for both: N. Salman and Dr. A. H. Kemp.

In Chapter 6: “On Rician statistical assumptions for geographic routing in WSNs”, under review in *IEEE Wireless Communications Letters*, 2013. Co-authors: N. Salman and Dr. A. H. Kemp.

c. Details of the work contained within these publications which is directly attributable to A. M. Popescu:

With the exceptions detailed in section d., the published work is entirely attributable to A. M. Popescu: the literature review necessary to develop the ideas behind the published manuscripts, the novel ideas proposed in the papers, the development of the MATLAB WSN simulator used in the analysis and all the work necessary in the editing of the manuscripts.

d. Details of the contributions of the other authors to the work:

Dr. A. H. Kemp is the co-author for all the publications listed above. They have been written under his supervision, benefiting from excellent technical and editorial advice.

Dr. B. Peng contributed with recommendations about how to structure a survey,

how to emphasize the originality of the work and how to provide concise, yet rich content to the reader.

I. G. Tudorache has provided information about routing protocols recommended for mobility in WSNs and aided with critical thinking about simulation scenario set-up and how to analyse and interpret the obtained simulation data.

N. Salman has provided provided the MATLAB functions necessary in the simulation of the LLS- and ML- RSS and ToA localisation. He has also provided advice in their understanding and good use with the WSN simulator developed by A. M. Popescu. His input includes recommendations on the localisation requirements for network setup and guidance in the understanding of how results are influenced by anchor numbers, placement, transmission range and environment noise. His experience with statistical theory has also been helpful in the development of the novel geographic routing algorithms. For the last manuscript he co-authored, he has provided the modified version of the LSS-RSS simulation and has facilitated the study of the Rician statistical assumption through theoretical advice.

This copy has been supplied on the understanding that it is copyright material and that no quotation from the thesis may be published without proper acknowledgment.

*To my adored parents, Raluca and Marius Popescu,
To my beloved grandmother, Emilia Stanga,
To my esteemed supervisor, Dr. Andrew H. Kemp,
And to my dear colleague and friend, Naveed Salman.*

Acknowledgements

It would not have been possible to write this doctoral thesis without the help and support of a number of kind people to whom I would like to give thanks here. They have been actively involved in my work improving its value and have continuously promoted my growth and given me the confidence to pursue my research.

I would first like to thank my supervisor, Dr. Andrew H. Kemp, who has patiently advised me on countless occasions and whose numerous revisions of my publications are invaluable. His constant encouragement and guidance have been vital in keeping me motivated throughout the period of my studies.

I owe a great deal of gratitude to my fellow colleagues in the Wireless Sensor Networks group. First and foremost I wish to thank Naveed Salman whose academic advice and friendship have helped me most. The numerous conversations we had discussing ideas have helped me learn a lot and greatly contributed to the development of my work. I would also like to thank Dr. Bo Peng for inspiring me through his own publications and Tudorache Ion Gabriel, Dr. Imtiaz Rasool and Dr. Hemat Maheshwari for their moral support and advice.

Above all I am thankful to my mother and father, Raluca and Marius Popescu, and grandmother, Emilia Stanga, for their unequivocal support, love and understanding. Undoubtaly it has been very difficult for them to be away from me for the long duration of my research, so thank you.

Abstract

The thesis first analyses the importance sensor placement has in a large scale WSN application using geographic routing. A simulation-based topological study is made for a forest fire prevention application using both deterministically and randomly placed nodes. Sensor deployment can be projectile, from the network edge, made through manual scattering or by air release. Results reveal the impact of sensor distribution, density or destination location on the routing component.

Furthermore, geographic routing analysis focuses on location information assumptions. Because all methods of localisation are imprecise, it is necessary to consider the use of estimated coordinates instead of the real ones and to first model the location errors as normally distributed. A more realistic evaluation of the routing component requires the use of positioning simulations, considering received signal strength (RSS) and time of arrival (ToA) ranging for localisation (both modelled in this thesis using the linear least square method (LLS) and maximum likelihood (ML) based Levenberg Marquardt (LM) method). Routing behaviour is analysed in terms of throughput, path lengths, energy consumption and failure causes. The energy expenditure of the two ranging methods is also analysed.

Efficient routing solutions for large scale WSNs are explored to cope with location error. A novel, low-complexity, error-resilient geographic routing method is proposed, namely the conditioned mean square error ratio (CMSER) algorithm. CMSER is

compared to other progress only forwarding methods. A modified version of the algorithm is proposed to further increase energy efficiency and simulation results also confirm this. Furthermore, because CMSEER is designed to make use of the Rice distribution (a statistical assumption valid only when the x and y coordinates of a node have the same location error variance) the precision of this approach is investigated. Although the routing behaviour is not severely affected by this simplifying assumption, because the variance of the errors can be very different in reality, a non-Rician version of the algorithm is proposed, which provides similar results under correct assumptions.

Contents

Acknowledgements	i
Abstract	ii
List of Figures	vii
List of Tables	x
List of Abbreviations	xi
List of Symbols	xv
1 Introduction	1
1.1 Problem statement	3
1.2 Research contribution	4
1.3 Thesis outline	6
1.4 List of publications	9
2 Overview of position based routing	11
2.1 Network types: differences and similarities	13
2.2 Comparison of routing types	15
2.3 Routing design factors	20

2.4	Conclusions	28
3	Geographic routing in realistic scenarios - from theory to practice	30
3.1	Presenting applications for geographic routing	30
3.2	WSN Simulations	36
3.2.1	Overview of WSN simulation environments	36
3.2.2	Wireless sensor network simulator	39
3.3	Node placement scenarios and their study	55
3.3.1	Previous work in node placement studies	56
3.3.2	Simulation setup	63
3.3.3	Simulation results	68
3.4	Localisation	76
3.4.1	Measurement techniques	76
3.4.2	Modelling location errors	79
3.5	Conclusions	83
4	Efficient geographic routing in the presence of location errors	85
4.1	Routing performance with a normally distributed position error	86
4.1.1	Simulation setup	86
4.1.2	Simulation results	89
4.2	Routing performance with RSS and ToA ranging	100
4.2.1	Simulations setup	101
4.2.2	Simulation results	106
4.3	Conclusions	115
5	Solutions for geographic routing resilient to location errors	118
5.1	Previous works	119
5.2	Error model	121

5.3	CMSER routing algorithm	122
5.3.1	Simulation setup	126
5.3.2	Simulation results	128
5.4	Modified version of CMSER routing algorithm	130
5.4.1	Energy saving feature	131
5.4.2	Simulation setup	134
5.4.3	Simulation results	137
5.5	Conclusions	141
6	On the Rician assumption for geographic routing design	144
6.1	Problem statement	145
6.1.1	Preliminary analysis	148
6.2	Non-Rician geographic routing solution	153
6.2.1	Simulations and results	155
6.3	Conclusions	161
7	Conclusions and future work	162
7.1	Conclusions	162
7.2	Future work	171
	Bibliography	174

List of Figures

2.1	Network types: centralised, decentralised, distributed	21
2.2	Greedy forwarding cases	24
2.3	Flooding cases	24
2.4	Examples of hierarchic networks with designated cluster heads	25
2.5	Recursive geographic routing	26
3.1	Example of a GRID distribution	58
3.2	Example of a random uniform node distribution	59
3.3	Example of a Gaussian node distribution	60
3.4	Example of a Pareto node distribution	60
3.5	Stensor division into strips	62
3.6	Example of a Stensor node distribution	63
3.7	Simulated forwarding algorithm	67
3.8	Packet delivery ratio	69
3.9	Average number of hops/packet for a successful transmission	70
3.10	Average number of hops/packet for all transmissions	70
3.11	Progress failure	72
3.12	Partial progress failure	72
3.13	Average energy spent for clear channel assessment	73
3.14	Average packet delay at MAC	74

3.15	Packet delivery ratio with D placed in the upper, right corner	74
4.1	Packet delivery ratio (Gaussian location error)	89
4.2	The total energy consumed in the network	90
4.3	Average energy consumption for successful transmissions	90
4.4	Average number of hops per received packet	91
4.5	Average energy consumption for all lost packets	91
4.6	Average hop count per lost packet	92
4.7	Average hop count per lost packet (cause: location error)	93
4.8	Percentage of failures due to location error	94
4.9	Percentage of failures due to connectivity failures	94
4.10	Percentage of failures due to progress failure	95
4.11	Percentage of failures due to congestion	95
4.12	Average energy consumption per network due to location error failure	96
4.13	Average energy consumption per network due to connectivity failure	97
4.14	Average energy consumption per network due to progress failure . . .	97
4.15	Average energy consumption per network due to congestion failure .	98
4.16	Localisation process	101
4.17	Loss Rate (black: LLS; colour: ML)	108
4.18	Average energy consumption for all lost packets [Joules] (black: LLS; colour: ML)	109
4.19	Average hop count per lost packet (black: LLS; colour: ML)	110
4.20	Percentage of failures due to location error and connectivity loss (black: LLS; colour: ML)	111
4.21	Percentage of failures due to lack of progress and congestion (black: LLS; colour: ML)	112

4.22	Energy consumed by the network (in colour - the energy spent on failed routing; in white - energy spent on localisation)	115
5.1	COND approach	124
5.2	Routing performance for scenario 1.	128
5.3	Routing performance for scenario 2.	129
5.4	Routing performance for scenario 3.	129
5.5	Routing performance for scenario 1, with M-CMSER	137
5.6	Routing performance for scenario 2, with M-CMSER	138
5.7	Routing performance for scenario 3, with M-CMSER	138
5.8	Average number of hops per received packet, in networks with ACK .	140
5.9	Total number of retransmissions in networks with ACK	140
5.10	Total number of transmissions in networks with ACK	141
5.11	Total energy consumption in networks with ACK	142
6.1	Varying α	151
6.2	Varying the anchor node placement and the noise values	152
6.3	CDF analysis	153
6.4	Routing performance (average σ^2 case)	158
6.5	Routing performance (maximum σ^2 case)	158
6.6	Performance based on RSS localisation	160
6.7	Performance based on RSS resulted σ_{ix}^2 , but with large σ_{iy}^2	161

List of Tables

3.1	MAC parameters	42
3.2	Simulation parameters	66
3.3	Simulated causes for failure	71
4.1	Simulation parameters	88
4.2	Network density (neighbours/node)	88
4.3	Simulation parameters	107
4.4	Network density (neighbours/node)	107
4.5	Energy consumption for ToA and RSS, with 9 anchor nodes	114
5.1	Simulation parameters	127
5.2	Simulation scenarios	128
5.3	Simulation parameters	135
5.4	Simulation scenarios	136
6.1	Results for test 1	149
6.2	Scenarios for test 2	150
6.3	Correspondance table for Ge simulation	157
6.4	Correspondance table for RSSe simulation	157

List of Abbreviations

2-D	Two Dimensional
3-D	Three Dimensional
ACE	Application Characterization Environment module
ACK	Acknowledge
AN	Anchor Node
ARQ	Automatic Repeat reQuest
AWGN	Additive White Gaussian Noise
C++	General-purpose programming language
CCA	Clear Channel Assessment
CDF	Cumulative Distribution Function
CMD	Command Packets
CMSE	Conditioned Mean Square Error Ratio
COND	Condition
CSMA/CA	Carrier Sense Multiple Access with Collision Avoidance mechanism

DATA	Data Packet
Ge	Gaussian-generated location error
GN	Gauss-Newton
GPS	Global Positioning System
GUI	Graphical User Interface
IEEE	Institute of Electrical and Electronics Engineers
LED	Least Expected Distance
LINUX	Computer Operating System
LLS	Linear Least Squares
LLS-RSS	Linear Least Squares Received Signal Strength
LLS-ToA	Linear Least Squares Time of Arrival
LM	Lavenberg-Marquardt
LR	Loss Rate
M-CMSER	Modified Conditioned Mean Square Error Ratio
MAC	Medium Access Control
MANET	Mobile Ad-hoc Network
MATLAB	Numerical computing environment and fourth-generation programming language
MED	Maximum Expected Distance

MEP	Maximum Expected Progress
MER	Maximum Expectation within Transmission Range
MFR	Most Forward within Radius
ML	Maximum Likelihood
ML-RSS	Maximum Likelihood Received Signal Strength
ML-ToA	Maximum Likelihood Time of Arrival
MSE	Mean Square Error
MSER	Mean Square Error Ratio
NAK	No Acknowledge
NAM	Network Animator
NLOS	Non-Line-of-Sight
NR-CMSER	Non Rician Conditioned Mean Square Error Ratio
NR-MSER	Non Rician Mean Square Error Ratio
NS-2	Network Simulator Version 2
OPNET	Optimized Network Engineering Tools
OSI	Open Systems Interconnection
OW-ToA	One Way Time of Arrival
PDR	Packet Delivery Ratio
PHY	Physical Layer

PLE	Path Loss Exponent
QoS	Quality of Service
QualNet	Communications Simulation Platform
RDF	Restrictive Directional Flooding
RGF	Recursive Geographic Forwarding
RP	Ranging Package
RSS	Received Signal Strength
RSSe	Received Signal Strength location error
SNR	Signal-to-Noise Ratio
Stensor	Stochastic sensor distribution using both X and Y axis
StensorX	Stochastic sensor distribution using the X axis only
TCL	Tool Command Language
TDOA	Time Difference of Arrival
TN	Target Node
ToA	Time of Arrival
TW-ToA	Two Way Time of Arrival
UDG	Unit Disk Graph
VANET	Vehicular Ad-hoc Network
WINDOWS	Computer Operating System
WSN	Wireless Sensor Network

List of Symbols

S	source node
R	range of regular sensor nodes (target nodes)
D	destination node
aUnitBackoffPeriod	a variable indicating the the units for the backoff period
minBE	minimum value of backoff exponent
maxBE	maximum value of backoff exponent
maxCSMABackoffs	maximum number of backoffs at MAC level
CCA_energy	energy spent for clear channel assessment
P_r	reception power
d	distance
d_0	reference distance
ω_c	carrier frequency
c	speed of light
G_r	antenna gain at receiver
G_t	antenna gain at transmitter
P_t	transmission power
λ	wavelength
L	circuitry losses
PL	path loss

X	Gaussian distributed random variable
μ	mean value of the Gaussian distribution
σ	standard deviation of the Gaussian distribution
dB	decibels
dBm	power ratio in decibels of the measured power referenced to one milliwatt (mW)
dBW	power ratio in decibels of the measured power referenced to one watt (W)
F	Fahrenheit
N	number of target nodes in a network
j	strip of Stensor network distribution
x_j	nodes per strip in Stensor distribution
Km	Kilometre
ha	Hectares
$d1$	distance 1
$d2$	distance 2
$F1$	forwarding node 1
$F2$	forwarding node 2
N	current node in a particular example
$pckts_d$	total number of delivered packets per network
$pckts_s$	total number of sent packets per network
$pckts_l$	total number of lost packets per network
PDR_n	packet delivery ratio per network trial
PDR	packet delivery ratio averaged over a number of trials
LR_n	packet loss ratio per network trial
LR	packet loss ratio averaged over a number of trials

$hops_r$	total number of hops of the received packets per network
$hopsP_{rn}$	average number of hops per received packet per network
$hopsP_r$	average number of hops per received packet averaged over a number of trials
$hops_l$	total number of hops of the lost packets per network
$hopsP_{ln}$	average number of hops per lost packet per network
$hopsP_l$	average number of hops per lost packet averaged over a number of trials
$hops_{le}$	total number of hops of the lost packets due to location error per network
$hopsP_{len}$	average number of hops per lost packet due to location error per network
$hopsP_{le}$	average number of hops per lost packet due to location error averaged over a number of trials
η_r	trials with at least one successfully received packet
η_l	trials with at least one packet lost
η_{le}	trials with at least one packet lost due to location error
C_F	failures due to lack of connectivity per traffic connection
NN	failures due to no neighbours except previous hops and source per traffic connection
CF_n	the percentage of connectivity failures per network
CF	the percentage of connectivity failures averaged over a number of trials
NP	failures due to no progress per traffic connection
PF_n	percentage of progress failures per network
PF	percentage of progress failures averaged over a number of trials

PPF_n	percentage of partial progress failures per network
PPF	percentage of partial progress failures averaged over a number of trials
$Mpkts_l$	number of packets lost due to congestion per traffic connection
CGF_n	percentage of congestion failures per network
CGF	percentage of congestion failures averaged over a number of trials
ERR	number of packets lost due to location errors per traffic connection
LEF_n	number of packets lost due to location errors per network
LEF	number of packets lost due to location errors averaged over a number of trials
$NodeDelay$	packet delay at MAC per connection (for all the transmitted packets)
$PcktDel_n$	average packet delay at MAC per network
$PcktDel$	average packet delay at MAC averaged over a number of trials
E_{CCA}	energy spent by by each node for CCA per packet
ME	energy spent at MAC per connection (for all the transmitted packets)
$MacEnergy_n$	average energy consumption per packet at MAC per network
$MacEnergy$	average energy consumption per packet at MAC averaged over a number of trials
$ConPckts_l$	number of lost packets per traffic connection
$EnergyLostPckt$	energy per lost packet
$EnergyPcktsLost_n$	average energy consumption for all lost packets over a network
$EnergyLostPckts$	average energy consumption for all lost packets avearged over a number of trials
E_i	initial node energy

E_{energTR}	energy consumed for transmissions and receptions by a node during a traffic connection, for all the packets forwarded by it
E_{totaln}	total energy consumption per network
E_{total}	total energy consumption averaged over a number of trials
E_{CF}	energy consumption of the lost packets due to loss of connectivity per traffic connection
E_{CFn}	energy consumption of the lost packets due to loss of connectivity per network
E_{CF}	energy consumption of the lost packets due to loss of connectivity averaged over a number of trials
η_{CF}	trials with at least one connectivity failure
E_{NP}	energy consumption of the lost packets due to progress failure per traffic connection
E_{PFn}	energy consumption of the lost packets due to progress failure per network
E_{PF}	energy consumption due to progress failure averaged over a number of trials
E_{Mpks_t}	energy consumption of the lost packets due to congestion failure per traffic connection
E_{CGFn}	energy consumption of the lost packets due to congestion failure per network
E_{CGF}	energy consumption due to congestion failure averaged over a number of trials
η_{CGF}	trials with at least one congestion failure
E_{ERR}	energy consumption of the lost packets due to location error failure per traffic connection

$E_{LocErrn}$	energy consumption of the lost packets due to location error failure per network
E_{LocErr}	energy consumption due to location error failure averaged over a number of trials
η_{ERR}	trials with at least one location error failure
E_{rcvc}	energy consumption of received packets per traffic connection
E_{pktsnd}	energy consumption of received packets per network
E_{pktsd}	energy consumption of received packets averaged over a number of trials
η_d	trials with at least one packet delivery
α	path loss exponent (PLE)
σ_{sh}	standard deviation for shadowing model
rv_{th}	sensitivity threshold
p_{size}	packet size
dr	data rate
$pkts$	number of packets/source
e_{tx}	energy per bit spent on transmission
e_{rx}	energy per bit spent for reception
l	network side length
η	number of trials (iterations)
SE	number of sensed events
s	second
m	metre
J	Joules
Kbits	Kilobits
W	Watts

$N(\mu, \sigma^2)$	Gaussian distribution of mean μ and variance σ^2
σ^2	variance of the Gaussian distribution
d_i	distance between the target node and anchor node i
M	number of anchor nodes in a network
$\boldsymbol{\theta}_i$	vector of real coordinates for node i
$\boldsymbol{\theta}_j$	vector of real coordinates for node j
d_{ij}	the real distance between two nodes i and j
\hat{d}_{ij}	the estimated distance between two nodes i and j
\mathbf{n}_{ij}	additive noise with Gaussian distribution for the estimated distance between i and j
w_{ij}	log-normal shadowing effect for the estimated distance between i and j
L_{ij}	path loss at distance d measured between nodes i and j
L_0	path loss at reference distance d_0
P_j	transmit power at the j^{th} target node
P_{ij}	received power at the i^{th} anchor node
\mathbf{n}_j	noise vector and variance for ToA location error
\mathbf{w}_j	noise vector and variance for RSS location error
$\hat{\mathbf{f}}_{ij}$	observed path loss
$\hat{\mathbf{f}}_j$	vector of observed path loss
\mathbf{f}	actual path loss vector
\mathbf{J}_j^k	Jacobian matrix at the k^{th} step
$\hat{\mathbf{s}}_j$	observed signal
$\mathbf{J}_{\text{ToA}j}^k$	Jacobian matrix at the k^{th} step for ToA ranging
$\mathbf{J}_{\text{RSS}j}^k$	Jacobian matrix at the k^{th} step for RSS ranging
\mathbf{A}^\dagger	Moore–Penrose pseudoinverse matrix

\hat{e}_{RSS}	energy consumed on RSS ranging between a target and an anchor
\hat{e}_{TOA}	energy consumed on the ranging between 2 nodes using ToA
\hat{E}	total estimated energy consumption over an entire network
\hat{E}_{RSS}	total estimated energy consumption over an entire network, when RSS is used
\hat{E}_{TOA}	total estimated energy consumption over an entire network, when ToA is used
S_i	relay node
I	the number of transmitting nodes along a routing path
F_j	forwarding candidate of a relay node
J	the number of neighbors of a relay node, with positive advance to destination
x_i	the real coordinate x of a node i
x_j	the real coordinate x of a node j
y_i	the real coordinate y of a node i
y_j	the real coordinate y of a node j
\hat{x}_i	the estimated coordinate x of a node i
\hat{y}_i	the estimated coordinate y of a node i
\hat{x}_j	the estimated coordinate x of a node j
\hat{y}_j	the estimated coordinate y of a node j
σ_{max}	the maximum standard deviation value during an iteration
σ_i^2	the variance of node i
σ_j^2	the variance of node j
σ_{ij}^2	the squared sum of the variances of two nodes i and j
$W_i \sim N(0, \sigma_i^2)$	Gaussian random variable with zero mean with standard deviation σ_i

$W_j \sim N(0, \sigma_j^2)$	Gaussian random variable with zero mean with standard deviation σ_j
$E(\hat{d}_{ij})$	the mean (expectation) of the estimated distance
$Var(\hat{d}_{ij})$	variance of the estimated distance
I_0	modified Bessel function of the first kind and order zero
I_1	modified Bessel function of the first kind and first order
$L_{\frac{1}{2}}$	denotes the Laguerre polynomial
M_{ij}	distance considered as the radius of a circular area in MEP algorithm
MSE_{ij}	the mean square error between nodes i and j
$MSE R_{ij}$	the mean square error ratio between nodes i and j
e_t	total energy dissipated per bit
$e_{tx-elec}$	energy spent on radio electronics during transmission (per bit)
$e_{rx-elec}$	energy spent on radio electronics during reception (per bit)
e_{tx-amp}	energy spent on signal amplification during transmission (per bit)
e_{elec}	energy spent on radio electronics (per bit)
β	constant value used in the calculation of the total energy per bit
M	energy-optimal position
m	slope
c	double the energy spent on radio electronics
d_{iM}	distance between node i and optimal position M
E_{trans}	total energy consumption spent for transmissions in a network
E_{rcv}	total energy consumption spent for receptions in a network
$TrNo$	number of total transmissions in the network
$HopNo$	average number of hops per received packet in the network
$R(\nu, \sigma_{ij})$	Rician distribution of ν mean and variance σ_{ij}

σ_{ix}^2	location error variance of node i for the x coordinate
σ_{iy}^2	location error variance of node i for the y coordinate
$MSE(\hat{\theta}_i)$	estimated error variance associated with node i obtained from the localisation
$\text{Cov}(\hat{\theta}_i)$	covariance matrix
θ_i	vector of real locations via LLS RSS
$\hat{\theta}_i$	vector of estimated locations via LLS RSS
s_{rss}	prescribed noise value for the RSS localisation simulation
$mean \sigma^2$	the mean value of the variance
σ_{RSS}^2	location error variance as resulted from the RSS localisation
$F_X(x)$	cumulative distribution function
Q_1	Marcum Q-function

1 Introduction

Technological progress in multiple fields, such as the booming success of telecommunication networks, the growth of the Internet and wireless communication and the advances in sensor technology, all paved the way for the development of wireless sensor networks (WSNs). A WSN comprises of spatially distributed autonomous devices (nodes) capable of sensing and measuring environmental parameters and of cooperatively forwarding the information to one or more devices situated in key positions (sinks/destinations). Envisioned as a bridge between the physical world and modern broadband networks, WSNs have become incredibly popular over the years because of the wide application potential. The increasing demand for WSNs in the industry, military, transport, agriculture, healthcare and many other branches encouraged the study of WSN principles and garnered the attention of the scientific community because of their unsolved challenges.

WSN expansion has been conditioned by the standardization of communication protocols, by the lack of effective energy resources in nodes, which would enable a long network life or by the quality of service (QoS) of data routing when limited by inaccurate localisation technology. The successful design and implementation of WSNs depends on maintaining the integrity and security of data over error prone wireless mediums, efficient energy management, optimal node distribution to ensure full network coverage and robust routing both in indoor and outdoor environments.

Consequently, WSNs require innovative algorithms developed to cope with sensor positioning, ranging and distributed communication and processing, while efficiently managing the available power and meeting application-specific challenges.

Position based routing is a particularly attractive type of routing and has increasingly captured the attention of the scientific researchers over the last decade due to advances in localisation technology. Although identified with geographic routing, the latter is considered as an encompassed category within the sphere of position-based routing, more attractive because of its numerous advantages. It is therefore seen as a promising solution to the challenges of the more restrictive WSNs which comprise of a large number of nodes with reduced battery lifetime or need to be deployed outdoors, in remote areas. Motivated by its intrinsic benefits, geographic routing constitutes the focus of the current thesis.

Geographic routing is proposed as a forwarding solution for point-to-point routing, where data packets are directed on a path established using only local information. Its need for local knowledge only increases energy efficiency by requiring very little node memory, few processing resources and by creating no overhead. To achieve geographic routing, each node needs to know two things: how to make routing decisions in any network topology in such a way that the data packets reach the destination, and where to transmit the data (so the location information of itself, the neighbours and the destination). Consequently, geographic routing research has taken two directions, one focusing on algorithms dedicated to acquiring location information in a given network topology and one focusing on the routing once the coordinates of the nodes are known. However, considering the two aspects independently is not practical and routing algorithms which neglect to consider the correlation between the two topics fail to perform realistically.

1.1 Problem statement

When designing geographic routing algorithms, if the connection between the localisation and the forwarding is neglected, the algorithms will not perform in reality as predicted by prior simulations [1–3]. Considering the position of nodes known with accuracy has led to the proposition of geographic routing algorithms with reduced efficiency in real-life applications and to the avoidance of their implementation [4].

Impractical routing is a result of unrealistic assumptions about network topology, density, radio coverage, power capacity of nodes, all leading to unrealistic network performance between theory and practice [5,6]. Inaccurate localisation is one of the most important examples of such an assumption. Few algorithms in the literature consider the fact that all positioning systems are inherently erroneous [3,7,8]. Most assume the use of the more accurate global positioning system (GPS) devices which are however too expensive for large scale networks. If other positioning systems are considered, location errors will vary in a different way, depending on the chosen ranging method.

With alternative localisation methods, such as those using received signal strength (RSS) or time of arrival (ToA) measurements, only a reduced number of nodes, called *anchor nodes*, need to be equipped with GPS devices, thus reducing the network costs. Anchor nodes can be static and benefit from more power and computational resources than regular nodes. The remaining nodes, called *target nodes*, are localised through ranging by the anchors and will not benefit from accurate location knowledge. With restricted energy resources and limited accuracy, target nodes need to make use of data forwarding strategies which consider their disadvantages. If designed to cope with error, the network throughput is maintained at acceptable levels and if designed to consume as little energy as possible, network lifetime is ex-

tended. Therefore, the objective of the present work is to create resilient geographic routing algorithms, ensuring quality of service and efficient management of network resources.

1.2 Research contribution

The current work is aimed at a good understanding of WSN requirements and of geographic routing principles. The main concerns regarding this type of routing are related to energy saving features and to location error tolerance. An investigation is made into the challenges faced by a basic geographic forwarding technique which has no error-coping capabilities, when node coordinates are known both with accuracy as well as in error. The scope is to compare its performance with previously proposed algorithmic solutions which are robust against location error, under similar constraints. The impact erroneous localisation has on the routing component is quantified via simulations. Consequently, the work proposes to identify geographic routing solutions to better address the identified problems in an energy efficient way.

To reach this goal, complex simulations are needed to imitate real-life network behaviour and to accurately evaluate the routing component. They facilitate the novel analysis of the network behaviour when nodes are deployed in a stochastic fashion, having different, application-dependent, random node distributions and when node coordinates are assumed both accurately known as well as in error [9]. These investigations are intended to be as realistic as possible, so the location error factor is proposed for simulation in two ways: either prescribed as a random value with a normal distribution [10] or used as a result of the localisation process itself which is simulated with RSS and ToA ranging [11, 12]. This also allows the evaluation and comparison of the energy spent by the network with each method, during both the

forwarding and the position estimation phase [13].

The results of the simulations support the proposal of two geographic routing algorithms: the mean square error ratio algorithm (MSER) and the conditioned mean square error ratio algorithm (CMSER), with a new approach on tackling location errors [14]. The forwarding alternatives are aimed at providing a high throughput at very little network cost. In addition, CMSER is then perfected to reduce energy expenses further. Its modified version (M-CMSER) is based on the approach of an existing algorithm in the literature, the least expected distance (LED), whose hybrid metric is aimed at improving the energy consumption [7].

A final contribution to the thesis is to question the widely adopted statistical assumption on which all of the location-error coping solutions are based. The assumption that inter-nodal distances are Rician random variables is an over-simplification which does serve its purpose, but is not completely realistic [7]. Its impact on the forwarding is analysed and shown to be higher when the estimated location errors for the x and y coordinates of each node differ in value, but the forwarding approaches are not aware of this difference. Several tests are used as proof as follows. The location error variance in the x and y coordinates of nodes is analysed via simulation and compared to the theoretically calculated values. The comparison is made numerically and via graphical visualisation of the error ellipses and of the cumulative distribution function curves. Two non-Rician algorithmic solutions are provided, by modifying the earlier proposed algorithms. Their performance is similar to the Rician ones, but they are based on accurate assumptions.

1.3 Thesis outline

This thesis comprises of six chapters and, following the introduction, it is organised as follows:

Chapter 2 comprises of an overview of wireless network types and the design requirements these impose on position based routing. Geographic routing is defined as a more restrictive type of data forwarding within the sphere of the position-based approach and addressed separately. The chapter is divided into three subchapters. The first one presents a comparison of two application-targeted types of networks (sensor and ad-hoc networks), which enables a better understanding of the challenges of each network type when trying to efficiently function in specific environments. Based on this analysis, the routing component can be more appropriately chosen. Scientists have provided a long list of algorithmic solutions classified by the literature depending on their approach. Subchapter 2 presents a classification of routing types motivating the focus of this thesis on position-based routing and the setting apart of geographic routing as a more promising forwarding approach. By understanding the network challenges and the solutions provided by already proposed algorithms, the unsolved issues can be identified and addressed accordingly. Thus, subchapter 3 presents the networking principles and design parameters which can lead to the proposition of novel and improved forwarding algorithms.

Chapter 3 addresses the design context of geographic routing algorithms and the need to correlate theoretical work with realistic application-driven requirements. Subchapter 1 presents possible application fields for WSNs in need of geographic routing due to the advantages it provides over other methods. Because theoretical propositions are made to improve network behaviour, they need to be tested in a simulation environment. Subchapter 2 analyses the appropriate software and moti-

vates the use of MATLAB over other available tools. A complex WSN simulator is developed and its functionality and parameters are described in detail. Aside from an optimal software choice, the realistic evaluation of theoretical propositions is also ensured by making correct, realistic theoretical assumptions. Subchapters 3 and 4 address widely employed assumptions related to sensor node placement and localisation. Considering different methods of sensor deployment related to possible WSN applications, a simulation study is made to analyse geographic routing performance for various node distributions. Subchapter 4 lists some of the most popular localisation measurement techniques used in the literature and briefly reviews recent work on geographic routing with inaccurate information knowledge. A preferred location error model is presented because of its use in an initial simplistic study of geographic routing behaviour.

Chapter 4 analyses the performance of geographic routing while considering erroneous location information. Geographic routing is inherently dependent on accurate positioning information. Realistic assumptions about the location knowledge are imperative when evaluating the true performance of a forwarding method. Network behaviour is studied via simulation and two location error models are alternatively employed: a simplistic one, which has been used previously in the literature, and a more realistic one, which includes a simulation of the localisation process. The first model assumes positioning errors normally distributed, while the second makes use of RSS and ToA ranging techniques. When using RSS and ToA measurements, the localisation techniques are simulated using both iterative and non-iterative algorithms, specifically the linear least square (LLS) method and the maximum likelihood (LM) based Lavenberg-Marquardt method. Each results in location errors of a different magnitude. Routing performance is analysed while varying the network density, illustrating the throughput, energy consumption, hop count and percentage

of failures due to inaccurate localisation, network congestion, lack of connectivity or of forwarding options. Furthermore, the energy consumption values are not estimated only for the routing process, but also for the localisation stage, for both ranging techniques. The realistic localisation assessment is based on values provided by Jennic, manufacturer of sensor devices for WSNs [15].

Chapter 5 proposes geographic routing solutions to efficiently forward data in networks with realistic assumptions of inaccurate localisation. Subchapter 1 presents previous algorithms proposed to cope with localisation error, while the following two introduce and describe the novel proposals: the conditioned mean square error ratio (CMSER) algorithm and the modified conditioned mean square error ratio (M-CMSER) algorithm. The performance of the new forwarding techniques is first compared in terms of packet delivery ratio (PDR) while varying the network density, communication range and standard deviation of location error. The energy consumed by the algorithms is estimated based on the route length of the received packets and on the hop count of the lost packets (the energy consumption is evaluated based on the number of hops per packet, each hop costing a similar amount of energy). To better compare the energy consumption of the two novel algorithmic solutions, the last subchapter presents the results of a more realistic simulation scenario, when reception acknowledgement is used. In these cases, if a tolerable location error is assumed, the PDR is the same for all algorithms. This allows the energy efficiency analysis of the algorithms based on the number of transmissions and re-transmissions which ensure the equal packet throughput.

Chapter 6 provides a more in-depth analysis of the geographic routing solutions previously proposed and tests the validity of an assumption on which MSER, CMSER and other algorithms in the literature are based on: that distances between nodes follow a Rice distribution. The condition for the Rician hypothesis is that the error

variance of the x and y coordinates of nodes is equal, a statement which is not always true in reality and whose validity is tested. For this, the simplistic error model used initially is replaced with the use of RSS localisation, simulated through the LLS method. The localisation process results in an estimation of the location coordinates and of the error variance, considering it equal for the x and y coordinates. Consequently the routing behaviour of Rician-based algorithms will be different from the case when the error variance is different for the x and y coordinates. The validity of the theoretical assumption is tested with the help of three simulations showing the results of network sampling, differences in the error ellipses and in the cumulative distribution function in the given cases. Two non-Rician algorithms are proposed, the adapted versions of MSER and CMSE (NR-MSER and NR-CMSE). The new forwarding methods are modified to still cope with location error and provide similar or better results, but most importantly to consider theoretically correct assumptions.

1.4 List of publications

The research papers, authored or co-authored by me during the course of my doctoral study, are listed in their chronological order as follows:

1. G. I. Tudorache, A. M. Popescu, Dr. A. H. Kemp, "Improved Mesh WSN Support For A Realistic Mobility Model", *7th International Symposium on Wireless Communication Systems (ISWCS)*, 2010
2. A. M. Popescu, G. I. Tudorache, Dr. A.H. Kemp, "Performance study of node placement for geographic routing in WSNs", *IEEE Swedish Communication Technologies Workshop (Swe-CTW)*, Stockholm, Sweden, pp. 13-18, Oct. 2011
3. G. I. Tudorache, A. M. Popescu, Dr. A. H. Kemp, "MANET routing protocols problem for the marginal mobility model", *41st European Microwave*

- Conference (EuMC)*, pp. 139-142, Oct. 2011
4. A. M. Popescu, G. I. Tudorache, Dr. A.H. Kemp, Dr. B. Peng, “Surveying Position Based Routing Protocols for Wireless Sensor and Ad-hoc Networks”, *International Journal of Communication Networks and Information Security* 4 (1), 2012.
 5. A. M. Popescu, N. Salman, Dr. A. H. Kemp, “Energy consumption analysis of geographic routing in WSNs with location error”, *18th European Wireless Conference*, Manchester, pp. 1-8, April 2012
 6. A. M. Popescu, N. Salman, Dr. A. H. Kemp, “Energy consumption of geographic routing with realistic localisation”, *IET Networks*, vol. 1, no. 3, pp. 126-135, Sept. 2012
 7. A. M. Popescu, N. Salman, Dr. A. H. Kemp, “Geographic Routing Resilient to Location Errors”, *IEEE Wireless Communications Letters*, vol. 2, no. 2, pp. 203-206, April 2013
 8. A. M. Popescu, N. Salman, Dr. A. H. Kemp, “On Rician statistical assumptions for geographic routing in WSNs”, under review in *IEEE Wireless Communications Letters*, 2013
 9. G. I. Tudorache, A. M. Popescu, Dr. A. H. Kemp, “PRP: Peripheral Routing Protocol for a WSN Realistic Marginal Mobility Model”, under review for publication in *IET Networks*, 2013
 10. A. M. Popescu, N. Salman, Dr. A. H. Kemp, “Energy Efficient Geographic Routing Robust Against Location Errors”, Accepted for publication in *IEEE Sensors Journal*, February 2014

2 Overview of position based routing

A focus of the scientific community is to design network-oriented position-based routing protocols and this has resulted in a very high number of algorithms being proposed, different in approach and performance, each suitable only to particular applications. Although numerous, as it can be seen from existing surveys [16–26], very few position-based algorithms have actually been adopted for commercial purposes. Because of this, as well as due to the need to understand the level of development and the evolution pace of research in the field of wireless networks, a vast literature review was necessary. This has helped to identify the general challenges of ad-hoc and sensor networks and to focus on a key component in network design: data routing.

Chapter 2 addresses the network layer and the design of position-based routing algorithms as detailed in [4]. Various types of forwarding methods are presented and compared, emphasizing the advantages of each. As a result, the main problems faced by position based routing are identified, tracing geographic routing boundaries and comparing trade-offs for the further improvement of existing algorithms. Also, a distinction is facilitated, differentiating geographic routing as a branch of position-based routing. The terms ‘position-based’ and ‘geographic’ are sometimes used in a generic way, when referring to location aided routing. The work in [20, 23] considered the two terms synonymous and the description of ‘geographic routing’

coincided at times with that of ‘position based routing’. The published survey [4] defines geographic routing as encompassed within position-based routing. Similarly, here, the distinction is used in the categorization of position based routing, bringing a novel factor in comparison with other more generic work on the topic. The two types of routing are explained in detail in subchapter 2.2 where it is also concluded that geographic routing has reduced memory requirements and benefits from a localised and energy-saving forwarding behaviour, while position-based routing algorithms may use global information of node coordinates and pre-computed paths.

In addition to this, surveying geographic routing algorithms has allowed application related analysis and suggestions. Prior literature has not provided specific details related to applications. While some authors make few application suggestions for their developed routing algorithm, others do not. Existing taxonomies are not developed in this specific direction and, while [18] does contain such information, it is not well explained.

Therefore subchapter 2.1 presents wireless sensor networks (WSNs) and ad-hoc networks and compare the two types. By understanding the main differences and various challenges in designing these two types of networks, one can have a better understanding of what is required from an efficient routing algorithm and what the novel research questions are. In subchapters 2.2 and 2.3, the focus is shifted to position-based routing and to geographic routing, the latter being considered more advantageous in comparison with other routing types. The notion of ‘geographic routing’ is clarified as a more restrictive and more efficient type of position-based routing. Then possible network design issues are identified and a description of the parameters used in the characterisation of routing algorithms is made.

2.1 Network types: differences and similarities

Position-based protocols are currently being thoroughly studied due to their application potential in networks with demanding requirements. Their main characteristic is the use of location information for routing decisions. Position-based protocols are generally designed for either ad-hoc networks or sensor networks (static or mobile). Leaving aside mobility issues which are challenging for both network types and comparing network demands, it can be stated that latterly developed position-based routing algorithms, if designed for static WSNs, can be used for static ad-hoc networks as well. However, WSNs are usually more demanding (as it will be revealed from the following paragraphs) and require better developed routing strategies.

Ad-hoc networks differ from WSNs through numerous aspects such as purpose, energy constraints, network lifetime, degree of mobility, scalability, device prices, node identification, cross-layer design, communication, fault tolerance and maintenance needs [21]. WSNs are designed for information collection, sometimes from remote areas where maintenance and sensor replacement is not possible [24]. Sensor networks consist of distributed autonomous sensor nodes which monitor physical or environmental conditions according to application demands and report the information to a single or to multiple sinks. Ad-hoc networks are designed for distributed computing and, in some cases, their resource saving requirements are not as demanding as the ones of WSNs, as it can be seen from the following paragraphs. The main concern of WSNs refers to energy constraints, while ad-hoc networks, and especially MANETs, need to benefit from exact location information and to adapt to mobility. However, this does not imply that all WSNs are static or that they should not benefit from accurate node localisation. Node positioning plays a vital role in data transmission and needs to be considered while designing routing algorithms which are position-based; without accurate position information, data packets may

not reach the destination or may be too power costly, considerably reducing the network lifetime.

WSNs are often created for applications with numerous nodes (more than ad-hoc networks) and mobility requirements. Node dynamism results in additional energy expenditure, increased node failure and affected connectivity and network lifetime. In addition sensor nodes have reduced size and limited battery power. This leads to increased power constraints for WSNs in comparison with ad-hoc networks.

The WSN size dictates sensor price i.e. economy of scale can be achieved. The degree of complexity of a sensor device should be minimal and any component which may increase node size or cost has to be carefully considered (such as GPS receivers) [18]. Also, because of the large number of nodes in mobile WSNs, the identification of nodes is no longer made through the hard wired unique MAC addresses as in the case of ad-hoc networks [5, 19]. In WSN end-to-end communication is preferred and the large amount of global identification overhead (tolerated in ad-hoc networks) has to be avoided. Instead of pre-wired identifiers, the nodes' identity is given by their location after deployment. The large amount of global identification overhead which can be tolerated in ad-hoc networks has to be avoided.

Other differences between WSNs and ad-hoc networks refer to layer and node communication. Because application level decisions may influence the design of all the layers, a cross-layer approach may be needed. Node communication sometimes differs for the two types of networks as well. WSN broadcast or multicast communication can replace the typical ad-hoc network unicast transmission.

However, though very different in purpose and level of demand on the routing component [18, 21], the two network types have important similarities: the unstable nature of their wireless communication, the lack of pre-deployed infrastructure, their mobile nature and ad-hoc deployment in some particular cases. WSNs can be dy-

dynamic when robots are used to carry the sensing equipment. Also, they can have an ad-hoc node placement when the distribution is not uniform, as in military applications. Therefore, even if the requirements for routing may seem different, both types can benefit from position-based routing. Because of scalability and energy efficiency issues, it is valid to consider that both WSNs and ad-hoc networks are suitable candidates for the implementation of a location based routing approach, such as geographic routing.

2.2 Comparison of routing types

This subchapter presents how different routing algorithms have been classified in the literature, what forwarding techniques fall under the name of “position-based” and why the name “geographic routing” is given to a separate category of algorithms. WSN routing algorithms have been classified by [18] as node centric, data centric, geo centric and QoS based. [18] also classifies them as destination initiated or source initiated, depending on the node where route setup is demanded and where the start-up point is. According to network architecture, routing algorithms can be categorized as implemented on a flat topology or a hierarchical one. In addition [22] mentions a classification which is regarded as optimal in this article’s perspective: as topology-based and position-based algorithms. The paper also does not use this classification in the analysis of its selection.

A first amendment to the classification in [22] is that position-based routing should not be made synonymous with geographic routing whose definition is more restrictive. Geographic routing is an elegant way to forward packets from source to destination, in very demanding environments, without wasting network resources or creating any impediment in the network design. Its requirements are minimal - it

only need information about the position of the sending node, that of its neighbours and of the destination. All its decisions are local and energy-saving. Therefore it is generally considered as an attractive routing method for both wireless ad-hoc and sensor networks. (However, as all location based algorithms, it does not completely lack drawbacks because it is based on localisation, an intrinsic source of communication errors.)

The work in [22] presents position based algorithms which make use of more location information than just that of the source, destination and of the forwarding node (which contradicts the definition of geographic routing given here or in [4]). Such an example is the distance routing effect algorithm for mobility (DREAM) protocol which requires a position data base of all the nodes in the network [27]. Furthermore, topology-based routing in [22] refers to proactive/table driven, reactive/on-demand and hybrid algorithms, which create routes ahead of events or on demand and memorize them at node level. Despite the fact that [22] is an overview of selected position-based routing protocols it also includes under this title topology-based routing algorithms because some make use of geographic coordinates. Here, it is considered more accurate to regard position-based algorithms as a general category of protocols which rely on location information and to categorize them into: topology-based and geographic routing. In addition, hierarchical position based routing is also discussed. Therefore, the following categorization will and further explain the differences of these sub-types of routing:

- Proactive (table driven or pre-computed) routing is achieved by creating lists or tables with destinations and possible paths towards the destinations. Periodically, these lists are distributed to nodes in the entire network, updating the link states. It makes use of broadcasting techniques for data updates at node level and for route creation. Through this mechanism, proactive routing

creates a lot of traffic, consumes excess bandwidth and a lot of power. Delays can also occur because of the slow network reaction to node mobility [21, 22].

- Reactive routing (demand driven) can be a lower cost option than proactive because it does not use periodic broadcasts and initiates route discovery only when a message has to be sent, thus traffic decreases and overhead is reduced. However, using flooding and route request packets (blind broadcasts) does result in energy expenditure and high latency. Scalability issues and network clogging can appear because of flooding [21, 22].
- Hybrid techniques of routing are designed to combine the advantages in both reactive and proactive routing, but in general their scalability can be a problem. They usually initiate routing through proactively determined routes and then certain demands in nodes are served according to reactive routing, through flooding. The advantages depend on the traffic requirements [22].
- Network architecture-based routing algorithms can be classified as operating on a flat topology or a hierarchical topology with either homogenous or heterogeneous sensor nodes. In a flat topology, all nodes are equal and are treated accordingly, while in a hierarchical topology, nodes are grouped on levels, and some nodes can become cluster heads having a different level of power. Geographic routing algorithms usually function on a flat topology, but they can be used in a hierarchical topology. However, some routing algorithms are purely hierarchical. In hierarchical routing groups or clusters of nodes are created and data belonging to cluster members is combined to transmit it from one cluster level to another. This type of routing takes advantage of energy saving benefits like aggregation. Also, it scales well because nodes can join and leave a cluster any time as long as they are not designated cluster heads. They are power efficient in finding routes, but they have excessive overhead due to the

use of proactive and reactive routing. Proactive and reactive routing is used depending on the hierarchic level of the node.

So, non-geographic routing protocols display a considerable number of problems such as a high overhead due to bandwidth consumption and maintenance energy expenditure, low scalability problems and slow reaction to topological changes because of the constant necessity for global network updates. On the other hand, geographic routing offers advantages resulting from the limited information needed at the node level. However it also suffers from an intrinsic problem that leads to inaccurate graph connectivity and persistent failures in both static and mobile networks.

- Geographic routing can theoretically be performed based solely on location information of nodes, which can be obtained via the GPS, where this is available, or via other location services. The source node has to be aware of its own position, the position of nodes within its range of communication (neighbour nodes) and of the destination. Therefore, the required node memory is minimal reducing bandwidth consumption and conserving energy. Nodes use broadcasting (on demand or periodically) to let their one hop neighbours know their location or use local positioning knowledge from anchor nodes used in the localisation process. Because discovery floods and state propagation are not needed, geographic routing results in minimal overhead. As a result of very little routing information being needed, no energy is spent on route discovery, queries or replies, node memory requirements are decreased and traffic overhead and computation time are considerably reduced. (Also, in this sense geographic routing is different from source routing in which the sender makes some or all the routing decisions by having mapped the network and specifying in the packet header the hops that the message has to go through.) The localised, yet distributed forwarding process leads to all nodes being involved

in the routing process, contributing to making routing decisions for a faster network reaction, avoiding delays and decreasing overall latency [23, 24].

Because geographic routing is based on knowledge of node coordinates, it relies on idealized assumptions about radios and their capacity to accurately serve node communication [5]. Two such impractical assumptions are the fixed radio range of nodes, described by unit disk graphs (UDGs) and the accurate location information they possess. The communication area of nodes is not predictable and proximity does not suffice. Obstacles may prevent nodes from being within range result in voids in the physical network topology and eventually in the failure of the forwarding strategy. Erroneous localisation can degrade the routing performance in a number of ways: such as packets being dropped, non-optimal paths being selected, creating routing loops or affecting routing correctness [1]. In dynamic networks, the localisation of mobile nodes is even less accurate. Distance measurements for mobile nodes are inherently noisy as their transient location leads to an inconsistent view of the positioning information [1].

To avoid the manual programming of the location in all nodes within a network, as the means of obtaining the location information, sensor nodes can either be equipped with GPS devices or use a location discovery algorithm based on cellular networks or ranging techniques [28] for distance measurements. However, all localisation methods have drawbacks: manual programming of nodes is sometimes difficult or impossible in remote areas or for large networks, the GPS increases device costs and power consumption and is less accurate indoors or where there is no direct line of sight between nodes and satellites, cellular networks require nodes to be in the range of the bases station which is not always made possible, common range estimation methods like Received Signal Strength (RSS) and Time-of-Arrival (ToA) have other flaws: RSS does not work well with large distances and ToA newly developed tech-

nology may require sophisticated synchronization mechanisms and energy-expensive trilateration procedures [28]. As a consequence, a number of papers have studied location errors and analysed their effects on geographic routing and its applications [1, 3, 7, 29–32]. Solutions are being provided for practical implementation, but accurate positioning systems are still being investigated.

2.3 Routing design factors

The performance of position-based routing algorithms can be judged according to the provision they offer for important design factors. Problems may appear during routing such as packets cycling around the network without reaching their destination, packets being dropped and never being retransmitted (due to node battery failure or to a maximum number of retransmissions being reached), packet copies being transmitted in the network redundantly and consuming energy unnecessarily. Routing performance can be rated by the way protocols handle network challenges such as these. So, it is necessary to analyse the qualitative and quantitative routing characteristics of position-based protocols, as proposed by [33] and listed by [20, 22, 23], as well as other features which have not been given the same consideration. This is especially important when considering the implementation of a certain position-based routing protocol for a specific application. The following network characteristics are used in the analysis of routing algorithms:

- **Loop Free.** Network information can be resent into the network to nodes that have previously received the same information. Thus sometimes data can circulate around the network on the same paths or between the same nodes which consider each other equally close to the destination. The result of such an event is the unnecessary consumption of network resources and packets

failing to reach their destination. Proposed algorithms and protocols may or may not possess the quality of being loop free. Ideally this will occur without consuming energy and memory for maintaining information of past traffic and routes.

- **Distributed Operation.** Networks can operate in a centralised, decentralised or distributed manner (Figure 2.1). Distributed algorithms can be classified as localised and non-localised. In localised algorithms, each node performs local computation and makes forwarding decisions using information related only to the position of itself, its neighbours and the destination. This is considered local behaviour with a global objective. Non-localised algorithms are either global, with each node knowing the positions of all the other nodes in the network and of their activity status, or zonal, nodes using localised algorithms within a certain perimeter, but using other routing mechanisms between zones [20]. Increased maintenance of routing tables at each node leads to the characteristic that non-localised algorithms have overhead, additional energy expenditure and less scalability. This is why localised algorithms are preferred.

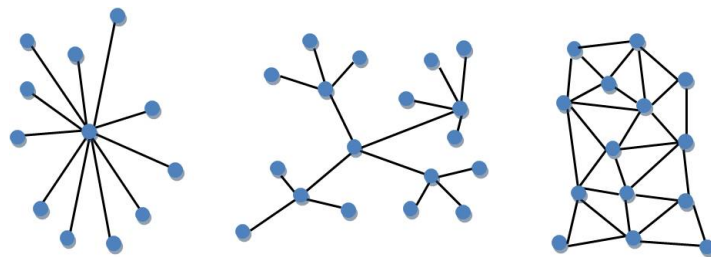


Figure 2.1: Network types: centralised, decentralised, distributed

- **Path Strategy.** Algorithms can make use of certain methods of finding a path for packet transmission. They can use either the single path strategy which requires only a single copy of a packet is present in the network at any

time, or the multipath strategy which requires a copy of the same packet to be sent on a few recognizable routes or on all possible routes (this last case is identified in packet forwarding as flooding) [20]. Combinations of the above mentioned strategies are also possible. However, the single path strategy is preferred for network resource conservation in an ideal localised algorithm [23].

- **Packet Forwarding.** There are three main forwarding strategies which can be used: greedy [34–43], flooding [27,36,44–47] and hierarchical [48]. Flooding can take place in several ways, as explained in the following paragraphs.

Greedy forwarding: is used when the message is able to advance from source towards the destination in a “greedy” manner (Figure 2.2a). It does not imply route establishment or maintenance at the next hop. The decision is made according to the optimization criteria of the algorithm and does not guarantee that a packet reaches its destination [49]. Metrics can be hop count, geographic distance, progress to destination, direction, power, cost, delay, a combination of these, etc. [50–54]. If the message has reached a node which has no closer neighbours to the destination (a void or hole), a recovery procedure is necessary (Figure 2.2b) making the forwarding method a hybrid. Recovery from such a concave node can be done through perimeter (face) forwarding [49,55–57] or flooding [37], [1,58–60]

Perimeter/face forwarding: it requires the mapping of the area (perimeter) of the void through exploration (tours) of the holes using the right-hand rule. Information about the traversed nodes is recorded in the traveling packet and later used by the node which encountered the void. The node decides the optimal route which can bypass the perimeter and forwards to one of its neighbours, the first in the established path (Figure 2.2b).

Flooding: it is the forwarding strategy in which every incoming packet is sent through every outgoing link i.e. to all neighbours (Figure 2.3a).

Restricted directional flooding (RDF): it implies the packet is sent to all single hop neighbours towards the destination (Figure 2.3b). The neighbours which receive the packet check whether they satisfy the criteria to forward the packet or whether they should drop it. From these neighbours, several of them participate in the forwarding, not just one, to increase the robustness of the algorithm. This means that multiple copies of the same original packet are in the network at a certain moment in time.

Directed/box flooding: is used in [46], which presents an algorithm that floods the data packet in a rectangular area (box) oriented in the direction of the destination.

Recursive geographic forwarding (RGF): proposed in [44], is a particular case of forwarding within a target region, where the packet is disseminated in an energy efficient way (Figure 2.5). The first node which receives the packet within the target region divides the area into 4 sub-regions and forwards a copy of the packet to them. The splitting and forwarding continues recursively until there is one or no node per region left. When the minimal region is empty the packet is dropped. The method is inefficient and sometimes does not terminate in low density networks.

Hierarchic forwarding: combines forwarding strategies according to hierarchical network structures (Figure 2.4). Some use zone based routing and some combine geographic routing with forwarding packets based on a proactive routing vector or on greedy strategies [22].

- **Path Selection Metric.** Path Metrics are very important to routing algorithms because they reflect their goal and motivate a certain path selection. If there is a certain quality that the algorithm targets to attain, such as real-time routing or power efficient routing, this can be done through the optimization of certain metrics. The most common routing metrics are the hop count, the power metric and the cost metric [20]. Other metrics can be used as presented

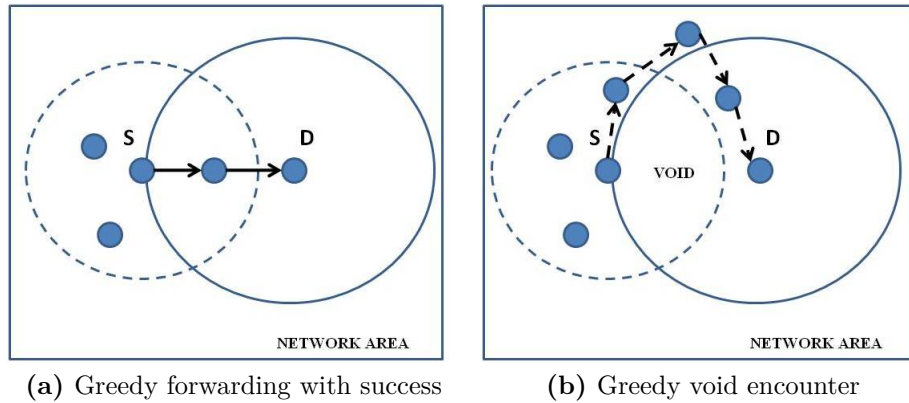


Figure 2.2: Greedy forwarding cases

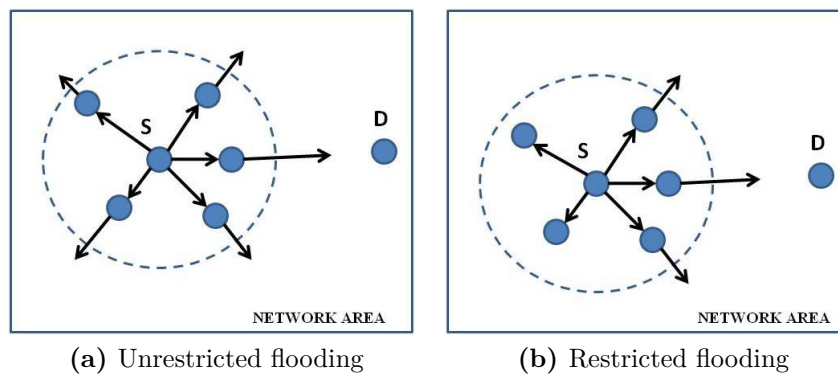


Figure 2.3: Flooding cases

in [61].

- **Memory (state).** As previously mentioned, there are routing algorithms which require nodes to maintain local or global information about the status of all the other nodes. Therefore, routing algorithms can be categorized according to the memory requirements of the nodes. If nodes need more than the position information of themselves, their neighbours and the destination, they are considered to have a memory requirement (statefull algorithms), even if the additional information is limited. Additional information may refer to the cost of the links to certain neighbours, the range of some nodes, node status, energy level, velocity, activity, cryptographic keys, destinations of nodes used

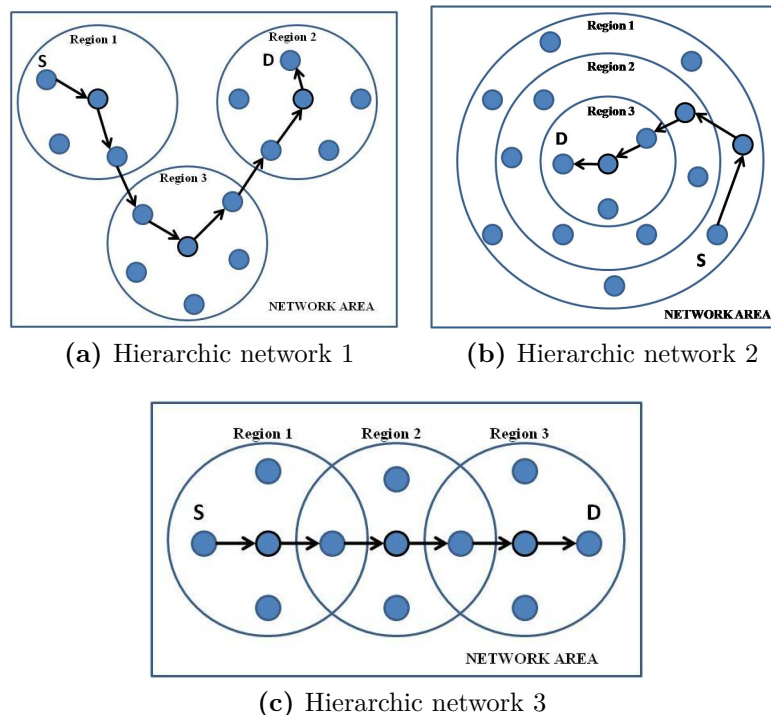


Figure 2.4: Examples of hierarchic networks with designated cluster heads

in recent communication. Otherwise, the nodes are considered to be without memory requirement (stateless algorithms). When mobility is involved, algorithms with additional memory requirements can have difficulties. Maintaining current accurate location information subject to topological changes causes high traffic, queues, congestion, overhead, latency and energy expenditure. Therefore it is desirable to avoid solutions which involve large memory demands at node level [20]. Note that geographic routing, according to the definition in this thesis, uses no memorization, so it is stateless. However, even if some protocols are categorized with memorization, they can be considered as belonging to the geographic routing category, because they do not store global information or routes to destination. Position-based protocols on the other hand represent a larger sphere, which includes geographic routing, and they do make use of more node memory.

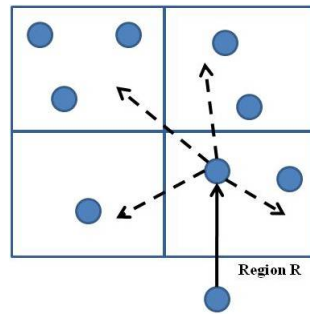


Figure 2.5: Recursive geographic routing

- **Guaranteed Message Delivery.** The main purpose of a wireless network is to be able to communicate node information to the destination for storage or further processing [23]. The performance level of the routing is reflected in the delivery ratio, which should be as high as possible, preferably 100% for the routing algorithm to actually guarantee all messages reach their destination. Packet delivery is improved either at a routing level or at the MAC level. In some articles, such as [44, 54], the message delivery is not analysed strictly from the routing perspective. The delivery performance of certain protocols is studied when the MAC layer is simulated as well, together with the ability to detect receipt failure through the Automatic Repeat reQuest (ARQ) technique and the ACK and NAK messages and retransmit data.
- **Scalability.** Ad-hoc networks as well as sensor networks have varying size and are forecast to reach sizes of thousands of nodes in the near future. This is only possible if routing algorithms allow network growth, without influencing network performance when new nodes join. This property is called scalability. Because scalability is not measured in a particular way and it depends on the outcome of a certain algorithm or protocol simulation, stating that an algorithm is, or is not, scalable is rather subjective. Algorithm simulations can be run under ideal conditions and may not even take mobility into consideration, therefore what may seem a scalable algorithm under certain constrictions, can

eventually prove otherwise. Here, scalability is classified as low, medium or high. Low, when the network which uses the protocol in discussion cannot grow beyond a relatively small size. Medium, when the network does not perform well over a certain size threshold or when size is restricted by a certain condition (density or topology). High, when the network's performance is not influenced by size.

- **Overhead.** The term “overhead” refers to excessive traffic and operating expense needed to accommodate network demands. The existence of a high amount of network traffic, as a result of the design of the routing algorithm, leads to a combination of unnecessary or indirect resource expenditure, such as computation time and energy, memory and bandwidth. Traffic overhead, translated into large or numerous excess packets, therefore increases bandwidth consumption and data processing requirements. According to this we can classify the overhead as: packet overhead and processing overhead, each having a certain degree: low, medium or high, as explained below.

Packet overhead: When large or numerous packets are sent in a network, excess bandwidth is consumed. Numerous packages are sent when the routing algorithms use excessive beaconing or signalling packets. Large packets are sent when information is piggybacked or when tables with node positions and path costs need maintenance at each node. To characterize packet overhead level, we will use the following: low - means light messages and no signalling beacons (unicast transmissions), medium – refers to a balance between packet size and packet number, high - comprises of both large and numerous packets (unicast, multicast, broadcast).

Processing overhead: Processing requirements increase when the data transmitted in the network is encrypted for security purposes. Encryption and decryption consume energy and supplementary bandwidth. The amount of data processing at

node level is also influenced by the number of computed operations (these being dictated by the routing algorithm design as well). To characterize processing overhead, we will use the following: low - translates into zero security and few demands on the processing unit, medium - means only one security method is used or data aggregation is employed, high - reflects a lot of processing activity and the use of multiple security methods [22].

- **Adaptive To Mobility.** Ad-hoc networks and sensor networks are currently being adjusted to serve the needs of more demanding applications and this implies nodes being mobile. Though early geographic protocols were designed for static ad-hoc networks only, it is now expected that routing should be able to take place in dynamic environments too. If the monitored events manifest no movement, then the routing algorithm is more stable - nodes sense and report their information and traffic is routed to fixed locations. If the events are dynamic and the network topology changes, for example in tracking applications, nodes require periodic reporting and the routing algorithm has to deal with increased traffic, overhead and energy consumption [17].

2.4 Conclusions

Constant scientific research is aimed at proposing novel and improved network protocols, as well as realistic routing algorithms which enable a long term, efficient network functionality. This chapter has presented the observed differences and similarities of WSNs and ad-hoc networks, their consequent requirements and the problems they give rise to when developing routing algorithms for them.

It has been established that position-based routing is an attractive type of routing, being given a lot of attention in the literature and promising more developments

in the near future. Furthermore, geographic routing distinguishes itself as a particularly advantageous method for packet forwarding, minimizing the communication overhead and being more energy efficient. It has thus been chosen for further investigations in the current work. Subchapter 2.3 lists routing factors which are necessary to characterize and compare the performance of geographic routing protocols and to establish potential areas of improvement for this type of forwarding.

Depending on these described features, the geographic routing protocols proposed in the literature have a certain degree of compatibility with specific application areas. To determine the compatibility degree, a time consuming analysis is required based on the theoretical behaviour of specific protocols. Supported by the published work in [4], the next chapter presents possible applications for geographic routing algorithms in WSNs. It presents all the areas where geographic routing could be implemented, but has not yet been because of certain unsolved issues. Chapter 3 aims to make the transition from theory to practice and to identify which geographic routing aspects can be perfected. It therefore brings forward practical problems relating to realistic node deployment and localisation. Possible tools of simulation and analysis are presented and a WSN MATLAB simulator is developed for further studies.

3 Geographic routing in realistic scenarios - from theory to practice

3.1 Presenting applications for geographic routing

The following chapter describes possible application fields and their applications as well as their requirements on routing. According to the design issues of a network, some position-based routing protocols offer certain advantages over the others. Whether they are power efficient, guarantee delivery, scale well or are real-time algorithms and take into consideration realistic channels or sensors with power scavenging abilities, each presents a characteristic that would make the protocol more appropriate for a type of application. This depends on the quality of service demanded by the application and the differences between the protocols, as explained in the following paragraphs.

There is a wide variety of applications which can be categorized as belonging to different areas such as industrial, home, health, environmental, military, automotive and commercial. The network challenges in each area are to some extent similar in the sense that all the routing protocols used in these network applications have to be as fault tolerant, as power efficient and low latency as possible and have to have a high delivery ratio. Also, the production costs of the network need to be kept

low. If it is a sensor network, sensor node capabilities can influence node costs and eventually network production costs. However, it is the network differences which recommend a specific routing protocol for a specific application. Applications differ through the operating environment, required QoS, number of events to be detected or tracked and dynamism of the events.

Industrial applications may require networks to function in an in-door environment (factories, warehouses) [62], attached to machinery [63] or dispensed throughout the compound [64], or in an outdoor environment. Possible applications refer to monitoring and control of industrial equipment, processes and personnel [18]. The QoS requirements are real-time communication and collaborative processing. Routing in such an environment can become especially difficult due to obstacles and noise which can affect the line of sight communication between nodes. Node deployment is of great importance in these cases because this affects routing performance. Nodes can be manually placed in the case of industrial applications, in a deterministic way, and data can be routed on predetermined paths. The manual deployment of nodes is not an impossible task in this case as the networks are probably of medium size. However, a predetermined approach could be applied only in the case of static routing. If nodes have to be attached to limited-moving machinery, a solution would be to increase the transmission range of each node to have sufficient coverage on a limited area of mobility. As a result power and bandwidth consumption would increase, consequently affecting routing.

Home applications refer to in-door environments. Higher bandwidth might be necessary for gaming or entertainment purposes, but considering strictly sensor network applications, QoS requirements are reduced [18,44,63]. Communication inside a home is safer, so less processing overhead is created by security needs and less energy is consumed. Home automation consists of sensor enabled appliances inter-

connected which communicate to a central control system [19]. Therefore, the size of the network is small due to the small number of events to be detected and tracked. Usually, there is also no movement involved in home sensor networks, so relatively static routing is recommended.

Health applications are defined here to be in hospitals and clinics, so inside buildings. Therefore they are in need of in-door routing for small or medium networks. Geographic routing may not be the best choice (as explained below). For tracking personnel and patients [39, 65], sensor mobility is required. Position-based routing, when implemented in different protocols, offers mobility adaptation and can actually outperform other routing methods in mobile scenarios. Among routing requirements of health applications are: reliability, robust routing, high fault tolerance and high delivery ratio. Latency cannot be tolerated in routing when it comes to the lives of patients. For example, if a heart attack is detected and signalled with delay, a human life might be jeopardized. Aggregation methods are not necessary and they cause latency. Energy constraints are the trade-off. If the network is positioned inside a building and not in a remote area, it is assumable that a power supply is available for battery recharging or sensors whose batteries fail can be recharged or replaced.

In medical applications, sensor nodes have to provide extra functions and are called smart sensors. They can be used on-body and off-body. On-body sensor networks are small in dimension and do not require geographic routing, but off-body applications may make use of position-based routing in certain cases. Sensor nodes for health applications in general have to be able to detect motion, so position, velocity, angular velocity and acceleration, and have to be able to detect personal features. In applications dedicated to monitoring the vital signs of patients, sensors are necessary for the detection of the heart rate, temperature, blood pressure and blood oxygen

level or for biochemical agents present in the blood stream. Fall detection, video surveillance, sleep disorder monitoring, heart attack identification, obesity problems, all require sensor networks. The collected data is stored, correlated and software management is necessary for issuing warnings in case of a threshold breach [66].

So, industrial applications, home applications and some health applications have two main characteristics in common: they require static routing (or reduced mobility) and small to medium networks. Geographic routing, which is the most advantageous for sensor networks, uses geographic coordinates which are not really appropriate for small, in-door networks. In a building of limited geographic area, the use of geographic coordinates does not make sense. However, position-based algorithms may be used, even without the need to be very scalable, because it is not really necessary for these networks to grow to a metropolitan size.

Environmental applications usually refer to network nodes distributed in certain fields (crops, forests, volcanoes, sea, air, space) and can be categorized as: physical world surveillance and emergency situation surveillance [19]. In both types of applications, networks have to be of medium to high size due to the number of events they may have to detect and track. In physical world surveillance, sensor networks can be used to track different parameters such as motion, sound, temperature, light, humidity, atmospheric pressure, etc. Their information is useful in tracking animal migration, climate change and the effects it has on crops, sea ice, snow and landslides [67]. The possibilities are extremely numerous. In emergency situation surveillance, nodes may have to track natural catastrophes, detect hazardous chemical levels, fires, floods etc. and the information provided through on-site reports can be used for management, crisis response, disaster relief and emergency rescue operations [37, 50].

The nature of the environmental application dictates the number of nodes, whether

they are static or mobile and the required QoS. Regarding this last feature, it can be said that the network length of life is one of the most stringent needs for environmental applications. Geographic routing algorithms with long network life time should have increased energy efficiency as well. To achieve energy efficiency network routing has to have very little overhead and make use of data aggregation to eliminate communication redundancy. Also, the power consumption of nodes has to be minimal because of their reduced battery power. If the node deployment is in a remote location node replacement or battery charging can be difficult or even impossible. Another requirement is robustness of algorithms. If the routing algorithm cannot reroute the message on a different path, node failure can cause routing failure. So robustness is also a recommended characteristic. As a difference between physical world surveillance and emergency situation surveillance, the latter has to be served by a routing protocol with very little latency and good data reliability, while the first is not as demanding on routing speed.

Military applications can refer to both indoor and outdoor networks. Ad-hoc networks are preferred to sensor ones because remotely deployed devices with battery failure are difficult to access and replace [24]. However, if sensor networks are chosen, it is because of the properties sensor nodes have. So, combat field surveillance, recognition missions, remotely controlled landmines that are target specific, intrusion detection and criminal hunting [17] are just a few of the application possibilities. Networks used in military applications should be designed for the multiple intelligently performed tasks according to the application demands: surveillance, recognition, targeting, tracking and control [45, 68, 69]. Geographic routing is recommended for outdoor military applications with large network implementations. The routing requirements for this area are similar to the environmental ones, but are more stringent regarding security and confidentiality [19, 70], something that will

reflect in processing overhead and energy consumption. Therefore energy efficiency demands have to be compensated by eliminating other power consuming factors.

Automotive applications may refer to two subcategories: for in-car purposes such as Internet access or entertainment or for large scale, out-door networks implemented using vehicles as nodes [71, 72]. Applications can make use of both mobile wireless sensor networks as well as mobile ad-hoc networks. A new type of network was considered in the '80, based on ad-hoc networks, and is now possible: vehicular ad-hoc networks (VANETs) [73]. The interest in this type of application comes from the mobility of the nodes which are fitted on vehicles and communicate through wireless technology. The applications can be multiple and all can make use of local information propagation. VANETs can be used for the extension of the wireless range of base stations, for traffic decongestion in busy areas, for driving assistance when supplementary information is needed about local gas stations, parking spaces, shops and restaurants, for driving safety when the weather changes or for avoiding accident areas. The size of such a network can reach metropolitan areas and the routing could take place by using both mobile as well as static vehicles. However, the disadvantages would be the speed and unpredictable directions of vehicles leading to connectivity issues [74]. Referring to dynamic topologies, geographic routing is superior in performance to other routing schemes. This is why it is recommended for automotive applications. The requirements of such applications on routing are robustness, high speed, precise localisation, good coverage and high fault tolerance.

Commercial applications refer to small indoor networks used in conferences and meetings, or to larger outdoor mesh networks or extensions to services provided by cellular infrastructure [24]. Commercial applications can use ad-hoc networks instead of wireless sensor networks because of their less demanding characteristics. Two such examples of static ad-hoc networks are given in [20]: Metricom

Ricochet [75] and Nokia Rooftop systems [55, 76]. For conference applications, the routing protocol has to consider a realistic lossy wireless channel and real time message delivery without delays and latency. Fault tolerance and high delivery ratio are primary requirements because the final purpose of the application is to guarantee communication. Mobility is not really needed in these applications, but for mesh networks and cellular infrastructure, mobility can imply robust routing requirements.

3.2 WSN Simulations

A very important step in WSN research is the ability to simulate and analyse network behaviour using commercially available software tools. An easy to use, versatile wireless network simulator is vital when studying network routing performance and the full impact of the stack layers on the network layer. Choosing the simulation tool however depends on multiple factors such as the desired complexity and level of accuracy and software/hardware costs. Each of these factors are discussed below.

3.2.1 Overview of WSN simulation environments

Network Simulator (NS-2) [77]: It is a widely used discrete event network simulator, popular in the academic study of mobile ad-hoc networks, mainly for the network layer. It is a powerful, open source tool which is constantly being changed and updated (currently has three versions). New versions are being proposed on a regular basis. Because of its popularity, there is support available online and there are numerous discussions on various simulated topics. It is appreciated because it is specifically developed for WSNs and its simulations are fast. NS-2 is however a huge package (50+ megabytes) which takes time to learn, to modify and to collect

data from. It uses two programming languages TCL and C++, both of which have to be familiar to the user. The functions have to be defined in C++ and then run using TCL. Also, additional knowledge is required in applying patches adapted to the version for which they were developed. It requires the LINUX operating system on the host computer which can be difficult to use by Windows users. In terms of efficiency, it supports IEEE 802.11 MAC and some radio propagation models, but its treatment of the OSI physical layer (PHY) and of the radio propagation model is incomplete. The results generated by NS-2 have been found unreliable at times by its users. It also has limited graphic visualization (only for static networks). With Gnuplot, Matplotlib, XGraph or Network Animator (NAM), one can animate packets over wired or wireless links.

Optimized Network Engineering Tools (OPNET) [78]: is another popular simulator used by both academia and industry, mainly for the MAC layer, which does not necessarily attract a lot of interest in the current study. It has been used extensively because of several benefits such as the Graphical User Interface (GUI) for topology design, a performance and display module which enable realistic analysis of performance and an Application Characterization Environment module (ACE) which can be used to import packet traces from various sources into the simulation. The tools provided by OPNET can be divided into three categories, for Specification, Simulation and Analysis. The Specification tools consist of five editors for the network, nodes, processes, parameters and probes. However, programming skills of proto-C and C language make the use of this simulator difficult. OPNET is a commercial software thus implying costs avoidable by using other environments. Learning and modifying it takes significant time and requires the Linux operating system as well.

QualNet Developer [79]: It is a new comprehensive virtual network environment

which allows the modification of all stack layers, of the communication medium and network dynamism related aspects. It makes available a number of tools which enable scenario design, 2-D and 3-D scenario animation, graphical statistic analysis and graphical packet tracing. One can modify scenarios, run batch simulations, visualize and compare results easily. Available documentation makes its use simple for beginners and does not imply having extensive programming skills unless one wants to define his own protocols and functions. To implement new functions, C++ knowledge is necessary. However, in comparison with NS-2, one only needs to know a single language, not two. A disadvantage is the fact that this software is commercial. However, although the software is made available in the University of Leeds, it is not widely used so online discussions and additional help is difficult to obtain.

MATLAB [80]: is a computing platform that enables various simulation projects. It has been particularly used for PHY layer studies in wireless communication. But in general, MATLAB is an easy-to-use mathematical simulation tool for different mathematical models, including the simulation of the network layer. One can use it for real-time simulations and analyse results easily. It is a commercial software, but it is widely used in academic studies and it is therefore made available in almost all Universities. As a consequence, there is a lot of online support and numerous discussions on various simulation topics. However, the main problem with this software is that there is no WSN library available and to develop such a library and to simulate all the stack layers can be quite difficult. A development group does exist however and an open source simulator has been made available at [81]. The Wireless Network Simulator can be tested and modified freely, but it is designed for proactive routing. Because it is structurally designed for route discovery, it cannot be modified for geographic routing (as defined in chapter 1).

Aside from the OPNET simulator, all the above presented simulation environments

have been made available for testing. Each has certain trade-offs and deciding which is best for future research is subjective. Although programming difficulties can be overcome, the process is time consuming. Price is also a problem and this is why OPNET has been rejected in favour of MATLAB. A MATLAB WSN simulator made available online was a good starting point for acquiring the programming skills, but a new complex simulator was designed specifically for this research.

3.2.2 Wireless sensor network simulator

To be able to compare the performance of geographic routing in a WSN, a MATLAB simulator was developed which allows the modification of the network topology, the use of accurate or erroneous localisation, with the ability to change the number and positions of the source(s) and destination(s), with the possibility to adjust energy-consumption related parameters and to imitate the behaviour of a realistic transmission channel. It was developed for static routing as in [7, 24], with a required complexity. This subchapter presents the general features of the developed simulator. The MATLAB functions are presented in the Annexes, each containing a short description of the simulated operations.

The MATLAB simulator imitates stack communication and includes the simulation of the Physical (PHY), the Medium Access Control (MAC) and the Network Layer. The other layers which were not included, such as the Transport or Application Layer, were not of interest to this research because of the focus on the routing aspect of the network functionality. The simulator consists of multiple MATLAB functions which make use of globally and locally defined variables. It is not a time-based simulation which runs for a predetermined amount of time. It is driven by a pre-established, uni-directional packet forwarding requirement which can have two possible outcomes: a successful or an unsuccessful delivery.

The first phase of the simulation is the network setup, according to the selected number of nodes and desired network coverage area. Network communication can be simulated based on accurate position knowledge or, more realistically, considering the nodes are distributed in a random manner and the nodes are not accurately informed of their position. The network setup stage (node deployment and localisation issues) will be discussed in more detail in the following subchapters.

The structure of the simulator is based on the fact that each transmitting node follows the same steps as in the following description. Network events (SE) trigger the sensor nodes called sources (S). The multiple sources [1,5,8,82] can be anywhere in the network so references in the literature select them in a random way [8,83,84], although some do consider them fixed for simplicity [7]. Another simplification is to consider a single S in the network [24,85] and, although this is less realistic, it reduces the simulation time. Each S can forward one [8,30] or more packets [83]. The developed simulator allows all these options. The number of S and of sensed events SE is differently set in each study and has an impact on the evaluation of the routing techniques in terms of time delay, traffic congestion and energy consumption, but not in terms of throughput efficiency.

The sensors act in a localised manner computing which of the nodes within the transmission range (R), entitled neighbours, are the best candidates to receive and forward the sensed data towards the destination (D). The best forwarding options are calculated based on the adopted forwarding strategy, which can be modified on choice. The employed routing strategies are discussed in the following chapters, depending on what routing algorithm is employed. Once the next hop is identified according to the chosen metric and transmission is attempted, the simulator is designed to optionally simulate, the behaviour of the MAC layer.

3.2.2.1 The MAC layer

The 802.15.4 MAC is described in the standard [86] as using a basic access mechanism, namely the Carrier Sense Multiple Access with Collision Avoidance mechanism (usually known as CSMA/CA). The CSMA functions in the following way: the transmitting node senses the medium. If the medium is busy with another transmission, then the node will postpone its transmission. If the medium is free, then the node can transmit. This is an effective approach when the medium is not heavily loaded, the transmission taking place with minimum delay. However, the risk of multiple nodes sensing the medium as free and transmitting at the same time, thus resulting in collisions, is not eliminated. To avoid collisions, and the possibility of additional delay by resending the packet by the upper layers, nodes use a retransmission algorithm entitled Exponential Random Backoff [87].

The Collision Detection mechanism is not a good solution because of price issues which increase with the implementation of a full duplex radio and mainly because of the fact that not all nodes are within range of each other or can hear each other interpreting a free medium when this may not be true [88]. To overcome these problems, the MAC uses a Collision Avoidance mechanism together with a Positive Acknowledgement scheme. A node which wants to transmit information senses the medium. If the medium is busy, then it postpones transmission. If the medium is free for a specified time, then the node can transmit. The receiving node checks the received packet and sends an acknowledgment packet (ACK). Receipt of the ACK indicates that no collision occurred. If no ACK is received, then the fragment is retransmitted until it gets acknowledged or is lost after a given number of retransmissions.

The Exponential Backoff Algorithm resolves contention between different nodes wanting to access the medium. This implies that each node chooses a Random

MAC parameters (unit)	Value
aUnitBackoffPeriod (s)	0.00032
Minimum value of Backoff Exponent (minBE)	3
Maximum value of Backoff Exponent (maxBE)	5
Maximum number of Backoffs (maxCSMABackoffs)	5
CCA_energy (J/bit) [89]	1.5e-0.7

Table 3.1: MAC parameters

Number between 0 and a given number, and waits for this number of slots before accessing the medium, always checking whether a different node has accessed the medium before. The slot time is defined in such a way that a sensor node will always be capable of determining if other nodes have accessed the medium at the beginning of the previous slot. This reduces the collision probability by half. Exponential Backoff means that each time the node chooses a slot and the message happens to collide, it will increase the maximum number for the random selection exponentially. The algorithm is executed if the medium is busy when the node is willing to transmit its first packet, after each retransmission or after each successful transmission. However, if the node wants to transmit a new packet and the medium has been free for more than a certain set time, the Backoff algorithm does not need to be executed.

With the simulation of the MAC layer in the present simulator, both the CSMA/CA mechanism and the Exponential Back-off algorithm are used with the parameters in Table 3.1. In agreement with the un-slotted version of IEEE 802.15.4 MAC layer [86, 87], when inter-node communication is attempted, each sensor checks if the channel is idle or not before sending a packet. When found busy, the assessment is repeated. The channel status is determined through Clear Channel Assessment (CCA) and the failure probability at node level is defined as proportional to the number of sources in the network (so the more packets are generated in the network, the higher the traffic level). If the MAC approves the transmission, the sending node either succeeds or

fails, depending on the accuracy of the location knowledge it has. The ARQ was implemented only for the research made at a latter stage (in Chapter 5). For the first stages of the work, packet reception does not trigger a reception acknowledgment. Although this would be a realistic assumption for practical applications, including the Automatic Repeat reQuest (ARQ) protocol, residing in the Data Link or the Transport Layer, goes beyond the scope of this research, which is to analyse the network layer behaviour. As a consequence, some packets travel for a certain number of hops and are lost without ulterior retransmission in several cases. This leads to an increase in loss rate (LR) and energy expenditure.

3.2.2.2 The Physical layer

The simulation makes use of a stochastic log-normal shadowing channel model as in [90]. The model is considered to take into account multipath shadowing and fading effects which occur in wireless environments. The propagation environment affects signal transmission in a complex way, difficult to model. Therefore, random variables are introduced according to different signal models.

The simplest channel model is the free space propagation model, which is used to predict received signal strength between transmitter and receiver in the case of non-obstructed line of sight [88], showing that received power decays depending on the distance between S and D . Examples of free space propagation are satellite communication and microwave line-of-sight. The Friis free-space equation describes the received power P_r at a distance d , between the transmitter and receiver affected by a path loss of 20 db/decade:

$$P_r(d) = \frac{P_t G_t G_r \lambda^2}{(4\pi)^2 d^2 L} = \frac{P_t G_t G_r \lambda^2}{(4\pi)^2 d_0^2 L} \left(\frac{d_0}{d} \right)^2, \quad (3.1)$$

where G_t and G_r are the antenna gains of transmitter and receiver, P_t is the transmission power, λ is the wavelength, L represents the circuitry losses in the transmission line or due to the antenna (if $L = 1$ then there are no losses in hardware systems), d_0 is the reference distance depending on the antenna technology (which is typically chosen to be 1m for indoor environments and 100m or 1km for outdoor environments) and $d \geq d_0$. The gain of the antenna is related to its physical size and its effective aperture. The wavelength is related to the carrier frequency ω_c , the speed of light c , $\lambda = \frac{c}{f} = \frac{2\pi c}{\omega_c}$.

Generally, the received power at distance d , is

$$P_r(d) = P_r(d_0) \left(\frac{d_0}{d} \right)^\alpha, \quad (3.2)$$

where α is the path loss exponent (for free-space, $\alpha = 2$).

The attenuation of the power between the transmitter and receiver, namely the path loss is expressed as:

$$PL(d)[dB] = P_t[dB] - P_r[dB] = 10 \log \left(\frac{P_t}{P_r} \right).$$

The free-space propagation model is most inaccurate when used by itself because in reality, in a mobile radio channel, there is not a single propagation path between transmitter and receiver. The magnitude and phase of the transmitted signal change depending on the channel due to constructive and destructive interference at the receiver. The log-normal shadowing channel model is used to mathematically model the fading effects of the electromagnetic transmission of information over the air. Shadowing, also called slow-fading, occurs when large obstructions obscure the main signal path between transmitter and receiver. The model accounts for the random variations in received power observed over distances comparable to the width of

obstacles found in the environment, such as buildings, cars, hills and trees. Both theoretical as well as measurement-based propagation models indicate the signal power between transmitter and receiver decreases logarithmically with distance for both indoor and outdoor channels [88]. The log-normal shadowing model is presented in the following equation:

$$PL(d)[\text{dB}] = PL(d_0) + 10\alpha \log\left(\frac{d}{d_0}\right) + X, \quad (3.3)$$

where α is the path loss exponent and the shadowing is represented by X , which is a Gaussian distributed random variable with a mean $\mu = 0$ and standard deviation σ . It expresses the shadowing effects occurring in the realistic situation in which wave propagation differs between transmitters and receivers found at the same distance from each other, due to other surrounding factors. The situation has been demonstrated through measurements and to predict this mathematically, the path loss at any value of the distance d is considered random and has a log-normal distribution [88].

3.2.2.3 The Network layer

During the research, different forwarding path strategies and simulator parameters have been used. The various changes are listed accordingly in the following chapters exactly as they have been used in each case. Although subchapter 3.3 is a study of geographic routing under different node distributions, it also clarifies the functionality of the simulator further because it is the first of this thesis explaining the operations of the network layer. The next paragraphs list general details about how the analysed network parameters are calculated by the simulator.

3.2.2.4 Simulation calculations

The simulator outputs a number of results which are presented in the following paragraphs. For simplicity, the calculations of the values detail several stages which take place in the simulation. The parameters are calculated for each traffic connection (which is initiated by a source node by sending data to the destination), for each network scenario (out of the total number of simulated trials) and then averaged over a total number of trials.

1. **Packet delivery ratio (PDR):** For each traffic connection in the network the simulator records the IDs and number of the received packets. The recorded number of received/delivered packets is added for all the connections in each network. The PDR of a network is calculated as: $PDR_n = \frac{(pckts_d * 100)}{pckts_s}$, where $pckts_d$ represents the total number of delivered packets and $pckts_s$ represents the total number of sent packets. The PDR displayed in the figures of the following chapters is however calculated as an average over η number of trials:

$$PDR = \frac{\sum PDR_n}{\eta}.$$

2. **Packet loss ratio (LR):** For each traffic connection in the network the simulator records the IDs and number of the lost packets. The recorded number of lost packets is added for all the connections in each network. The LR_n of a network is calculated as: $LR_n = \frac{(pckts_l * 100)}{pckts_s}$, where $pckts_l$ represents the total number of lost packets and $pckts_s$ represents the total number of sent packets. The LR displayed in the figures of the following chapters is however calculated as an average over η trials:

$$LR = \frac{\sum LR_n}{\eta}.$$

3. **Average hop count per received packet ($hopsP_r$):** For each traffic connection

in the network the simulator records the IDs and number of the received packets. The number of hops for each received packet is also recorded. The average number of hops per received packet in the network, $hopsP_{rn}$ is calculated as: $hopsP_{rn} = \frac{hops_r}{pckts_d}$, where $hops_r$ is the total number of hops of the received packets in the network and $pckts_r$ is the total number of received/delivered packets in the network. The average hop count per received packet, $hopsP_r$, is obtained by averaging the sum of the values $hopsP_{rn}$ of each trial, over η_r trials which have had received packets. If no packets are received in any trial, that particular network is not used for averaging.

$$hopsP_r = \frac{\sum hopsP_{rn}}{\eta_r}.$$

Also, if more routing algorithms are tested and compared, then only those packets which are received in all the networks are of interest in the analysis of the path length. Consequently, the simulator identifies these commonly received packets and calculates the hop count only for them. Similarly, only the iterations with commonly received packets are taken into consideration in the calculations.

4. Average hop count per lost packet ($hopsP_l$): For each traffic connection in the network the simulator records the IDs and number of the lost packets. The number of hops for each packet (lost and received at D) is also recorded. The average number of hops per lost packet in the network is calculated as $hopsP_{ln} = \frac{hops_l}{pckts_l}$, where $hops_l$ is the total number of hops of the lost packets in the network and $pckts_l$ is the total number of lost packets in the network. The average hop count per dropped packet, $hopsP_l$, is obtained by averaging the sum of the values of $hopsP_{ln}$ obtained for each network over η_l trials which have had packet loss. If no packets are lost in any trial, that particular network is not used for averaging.

$$hopsP_l = \frac{\sum hopsP_{ln}}{\eta_l}.$$

5. **Average hop count per lost packet due to location error** ($hopsP_{le}$): For each traffic connection in the network the simulator records the IDs, number of the lost packets due to location errors and the number of hops for each packet. The average number of hops per lost packet due to location error in the network is calculated as $hopsP_{len} = \frac{hops_{s_{le}}}{pckts_{le}}$, where $hops_{s_{le}}$ is the total number of hops of the lost packets due to location error in the network and $pckts_{le}$ is the total number of lost packets due to location error in the network. The average hop count per dropped packet $hopsP_{le}$ is obtained by averaging the sum of the values $hopsP_{len}$ obtained for each trial, over η_{le} trials which have had packet loss due to location error. If no packets are lost due to location error in any trial, that particular network is not used for averaging.

$$hopsP_{le} = \frac{\sum hopsP_{len}}{\eta_{le}}.$$

6. **Percentage of connectivity failures** (CF): For each traffic connection in the network, the simulator records the sum of the number of packets lost due to no connectivity, C_F , along with their IDs. For a specific case, the simulator can also consider the sum of the number of failures due to no new neighbour except previous hops, NN . For each network, the simulator adds the number of failures due to low connectivity for all the traffic connections and calculates the total number of lost packets. The percentage of connectivity failures in a network CF_n , out of all the failed transmissions which take place (total number of lost packets in the network), is calculated as follows: $CF_n = \frac{[\sum C_F + \sum NN] * 100}{pckts_l}$. The simulator computes the percentage of connectivity failures for η_l trials with packet loss:

$$CF = \frac{\sum CF_n}{\eta_l}.$$

7. **Percentage of progress failure (PF):** For each traffic connection in the network the simulator records the IDs and number of the packets lost due to no progress, NP . For each network, the simulator adds the number of packets lost due to no progress and calculates the total number of packets sent over all the traffic connections. The percentage of progress failures in a network, out of all the transmission failures which take place (total number of packets lost) is calculated as: $PF_n = \frac{\sum NP*100}{pckts_l}$. The simulator computes the percentage of progress failures for η_l trials with packet loss:

$$PF = \frac{\sum PF_n}{\eta_l}.$$

8. **Percentage of partial progress failure** when previous hops are eliminated (PPF): For each traffic connection in the network the simulator records the IDs and number of packets lost when no neighbours are available for forwarding, after the S and previous hops have been eliminated from the neighbour list, NN . For each network, the simulator adds the total number of packets lost due to partial progress and calculates the total number of packets lost over all the traffic connections. The percentage of partial progress failures in a network, out of all the transmission failures which take place (total number of packets lost) is calculated as: $PPF_n = \frac{\sum NN*100}{pckts_l}$. The simulator computes the percentage of partial progress failures for η_l trials with packet loss:

$$PPF = \frac{\sum PPF_n}{\eta_l}.$$

9. **Percentage of congestion failures (CGF):** For each traffic connection in the network the simulator records the IDs and the total number of packets lost due to congestion ($Mpckts_l$), after the MAC has tried to send the packets for a maximum

allowed number of times. For each network, the simulator adds the total number of packets lost due to congestion and calculates the total number of packets lost over all the traffic connections. The percentage of congestion failures in a network, out of all the transmission failures (total number of packets lost) which take place is calculated as: $CGF_n = \frac{\sum Mpkt_{sl} * 100}{pkt_{sl}}$. The simulator computes the percentage of congestion failures for η_l trials with packet loss:

$$CGF = \frac{\sum CGF_n}{\eta_l}.$$

10. **Percentage of location error failures (LEF):** For each traffic connection in the network the simulator records the IDs and number of packets lost due to location errors (*ERR*), when *S* forwarded the packets to a node in its list of neighbours which was actually out of the communication range. For each network, the simulator adds the total number of packets lost due to location error and calculates the total number of packets lost over all the traffic connections. The percentage of location error failures in a network, out of all the transmission failures which take place (total number of packets lost) is calculated as: $LEF_n = \frac{\sum ERR * 100}{pkt_{sl}}$. The simulator computes the percentage of congestion failures for η_l trials with packet loss:

$$LEF = \frac{\sum LEF_n}{\eta_l}.$$

11. **Average packet delay at MAC (PcktDel):** For each traffic connection in the network the simulator records the time spent by the MAC of each node for CCA for each packet, until they are either sent or lost (*NodeDelay*). For each network, the simulator adds the total number of recorded delays by all the nodes at all transmissions and also calculates the total number of packets sent over all the traffic connections. The average packet delay at MAC per network, $PcktDel_n$, out

of all the transmissions which take place (total number of sent packets) is calculated as: $PcktDel_n = \frac{\sum NodeDelay}{pkts_s}$. The simulator computes the average packet delay at MAC for η trials:

$$PcktDel = \frac{\sum PcktDel_n}{\eta}.$$

12. **Average energy consumption per packet at MAC (*MacEnergy*):** For each traffic connection in the network the simulator records the values of the energy spent by each node for CCA per packet, until the packets are either successfully sent or lost, E_{CCA} . The energy values of all the participating nodes are added and stored for each connection: $ME = \sum(E_{CCA} * pkts_s)$. For each network, the simulator adds the total energy consumed (by all the nodes) during all the traffic connections. It also calculates the total number of packets sent over all the traffic connections. The average packet delay at MAC per network, $MacEnergy_n$, out of all the transmissions which take place (total number of sent packets) is calculated as: $MacEnergy_n = \frac{\sum ME}{pkts_s}$. The simulator computes the average energy consumption per packet at MAC for η trials:

$$MacEnergy = \frac{\sum MacEnergy_n}{\eta}.$$

13. **Average energy consumption for all lost packets (*EnergyLostPkts*):** For each traffic connection in the network the simulator records the IDs, number ($ConPkts_l$) and the energy spent to route each lost packet ($EnergLostPckt$). For each network, the simulator adds the total energy consumed by all the nodes on all unsuccessful transmissions over all the traffic connections. So the energy consumption for all lost packets per network is calculated as: $EnergyLostPkts_n = \sum(EnergLostPckt * ConPkts_l)$. The simulator computes the average energy con-

sumption for all lost packets, for η_l trials with packet loss:

$$EnergyLostPckts = \frac{\sum EnergyLostPckts_n}{\eta_l}.$$

14. **Average total energy consumption per network** (E_{total}): This value reflects the power consumption of the entire network for both successfully delivered and lost packets. The simulator is designed to store a certain (user allocated) battery power level for each node, E_i . During each traffic connection, the simulator subtracts for each node the energy consumed for transmissions and receptions, $EnergyTR$, for each node which participates in the routing from the allocated available energy E_i . Consequently, each node will have a recorded energy level left at the end of the routing process, for each traffic connection. For each network, the simulator calculates the total energy consumption for all N nodes, E_{totaln} . It adds the recorded remaining energy levels for all N nodes and subtracts them from the total allocated power levels. It also considers the previously calculated energy consumption values resulting from the CCA, namely the ME , for all traffic connections. Consequently: $E_{totaln} = \sum(E_i * N) - \sum(EnergyTR * N) - \sum ME$. The simulator computes the total energy consumption for η trials:

$$E_{total} = \frac{\sum E_{totaln}}{\eta}.$$

15. **Energy consumption due to connectivity failure** (E_{CF}): For each traffic connection in the network the simulator records and adds the number of lost packets due to loss of connectivity, C_F , and calculates the energy consumption of these packets, E_{CF} , which depends on the energy consumed for transmission and reception of the participating nodes. For each network, the simulator adds the recorded energy consumption of each traffic connection: $E_{CFn} = \sum E_{CF}$. The simulator computes

the energy consumption due to connectivity failure for η_{CF} trials with connectivity failures:

$$E_{CF} = \frac{\sum E_{CFn}}{\eta_{CF}}.$$

16. **Energy consumption due to progress failure (E_{PF}):** For each traffic connection in the network the simulator records and adds the number of lost packets due to progress failure, NP , and calculates the energy consumption of these packets, E_{NP} , which depends on the energy consumed for transmission and reception of the participating nodes. For each network, the simulator adds the recorded energy consumption of each traffic connection: $E_{PFn} = \sum E_{NP}$. The simulator computes the energy consumption due to progress failure for η_{PF} trials with progress failures:

$$E_{CF} = \frac{\sum E_{PFn}}{\eta_{PF}}.$$

17. **Energy consumption per network due to congestion failures (E_{CGF}):** For each traffic connection in the network the simulator records and adds the number of lost packets due to congestion failure, $Mpks_{l}$, and calculates the energy consumption of these packets, $E_{Mpks_{l}}$, which depends on the energy consumed for transmission and reception of the participating nodes. For each network, the simulator adds the recorded energy consumption of each traffic connection: $E_{CGFn} = \sum E_{Mpks_{l}}$. The simulator computes the energy consumption due to progress failure for η_{CGF} trials with progress failures:

$$E_{CGF} = \frac{\sum E_{CGFn}}{\eta_{CGF}}.$$

18. **Energy consumption per network due to location error failure (E_{LocErr}):** For each traffic connection in the network the simulator records and adds the

number of lost packets due to location error failure, ERR , and calculates the energy consumption of these packets, E_{ERR} , which depends on the energy consumed for transmission and reception of the participating nodes. For each network, the simulator adds the recorded energy consumption of each traffic connection: $E_{LocErrn} = \sum E_{ERR}$. The simulator computes the energy consumption due to location errors for η_{ERR} marked trials with progress failures:

$$E_{CGF} = \frac{\sum E_{LocErrn}}{\eta_{ERR}}.$$

19. Energy consumption for the received/delivered/successful packets (E_{pckts_d}): For each traffic connection in the network the simulator records and adds the number of received packets and calculates the total energy consumption of these packets (E_{rcvc}). For each network, the simulator adds the recorded energy consumption of each traffic connection: $E_{pcktsn_d} = \sum E_{rcvc}$. The simulator computes the energy consumption of the received packets for η_d trials with at least one received packet:

$$E_{pckts_d} = \frac{\sum E_{pcktsn_d}}{\eta_d}.$$

Also, if more routing algorithms are tested and compared, then only those packets which are received in all the networks are of interest in the analysis of the energy consumption for the received packets. Consequently, the simulator identifies these commonly received packets and calculates the energy only for them. Similarly, only the iterations with commonly received packets are taken into consideration in the calculations.

3.3 Node placement scenarios and their study

Network performance is greatly influenced by network topology which, if inappropriate for the specific scenario, can lead to premature power depletion, to low packet delivery ratio (PDR) and a short network lifetime. All applications described in subchapter 3.1 require the use of numerous sensor nodes, properly deployed. In addition to this, deterministic node placement in WSNs has been well investigated, while stochastic placement requires further study. The randomness factor creates difficulties for high performance routing in WSNs. Considering these two factors, the network size and the need to deploy nodes randomly, a fire prevention application has been chosen here for further study. In theory, it requires the network to be functional for an extended period of time, while consuming as little energy as possible. The current work analyses how the node placement affects network performance when geographic routing is employed, for this particular case.

WSNs are needed for forest surveillance and fire prevention [2,91–93]. Forest fires can be caused by either the forces of nature or by man. Accidental natural fires can start because of lightning or extreme solar heat. Once wood heats up and reaches 572° , it generates a combustible gas which in reaction with oxygen creates flames [94]. Man caused fires, which seem to be the cause of 95% of forest fire hazards [93], can be caused intentionally or through negligence, as a consequence of forestry activities, improper extinction of fires, careless smoking or other unpredictable activities such as auto or aero accidents (burnt Chinese lanterns) or plant pollution [93]. The flames of an initially small fire can grow easily in forests even on cold days because of unpredictable weather conditions such as wind currents. This is why fire prevention is of utmost importance in areas of high risk for human and environment protection. Forest regions can be kept under surveillance by means of WSNs.

Sensors can detect parameters such as humidity, air and soil temperature or wind velocity informing of potential fire hazards. The information can be reported to a control station (a sink/destination). Because large areas of forest can be monitored, the sensors need to use their battery levels in a considerate way (wasting as little power as possible) and thus may have a limited range and communicate in a multi-hop fashion. Considering such a scenario and the implementation of a network for fire prevention, the aim is to determine how to distribute sensor nodes (over a medium to large area) to obtain a good performance of the network when using geographic routing. Because of the nature of the considered application, there are many possibilities to distribute the nodes. Given that the WSN may need a remote setup and knowing the size and coverage necessities, simulation is necessary before physical deployment, as proven by [2].

3.3.1 Previous work in node placement studies

Though previous studies [95, 96] investigated various algorithms with a stochastic node distribution and, although particular problems related to geographic routing have been analysed (e.g. the presence of the sink routing energy hole problem [97, 98] and of routing holes [99]), geographic routing behaviour with different stochastic node placements has not been studied.

A performance study of a WSN with 3 node placements has been made by [96] which investigated network lifetime in terms of event sensing ratio, tolerance against random failure and battery exhaustion. It considered circular node placements in rectangular surfaces where the base station is central. The nodes were either distributed normally (Simple diffusion placement), in a random uniform manner (Constant placement) or uniformly scattered in terms of radius and angular direction (R-random placement). In terms of routing, a minimum hop strategy was employed.

The authors in [100] proposed several indexes to estimate uniformity of node distributions and uses six cases of node distributions for the investigations: the Grid, the random distribution and special cases of node distributions clustered in certain regions of a rectangular surface.

When investigating geographic routing behaviour, [99] has looked at the routing hole problem for uniform, normal and skewed distributions. The observations referred to the size of the routing holes, the number of hops necessary to circumvent them and the likelihood of encountering a routing hole as a function of distance.

When investigating the sink-routing energy hole problem for a uniform distribution, which can be encountered in geographic routing as well, [97] developed a novel non-uniform power-aware node deployment scheme to maintain continuous connectivity-coverage and conserve energy. This comparative study analysed the coverage and quality of delivered data in a circular network with one central destination.

The energy hole problem is also studied in [98] for a circular area with a central destination where nodes grow in a geometric progression from outer-to-inner coronas, except the outermost. Q-switch routing is used here; nodes in outer coronas divide the load to multiple nodes towards the destination. These nodes are chosen to have maximum residual energy; they have more power resources because they have been used less during previous transmissions. The proposed non-uniform deterministic distribution is compared with non-uniform random and uniform node distributions.

[96] investigates energy holes at the periphery, for sensing nodes, as well as centrally, for routing nodes. A Power Law distribution is proposed which claims to offer a higher density of nodes near the destination and a lower density but with constant number of nodes at the periphery. In multi-hop networks it is desirable to have more nodes in the active areas of the network where traffic is served constantly. The sensor devices used more often are the first ones to be depleted of energy and, if

they are found near the destination, they can leave it isolated when their battery is exhausted. The paper uses the uniform and normal distributions for comparison.

In [101] a new distribution is proposed (Stensor) when trying to solve the coverage problem for random target surveillance. The objective of the new distribution is to cover the network area with limited randomness. This proposal has been included here, for comparison with the well known uniform distribution.

The present node placements have been used throughout the literature for comparison purposes or simply for the analysis of various routing algorithms:

A. Grid Placement: Is a uniform deterministic way of placing nodes exactly at the intersection of the lines of a Grid [102] in a rectangular or square area (Figure 3.1). The space between the nodes is entitled grid pace and can be varied in size (here it is equal to the R). If the size of the grid pace is larger than the R of the nodes, the communication cannot take place. The grid can be filled entirely or partially with nodes.

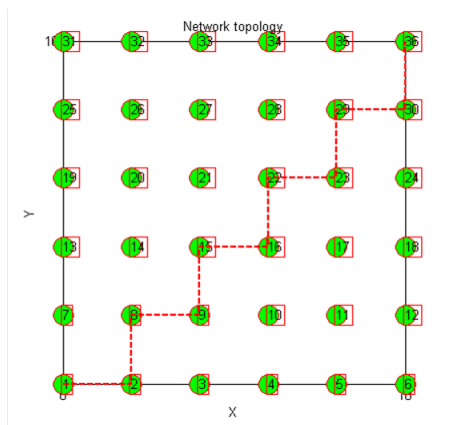


Figure 3.1: Example of a GRID distribution

B. Random Uniform Placement: The uniform or rectangular distribution states that, for all values of a random variable X , the probability of occurrence is equal. If the random variable X is the node location, then the probability of the coordinates

of nodes to be within the given network surface is equal for all nodes and has the following distribution function:

$$f(x) = \begin{cases} \frac{1}{b-a}, & a \leq x \leq b, \\ 0, & \text{otherwise} \end{cases}.$$

Therefore, when node coordinates are randomly generated within the given surface interval, they will also be uniformly distributed, meaning with equal probability of occurrence. This is considered to result in a network with a uniform node density, referred to as Constant Placement in [96, 102] (see Figure 3.2).

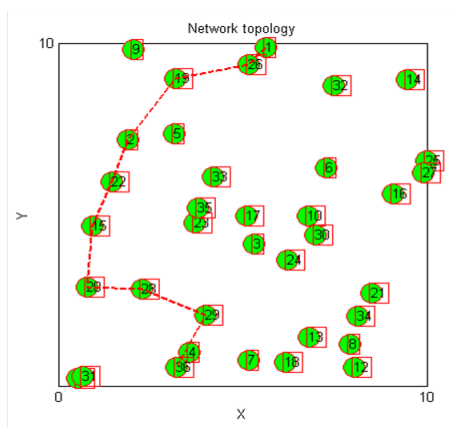


Figure 3.2: Example of a random uniform node distribution

C. Gaussian Placement: The normal distribution describes the behavior of a random variable X whose probability of occurrence is higher near the mean value μ and decreases with a certain variance σ^2 , $f(x, \sigma) = \frac{1}{\sigma\sqrt{2\pi}}e^{-\frac{(x-\mu)^2}{2\sigma^2}}$. The node placement characterizes the distribution of nodes when scattered from an air manned vehicle such as an airplane. It has been referred to as Simple Diffusion in [96]. The node density is not constant, but higher around the distribution central point and lower as the distance increases (see Figure 3.3).

D. Pareto Placement: This was originally used to describe the allocation of

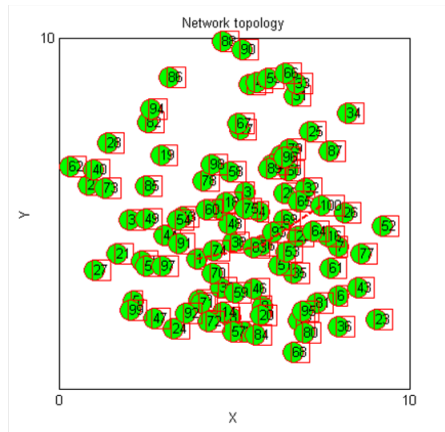


Figure 3.3: Example of a Gaussian node distribution

wealth among individuals showing that in any society a larger portion of the wealth is owned by a smaller percentage of the people. In the same manner, the distribution can be used in WSNs successfully to illustrate projectile distribution of nodes. Nodes thrown from a corner of the network have a greater density close to the distribution point, while few nodes reach further distances. This placement has been named Skewed Distribution (see Figure 3.4). The generalized Pareto distribution function is the one used for the current study and it has the following mathematical expression: $f(x|k, \sigma, \theta) = \frac{1}{\sigma} (1 + k \frac{(x-\theta)}{\sigma})^{-(1+\frac{1}{k})}$, where the parameters are $k = 1$, $\sigma = 1$, $\theta = 0$, [103].

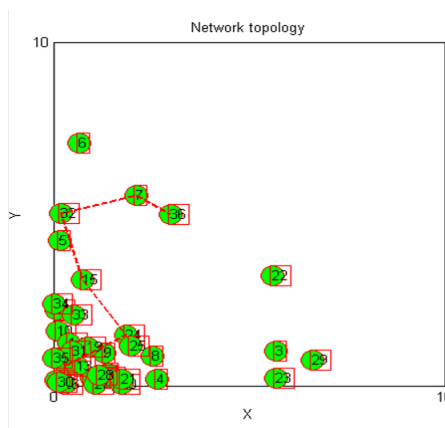


Figure 3.4: Example of a Pareto node distribution

E. Stensor Placement: It aims to place nodes in a uniform, yet random manner by means of an algorithm which identifies the node location distribution process with a Poisson process [101]. Having N nodes, the network surface can be divided into \sqrt{N} strips. Each strip j is considered to be able to host a certain number of nodes, randomly located within the strip. The number of nodes within each strip j of the network is modelled by a random variable X governed by the Poisson distribution with mean λ , $f(x, \lambda) = \frac{\lambda^x e^{-\lambda}}{x!}$. The process is iterative and continues as long as $\sqrt{N} > 1$. The division into strips is performed each time along the widest axis. For each partition a random number r is generated within the interval $(0, 1)$ and the algorithm decides the number of nodes per strip x_j using the cumulative distribution function: $Pr(X_j \leq x) \leq r \leq Pr(X_j \leq x + 1)$. The process is shown in Figure 3.5 with corresponding results in Figure 3.6.

As an example, a number of $N = 36$ nodes need to be distributed in a 10x10 (m) network. The nodes are shown in the first sub-figure of Figure 3.5 as they appear after the distribution process has finished. At the first step of the algorithm, the network surface is divided into 6 strips (marked with red colour) and each strip is calculated to possibly receive a random number of nodes r (respecting the cumulative distribution function). So N becomes 7, 8, 2, 8, 6 and 5 for each strip (these values appear in the green boxes at the bottom of each strip of the first sub-figure). During the second step of the algorithm, each strip with $\sqrt{N} > 1$ is then divided further into more strips, the same way as before. Where necessary, the values are rounded to the next smallest integer number, so for strip 3, which has 2 nodes allocated, there will be no further division. Only strips 1, 2, 4, 5 and 6 are divided into 2 strips each and are allocated a random number of nodes r equal to: 1&6, 4&4, 4&4, 4&2, 4&1. It is kept in mind that each initial strip had a number of total nodes allocated and that this second division must make use of that previous r number,

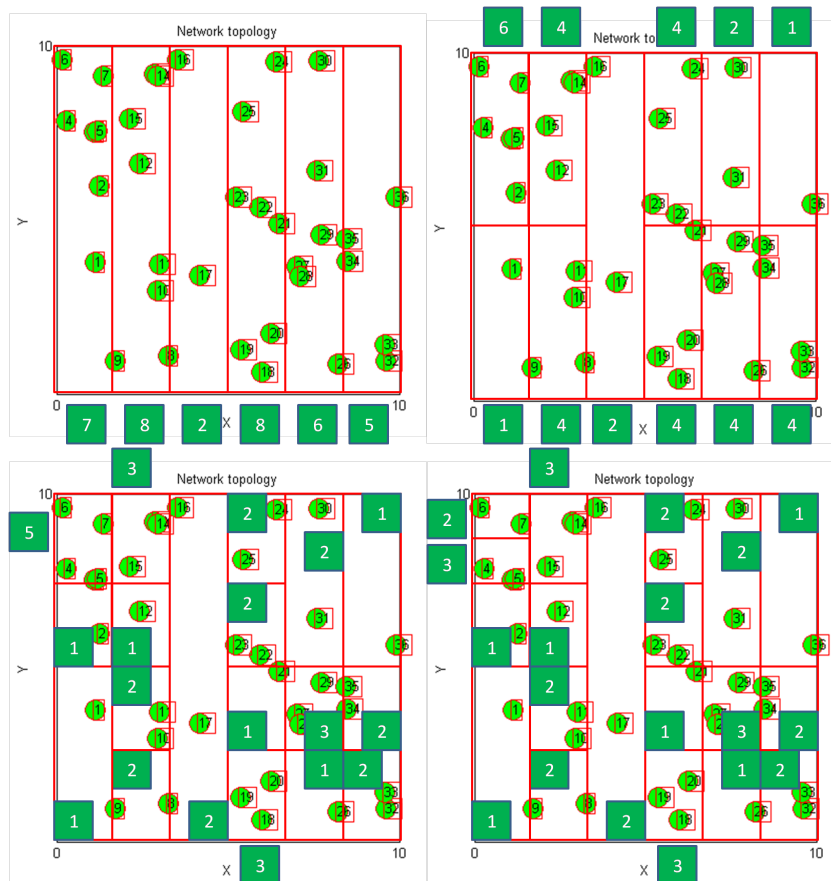


Figure 3.5: Stensor division into strips

so for $1 + 6 = 7$, $4 + 4 = 8$, $4 + 4 = 8$, $4 + 2 = 6$, $4 + 1 = 5$ (visible in green boxes above and below the strips in the second sub figure). The algorithms continues in the same manner until no more divisions are possible and the next two steps of this case can be seen in the third and fourth sub-figures of Figure 3.5. The final result is clearly displayed in Figure 3.6.

F. StensorX Placement: This distribution is a novel proposal and a modification of the Stensor placement in [101], with the difference that the division into strips at each step takes place along the same axis as in the first iteration. Thus the placement is less uniform. So if the x axis was the longest at the first step of the iteration, then all strip divisions take place along the x axis.

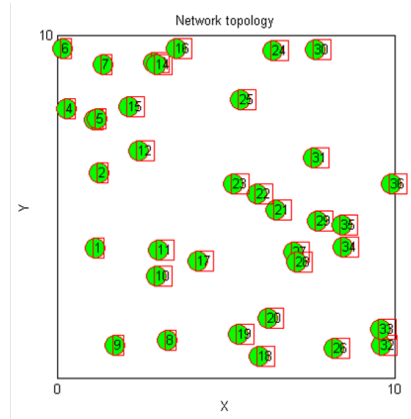


Figure 3.6: Example of a Sensor node distribution

3.3.2 Simulation setup

To be able to compare the performance of geographic routing in a WSN with various network topologies whose nodes are placed according to the distributions described in subchapter 3.3.1, we have used the MATLAB simulator in subchapter 3.2.2. Network analysis is initiated by considering a network area of approximately 4 Km², as a square surface, similar to the size of Sherwood Forest (423.6ha = 4.23Km² [104]), with a centrally placed destination as in [8] and with relatively low traffic. The motivation for this dimension of the network is influenced by the desire to explore geographic routing behaviour for large networks. A number of papers in the literature consider circular sensor networks of specific diameters [1, 96], while others consider square or rectangular surfaces of 50x50m [82], 200x200m [105], 300x300m [7], 500x500m [7], 1000x1000m or slightly bigger [3, 5, 95, 101, 106] and 2000x2000m [5, 8, 55, 107–109]; it is therefore considered as a realistic assumption to decide on such a geometric shape and value for the WSN simulations here.

The value of the communication range R is established in the literature in such a way that connectivity is ensured, by calculating the node density in networks with a random uniform distribution; R is attributed values of 10m [7, 110], 20m [7, 29],

30m [29], 40m [83, 111], 60m [7], 80m [53], 90m [106, 109], 100m [96], 150m [8], 250m [1, 3, 108]. Because this study investigates stochastic node placements, which are not always uniform, $R = 100$ is chosen similarly to that in [96] and the density of the nodes in the network is varied by modifying the total number of nodes N . In [8], where the considered network is 2000x2000m, $R = 150$ and $N = 900$. Similarly, for a 2000x2000m area, in [107] the network is populated by only $N = 210$ nodes and in [55] by $N = 200$ nodes, while $R = 250$. So for the same area considered here, the references use larger R , but a smaller N , changing the network connectivity.

The number of trials η used in the simulations is also chosen differently for each reference in the literature, having values of 20 [3, 95], 50 [5, 8], 100 [7, 53, 83, 112] and reaching 1000 iterations in [30]. Although a higher number of iterations extends the simulation time, after several trials, it has been decided that $\eta = 1000$ provides the most accurate results for the large scale network case considered here.

Nodes are considered to have been stochastically distributed, having fallen on the lower branches of the trees, at approximately the trunk level, as in [92]. The current work examines the network performance averaging the results over a high number of trials. The study looks at the PDR, the average number of hops per packet for successful transmissions as well as non-successful ones, the delay caused by MAC retrials and the energy spent for repeated channel assessments. Because packet delivery can fail not just when networks are sparse, but also because of the lack of forwarding choices which offer advance to D , we analyse this aspect as well and point out simulation-dependent results.

The network parameters in Table 3.2 and other basic network information (parameters which are varied for the current work) are loaded, the topology is setup and the distribution is plotted. The distances between all nodes are calculated based on the location information made available during network topology setup. The battery

level is set the same for each node, to suffice all packet transmissions. The number of nodes for each network simulation, under all topologies, is increased gradually to obtain better connectivity. Packet forwarding provides advance to D . Each node determines its neighbors based on the SNR and on the received signal power which is calculated considering a realistic channel with log normal shadowing. The simulation makes use of the MAC layer. Nodes within R are considered as potential forwarding options. The forwarding geographic algorithm is based on the assumption that nodes are aware of S and D coordinates and that they can also locate or know the coordinates of the other nodes within R (namely of the neighbours) via the anchor nodes.

The positions of the sources S are random in each trial and each detects SE events and forwards the information to D . The number of S and SE is set so that the network traffic is not high, imitating the real scenario of a forest fire, where multiple sources would detect the spread of the fire in random locations and send the detected parameters several times (as an alarm).

Each time a node wants to send a packet, the node checks whether D is within R . If it is not, the list of neighbour nodes (kept in each node) is tested to blacklist previous hops and to determine which node is closest to D . Figure 3.7a illustrates this process: current forwarding node N , eliminates the source node S from the neighbour list and considers node $F1$ and $F2$ as forwarding possibilities. The distances between the neighbours and the destination D ($d1$ and $d2$) are compared to the distance between current node N and D (d) and $d2$ is found to be the shortest. Therefore node $F2$ will be the next hop with the most progress towards D . The elimination of previous hops from the neighbour list is optional, but it has been implemented here to avoid undesired loops and backward progress - sources of useless energy consumption. (This implies a list with the previous hops is forwarded in the

Simulator parameters (unit)	Symbol	Value
Transmission range (m) [106]	R	100
Transmission power (W) [2]	P_t	600e-3
Distance of reference (m) [92]	d_0	1
Path loss exponent [92]	α	4
Standard deviation for shadowing model (dB) [92]	σ_{sh}	5.6
Sensitivity threshold (dBm) [95]	rv_{th}	-81
Packet size (bits) [95]	p_{size}	1024
Data rate (Kbits/s) [86]	dr	250
Number of packets/source [5]	$pkts$	10
Energy per bit spent on transmission(J/bit) [96]	e_{tx}	2.5e-07
Energy per bit spent for reception (J/bit) [96]	e_{rx}	1.5e-0.7
Initial node energy (J) [95]	E_i	1
Network side length (m) [8, 104, 107]	l	2000
Number of trials [53]	η	100
Number of sensed events [84]	SE	20
Number of nodes	N	441-1200

Table 3.2: Simulation parameters

header of each packet, slightly increasing the packet size.)

Each transmitting node follows the same algorithm as illustrated in the simulation flowchart in Figure 3.7b, which also shows that once the next hop is identified and transmission is attempted, the MAC layer CSMA/CA mechanism comes into play checking if the channel is idle or not before sending a packet. The channel status is determined through clear channel assessment (CCA), as explained in subchapter 3.2.2. The CCA is simulated in a simplistic way by considering that the output of the MATLAB function should be either 1 (idle channel) or 0 (busy channel). The simulation offers two possibilities: to either have random output or to control the probability of the output. A matrix of 100 values of zero and one is used. When the probability of a certain outcome is under the control of the user, the percentage of zeros is prescribed (e.g. for a desired 98% probability of an idle channel, there will be 98 % ones in the matrix and 2 zeroes). In accordance with the the IEEE 802.15.4 un-slotted MAC which has been implemented, when the channel is found busy, the

transmitting node attempts retransmission for 5 times increasing the delay of the packet delivery (as in Table 3.1) [86]. When all the packets have been transmitted and have been either lost or received at D , the route is plotted.

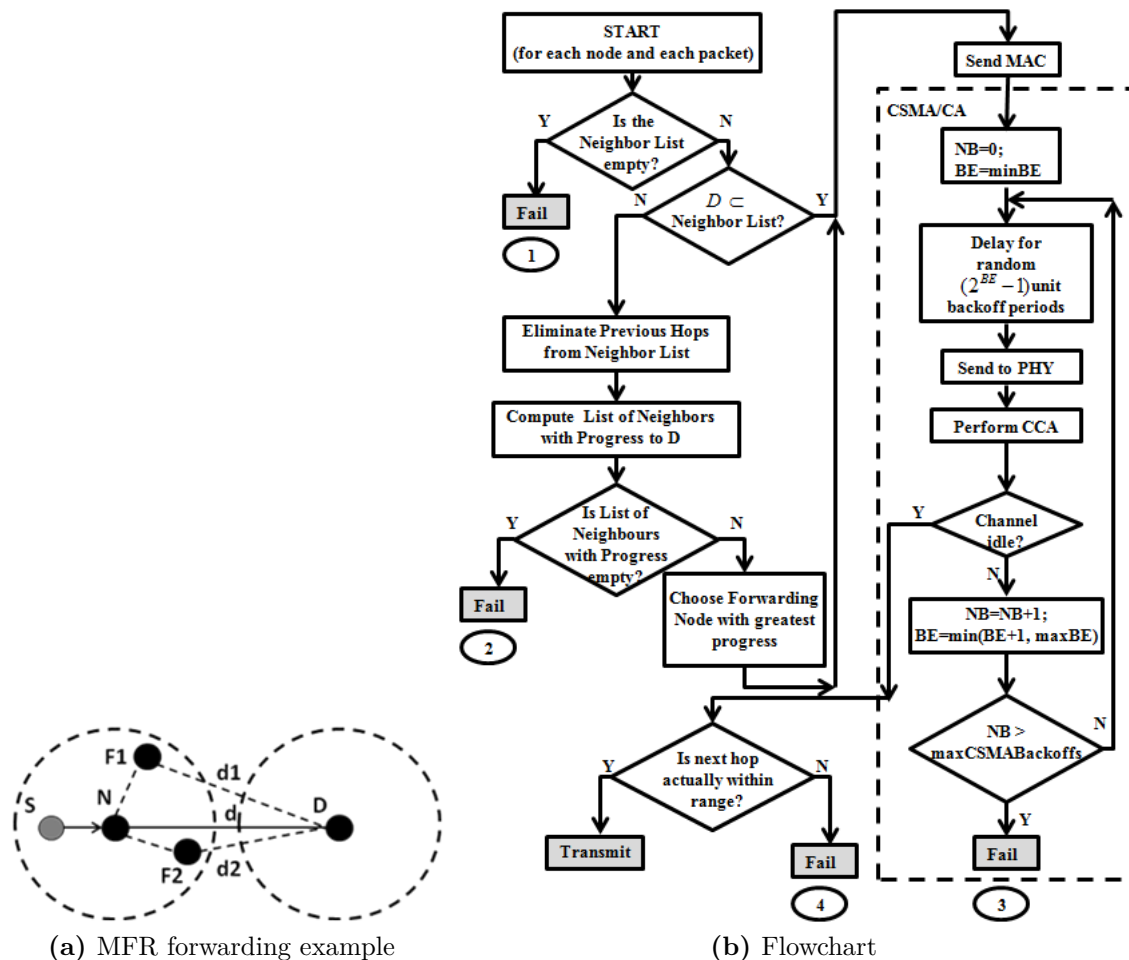


Figure 3.7: Simulated forwarding algorithm

No packet reception acknowledgment is simulated here. Therefore, for any packets sent, if forwarding node $F2$ does not have any forwarding options itself and loses all the packets, the sending node will not be aware of the situation so the information will not reach D . In addition, forwarding to nodes which may lose the packets can result in energy spent uselessly. This power expenditure can be observed by analyzing the number of registered hops for a transmission when the packets do not

reach D .

3.3.3 Simulation results

For the Grid, the number of nodes that covers the established network surface is 441. This is the maximum number which can be used when the grid pace is equal to the R (as in Table 3.2). As a consequence the network with a deterministic uniform node distribution (a Grid) cannot have its size increased, unless the grid pace and R are decreased, so it has not been included in the described comparison. When the network has a grid placement with a complete coverage, accurate localisation information and no assumption of channel noise, the packet forwarding is not negatively affected, having an ideal performance.

Figure 3.8 illustrates the PDR of the network for each random node distribution, as the number of nodes increases. As expected, the networks increase their PDR because of higher node density and better connectivity. The best performance is obtained for the Gaussian distribution whose results are above 90% for all network sizes. The Gaussian distribution is favoured by the presence of D in the centre of the network, where the node density is at its highest. For the other node distributions, D can be isolated at times and the packet delivery may fail more often. This is confirmed by the slope of the second best distribution (StensorX placement), in terms of PDR, is clearly steep, evolving from 40% to nearly 100% with the increase of node density. Surprisingly, the StensorX outperforms the Stensor placement which being more uniform should provide better results. The Stensor distribution also does not reach 100% delivery ratio, for any network size. As anticipated, the Pareto distribution, which covers only a corner of the network, fails to deliver any of the packets due to either lack of connectivity or because most of the neighbour nodes do not offer progress to D as seen in Figure 3.11 and Figure 3.12. For a random

distribution of nodes in the network, the PDR is low, less than 10% of the packets being delivered, even in high density networks.

Although some of these distributions are expected to perform badly (e.g. the Pareto distribution) because of their network coverage, they are still included in this study to illustrate their differences and to show the importance that the node placement has for geographic routing. Having not been investigated previously in the literature and avoiding to consider their potential (if used superimposed) can lead to their avoidance in applications.

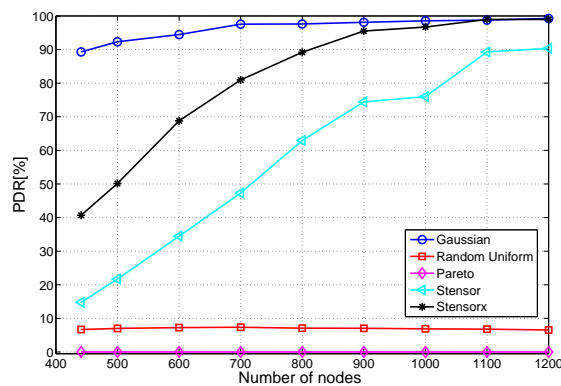


Figure 3.8: Packet delivery ratio

Of course, high PDR implies more energy expenditure, proportional to the network effort made to deliver those packets. However, the energy consumption figures are of concern when energy is spent without results. Such a case is observable when nodes forward packets without these reaching D or when longer routes are used because of the node distribution and density. Figure 3.9 and Figure 3.10 present the number of hops in the routes chosen by the geographic routing for each topology. When analyzing the number of hops in the case of successful deliveries, the Gaussian distribution is the most efficient in terms of PDR and of hops. Its average hop count is almost a constant of 5 hops per packet for all network densities. For StensorX placement, though it provides high PDR, the average number of hops per packet

for successful transmissions is 7, similar to that of the networks where Random Uniform distributions are used. For Stensor Placement, the average number of hops per packet becomes the same only for more than 800 nodes, being the highest in comparison with the rest, 8 hops per packet.

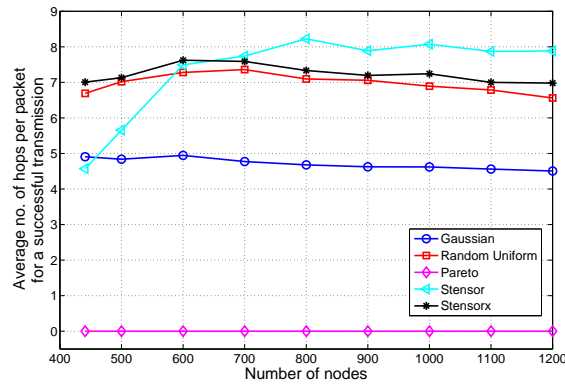


Figure 3.9: Average number of hops/packet for a successful transmission

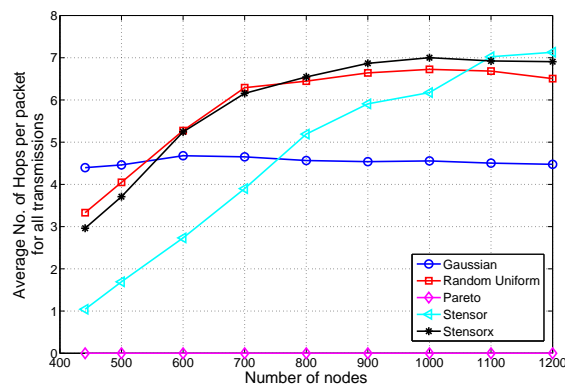


Figure 3.10: Average number of hops/packet for all transmissions

Because of the implementation of the current simulation (without acknowledgment of received packets), where packets are sometimes forwarded even if they do not reach D, the additional spent energy is reflected in the average number of hops per packet when this number is analysed for both successful and non-successful transmissions. Figure 3.10 shows how the less energy efficient distributions are the StensorX and the Random Uniform which route more packets that do not reach D. The average

Flowchart No.	Type of failure	Cause
-	Battery Exhaustion	node power is depleted preventing all communication
1	Connectivity Failure	no neighbors in the R of the transmitting node
2	Progress Failure	forwarding options are further from D than the current transmitting node
-	Partial Progress Failure	no forwarding candidates after neighbour selection is performed and the S and previous hops are eliminated (cause related to avoiding network loops and backward progress)
3	Congestion Failure	high network traffic resulting in the channel being found busy during assessment for the maximum number of allowed retries
4	Location Error Failure	the transmitting node does not know the correct position of its neighbors disregarding forwarding possibilities or attempting to transmit to nodes which are out of its actual range

Table 3.3: Simulated causes for failure

number of hops per packet in these cases increases with network density, varying from 3 to 7. The Gaussian distribution however renders a constant number of hops, just as before.

Failure in packet delivery can be due to five potential reasons, as listed in Table 3.3. The flowchart in Figure 3.7b indicates at which point in the simulation the failures in Table 3.3 could take place.

Power depletion is not possible within the present simulation because nodes are assigned enough energy. Networks analysed here are dense and the failure probability at node level is defined as proportional to the number of sensed events SE in the network. Location Error Failure is not possible here either because we assume all nodes know their exact coordinates. For the following, Figure 3.11 and Figure 3.12 demonstrate how the distributions affect routing failure because of lack of insufficient neighbouring nodes or nodes which do not offer advance to D . When progress

failure is involved, we can imply that routing holes are encountered and that a recovery algorithm for geographic routing can increase the PDR. However, a recovery method has not been simulated because of the aim to study pure geographic routing performance for different distributions. Nonetheless, progress failure decreases with density when forwarding choices increase and is at its highest and almost constant for Pareto due to the shape of this distribution. Partial progress failure for the Pareto distribution has a random shape due to the fact that this network topology can be obtained by projectile distribution, where the random factor makes nodes ‘fall’ closer or further away from the centered D resulting in a varying failure rate.

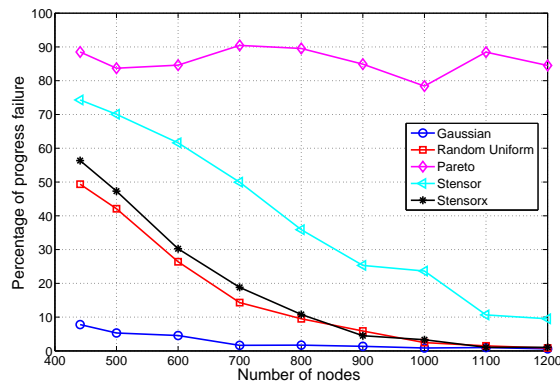


Figure 3.11: Progress failure

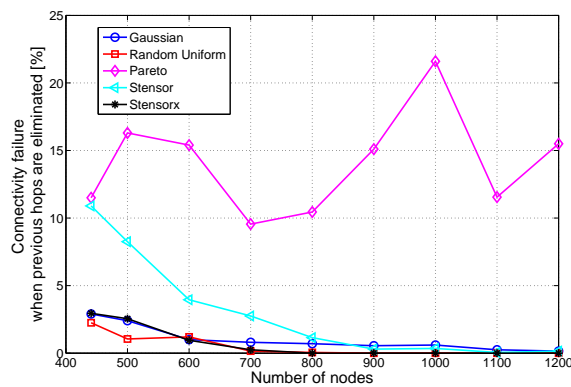


Figure 3.12: Partial progress failure

Though the failure rate is not affected by congestion in these cases, energy expen-

diture is influenced by it and this aspect can be analysed at MAC level. Every time the channel is detected busy because of high traffic, nodes delay the transmission increasing the delay per packet. Assessing the channel results in energy expenditure. Figure 3.13 presents the energy expenses on CCA for each distribution and Figure 3.14 presents the delay at MAC. The consumed power increases proportionally with the density of the networks. Random Uniform and StensorX placements have the highest energy consumption and delay. The Stensor placement resulted in less energy consumption and delay at MAC for networks smaller than 800 nodes. For denser networks this distribution suffers an increase resulting in higher figures than for the StensorX and Random Uniform networks. The Gaussian distribution has however, almost the lowest rates for both delay and power consumption at MAC. However, the Gaussian energy consumption and delay is motivated by the PDR.

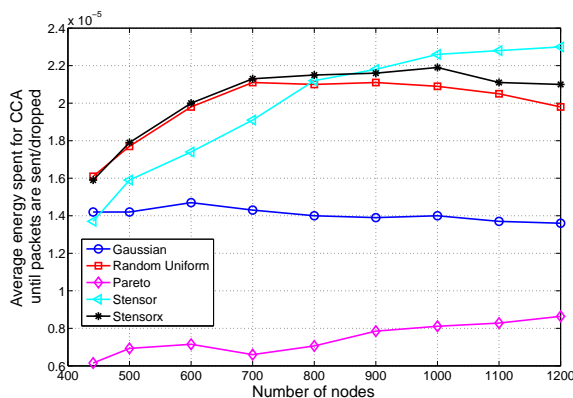


Figure 3.13: Average energy spent for clear channel assessment

A comparison of these random distributions when D is placed in the upper right corner of the network has also been included in the investigation. Placing D in the center of the network favours Gaussian placement and it is not the only possible sink position in a forest fire prevention application. Figure 3.15 illustrates the PDR of the different networks while using the parameters as in Table 3.2. As predicted, the Gaussian and Pareto networks are not functional and the PDR is next to zero

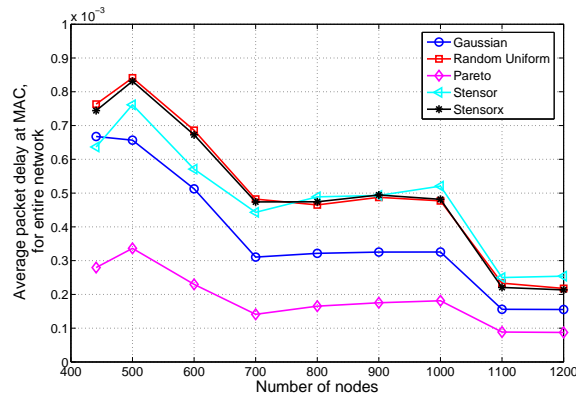


Figure 3.14: Average packet delay at MAC

because D is basically isolated and the networks are disconnected. The Uniform Random, the Stensor and StensorX networks perform similarly having an improved performance with the increase in density. The Stensor networks perform best in lower density and the StensorX and Uniform have a similar, better performance in denser networks, reaching 90% PDR in the denser cases. The reason why 100% PDR is not reached even for the highest of node densities is because D is isolated in more than 10% of the cases.

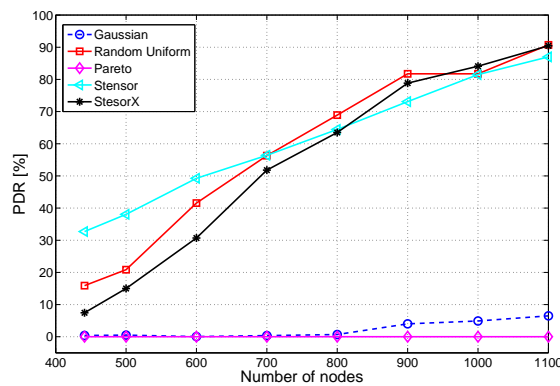


Figure 3.15: Packet delivery ratio with D placed in the upper, right corner

Energy consumption varies for sensor networks of the same size and for simulations with the same parameters, depending on the distribution of the nodes. From the above simulations, we can conclude that for a fire prevention application over a large

forest area, with a centered destination D and geographic routing at the network layer, it is recommended to place the nodes according to the Gaussian distribution. This is the most successful in terms of throughput and energy consumption as it offers highest PDR with the least number of hops per packet as well as the least amount of delay and energy consumption at MAC level. However, if D is not centrally placed, the networks with Gaussian distribution of nodes may not lead to the same positive results.

With D placed differently other node placements such as StensorX and Stensor can have a better performance. The differences between Stensor and StensorX are marginal. The Random placement, though similar in terms of hop count and MAC performance with the Stensor Placement, is certainly not as successful in terms of PDR. The Pareto distribution is also not recommended for this application unless the nodes are projected from multiple corners of the network, providing better coverage.

For a fire prevention application, high PDR is critical. If information about fires does not reach the destination, this can have serious consequences. Considering the study of this large scale application has a clarification objective, useful in the research of geographic routing behaviour, where it is imperative to choose a specific node distribution and destination placement. It provides an indication of what to expect in terms of performance of the same forwarding algorithm, when the network conditions are changed. It also raises awareness about other network factors which can influence the routing behaviour, such as the location knowledge nodes actually have about their neighbours and the accuracy of the employed positioning system. The localisation aspect is presented in subchapter 3.4 and thoroughly explored in the following chapters of this thesis.

3.4 Localisation

Localisation is necessary for sensor networks and it can be used for various purposes such as event reporting, data centric storage and naming schemes [1]. However, localisation's most important use is considered to be in routing schemes because inaccurate position knowledge of sensor nodes affects the forwarding process. For dense networks, even small inaccuracies can lead to premature packet loss, choices of non-optimal routing paths or routing loops. All these result in unnecessary energy expenditure and reduced network life-time. Accurate localisation is therefore essential in position-based routing. According to the position knowledge, sensor nodes can be divided into two categories: anchors (or beacon nodes) and targets (or blind-folded nodes). Anchor positions are usually known with accuracy (either through GPS or installation measurements). GPS use is however economically unjustifiable for each node in a large or inaccessible network. The coordinates of target nodes are estimated using localisation algorithms, the absolute positions of the anchors and inter-sensor node range measurements, as described in subchapter 3.4.1. Location discovery algorithms present advantages and disadvantages as well depending on the adopted measurement techniques. Furthermore, in mobile networks, dynamic nodes using beaconing can introduce inaccuracies and offer an inconsistent view of the positions. The location dissemination services sometimes used to aid in geographic routing, such as the Grid Location Service (GLS) [74], can further affect the network performance.

3.4.1 Measurement techniques

Measurement techniques can be classified as based on angle, distance or RSS profiling techniques [28]. They are briefly presented in the following paragraphs.

1. Angle-of-arrival (AOA): It is a technique which aims to determine the direction of a radio wave incident on an antenna array, by measuring the time difference of arrival (the delay) of the radio wave at individual elements of the antenna array.

a. Using the receiver antenna's amplitude response. This technique uses beamforming, meaning the anisotropy in the reception pattern of an antenna. When transmitted signal strength varies, the receiver cannot detect this due to varying amplitude of the signal and due to anisotropy – the solution: the use of a second non-rotating omnidirectional antenna or the use of 2-4 stationary antennas with known anisotropic patterns.

b. Using receiver antenna's phase response. The technique derives the results from the measurement of the phase differences in the arrival of a wave front and requires a large receiver antenna or an antenna array. The drawbacks are the limited accuracy because of direction, shadowing and multipath reflections.

2. Distance related measurements: (inherently noisy)

a. Time of arrival measurements (ToA). It is a time-based ranging system which utilizes the propagation delay in the transmitted signal to estimate the distance. It can be classified into two techniques based on the number of transmitted packets for distance estimation:

- **One-way propagation time of arrival measurements (OW-ToA)** refer to the difference between the sending time of a signal at the transmitter and the receiving time of the signal at the receiver. The drawbacks are the following: the method requires highly synchronized local clocks between the nodes and it is not favoured by WSNs as the demand for highly accurate clocks increases the complexity and cost of the sensor nodes.

- **Two way (Roundtrip) propagation time of arrival measurements (TW-**

ToA) refer to the difference between the time when a signal is sent by a sensor and the time when the signal returned by a second sensor is received at the original sensor. The method requires the nodes to exchange two packets for distance estimation and eliminates the requirement of clock synchronization between the nodes. Location estimation accuracy is exceedingly dependent on the distance measurement accuracy, which can be corrupted by additive white gaussian noise (AWGN), multipath propagation, direct path excess delay, non-line of sight propagation error, multiple access interference, clock drift and clock offset. The method also implies a specific CCA delay. In this thesis, TW-ToA will be used because it does not require a sophisticated synchronization mechanism.

b. Lighthouse approach. It derives the distance between an optical receiver and a transmitter of a parallel rotating optical beam by measuring the duration that the receiver dwells in the beam. The drawback is that this requires line-of-sight between receiver and transmitter.

c. Time difference of arrival (TDOA). It uses measurements of the transmitter's signal at a number of receivers with known locations to estimate the transmitter position. The drawbacks are the cost associated with the data exchange as well as the need for very accurate synchronization among receivers.

d. Received signal strength (RSS) measurements. The method is based on the emission at the transmitter side of a signal using fixed reference power known to the receiver while the receiver measures the power of the received signal and derives the distance from the calculated attenuation. The RSS is a straightforward, inexpensive technique with no requirement for additional hardware [28]. However, signal strength depends on the channel behaviour. Thus an accurate propagation model is necessary for simulation. In real-world conditions, while measuring the RSS, there are two main sources of error: multipath, due to reflection and scattering in

non-line of sight environments, and shadowing errors, as a result of signal attenuation due to environmental hindrance. Thus, because the RSS technique is sensitive to environmental changes, it offers more accurate estimates over shorter distances.

3. RSS profiling techniques

They refer to constructing a form of map of the signal strength behaviour in the coverage area. This can be done a priori or online by using sniffing devices with known locations. The map is stored in a central location and used by target nodes to estimate locations using the RSS measurements from anchor nodes.

3.4.2 Modelling location errors

In order to properly use the WSN simulator developed for the current research, its design has to consider error sources, error propagation and their impact on the routing. Most existing routing protocols assume accurate location information and do not study the effects of localisation errors on the forwarding algorithms. However, because of its vital necessity for accurate position information, research has also been aimed at investigating the impact of inaccurate ranging measurements on various position based algorithms.

3.4.2.1 Previous work

[1] presents a theoretical model of how location inaccuracy and inconsistency affect routing. Four metrics are provided for quantization and analysis of greedy routing and recovery procedures: absolute location accuracy, relative distance accuracy, absolute location inconsistency and relative distance inconsistency. However, these metrics are not considered in the literature further. Early work researching geographic routing considered it equivalent to greedy forwarding over geographic

coordinates. However greedy forwarding fails when reaching a local minimum. As a consequence, further studies analysed algorithms with two components: greedy and perimeter/face forwarding. The effect of localisation errors on geographic routing was first studied for both components in [30], for the Greedy Perimeter Stateless Routing (GPSR) protocol. Results showed noticeable impact of location inaccuracy on perimeter forwarding. While [30] was pointing out that errors of only 10% of the considered communication range have severe effects, a simulation study performed the same year in [113], but without referring to geographic routing, concluded that location error was tolerable for only 40% of R . However, the error model used in early studies [30, 110] was considered to be uniform random, having the error uniformly distributed within a certain range - a less realistic approach. In addition, [110] considered static stable networks with an ideal wireless environment, without the intervention of a MAC layer.

A number of other authors investigated the impact of location errors on geographic routing in the following years in [3, 29, 114], all of which reconsidered the error model. By following the example of [7], the authors of [3, 114] considered the error distribution to be two dimensional Gaussian and even exponential in [114]. The behavior of basic greedy routing and flooding is analysed through simulations in [110], for a less realistic network model and without considering a MAC layer, the possibility of collision or of interference. However [110] included the use of second order neighbourhood information and the existence of obstacles in conjunction with location errors. In [3] a new algorithm, robust to location errors, is proposed based on the investigation of the Most Forward within Range (MFR) algorithm. In addition, [3] also considered imperfect transmission ranges. The findings of both [110] and [3] reflect the substantial degradation of routing performance in terms of transmission failure and backward progress, for both static and mobile networks.

In [29] a new approach on the subject is taken with a direct investigation of geographic routing performance as a function of the number of anchor nodes used for localisation, of the noise level in the network and the radio range. The issue of how to make geographic routing more resilient to location errors has been tackled by [3, 7, 29, 85, 111, 114–116]. In [3] a strategy called Maximum Expectation within transmission Range (MER) is proposed. The work incorporates location errors in the developed objective function by considering the error probability when making routing decisions. In [116] not just localisation inaccuracy is considered, but also realistic link reliability. In [111, 115] the focus is on the resilience of the ALBA-R protocol, claimed to be completely robust to location errors due to a connectivity related mechanism, while in [114], GPSR and BGR are studied and fixes are proposed. In [117] IEEE 802.15.4 networks with large scale location errors and unstable communication links are considered. [117] proposes a location estimation and dynamic link detection scheme for geographic routing in NLOS environments which, although successful, consumes a lot of energy.

[29] is the only work investigating geographic routing performance as a function of the number of anchor nodes used for localisation, of the network noise level and of R. Although the study mentions the localisation process and recognizes that different error characteristics introduced by this, no details are given about the assumed type of localisation. Moreover, the emphasis is only on PDR. In [110] there is a brief analysis of the average power consumption per node when the location error is varied, but little insight is provided into how different methods of localisation affect geographic routing. The subject of energy efficiency in the presence of location errors is further studied in [7]. Behavioural information is given about a selected number of power efficient algorithms by comparatively analyzing their energy consumption with accurate and imperfect location information. A solution is provided through

the Least Expected Distance (LED) algorithm in [7], which aims to preserve the power saving features of basic geographic routing while coping with location errors. Although valuable through the assumption of a variable transmission power and thus of R and of a Gaussian error model, the work gives no attention to the energy impact of various localisation methods or of the MAC layer.

3.4.2.2 Location Error Model

In the initial stages of this research the positions of the nodes are known with accuracy. As the simulations become more realistic, the existence of location errors is assumed. The initial simplifying assumption is that all nodes in the network know their measured position and that of their neighbours. Their location errors are independent and follow a two-dimensional Gaussian distribution $N(\mu, \sigma^2)$, with the probability function:

$$f(x) = \left(\frac{1}{\sqrt{2\pi\sigma^2}} \right) \exp \left(-\frac{(x - \mu)^2}{2\sigma^2} \right), \quad (3.4)$$

where μ is the mean (and it is zero) and σ^2 is the variance. Instead of presuming that a node's position can be localised with equal probability within a circular disk of range R , centered at the actual coordinates, as in [24, 110], the considerations are that the estimated coordinates will have a higher probability of being near the actual coordinates and a lower probability to be further away [3, 29, 114]. Assuming the real coordinates known, the Gaussian errors are introduced with a zero mean μ and finite standard deviation σ .

Previous work with a uniform random error model specifies the location error as a percentage of the node radio range [24, 110]. When errors are considered normally distributed, σ is set within a range, upper limited by a percentage of the sensor

radio range R [3, 114]. For comparison purposes, the present work also considers σ as correlated to the value of R and it is varied as a percentage of it. As the error model is Gaussian, the error itself can vary between $(-3\sigma, 3\sigma)$ which for $R = 100\text{m}$ is equal to a range of $(-90\text{m}, 90\text{m})$. In [24] the error is varied between $(0, 80\text{m})$, in [114] it is set in the interval of $(0, 120\text{m})$ and in [3] $\sigma = 40\%$ of R and is in the range of $(3\text{m}, 50\text{m})$.

3.5 Conclusions

Geographic routing performance can be affected by many application- and environment-dependent factors and, while some can be managed deterministically, the ones which are random in nature require statistical modelling. Chapter 3 has shown how simple assumptions about network topology or destination placement can make a massive difference in the PDR of the same routing algorithm. Because the outcome of WSN simulations is severely influenced by the assumptions one makes when designing the network, it is important to establish which node distribution and destination position would lead to less biased results for the further analysis of geographic routing. It has been concluded that an assumption of a Random Uniform node distribution (with the destination in the corner of the covered area) is the most suitable for the network simulations in the next chapters. This decision is based on the degree of randomness of the distribution which can be considered as a “worst case scenario” and on the fact that it is also one of the most popular choices in the literature [96, 99, 100, 102, 118]. Another contribution of this chapter is that it gives a measure of the impact apparently insignificant assumptions can have on the routing component. It not only shows the differences in routing performance in slightly different circumstances, but it directs the attention to other issues, such as the actual

position knowledge nodes have about themselves and their neighbours. This is why subchapter 3.4 is focused on presenting localisation methods employed in WSNs and on the localisation accuracy assumptions made in the literature when designing geographic routing algorithms.

So an efficient geographic routing algorithm will successfully transmit data based on how well random network events are modelled and managed. The aim is to obtain good network results even with insufficient node density, random node placement, noisy environments, limited node power or inaccurate localisation. Unfortunately, existing forwarding protocols use theoretical simplifying assumptions, which impact the routing performance in simulations and real life implementations to such an extent that geographic routing has been avoided in practical applications. To improve the algorithmic behaviour or propose other solutions, it is first necessary to further analyse and measure the effects of another unrealistic assumption, that of accurate location information. Thus, the following chapter will study the impact of inaccurate positioning knowledge on geographic routing when coordinates are known both with accuracy as well as in error. Evaluations will be made for both a normally distributed location error as well as for errors resulted from the simulation of the positioning process.

4 Efficient geographic routing in the presence of location errors

This chapter presents the problem of efficient geographic routing in terms of throughput and energy consumption in realistic conditions of inaccurate localisation. The routing performance is analysed when the localisation is both simplistically (subchapter 4.1) and realistically simulated (subchapter 4.2).

Because positioning systems are inevitably imprecise due to inexact measurements and location errors lead to poor performance of geographic routing in terms of PDR, this is the aspect predominantly studied in the literature [3, 30, 110, 114]. Little attention has been given to the effect erroneous localisation has on power consumption [7, 110]. The importance of an adequate throughput is not neglected, so the PDR is analysed as a confirmation of the results previously obtained by [3, 30, 110, 114]. However, if the network is not energy efficient there can be severe consequences: the power depletion of key nodes, isolation of certain network areas, failure to deliver packets, slow network reaction and reduced lifetime. It is therefore considered necessary to study the energy consumption in WSNs which make use of geographic routing by investigating scenarios that incorporate localisation inaccuracies.

4.1 Routing performance with a normally distributed position error

As detailed in subchapter 3.4.2, although previous work predominantly assumes a simplistic random uniform error model such as [30, 110], the present investigation considers a normally distributed position error, as more recently done in [3, 7, 29, 85, 114, 119]. The routing behavior is evaluated using the MATLAB simulator described in subchapter 3.2.2, but assuming that nodes can be localised with error, the standard deviation σ of position error is considered between 10-30 % of R . The considered values are chosen based on the observation made in [30], that a σ of more than 10% of R would already be problematic for the PDR. It is found that when there is location error, more energy consumption is spent for the lost packets because of increased loss numbers, while the received packets have increased energy expense due to the length of the routes. Also, investigations shed light on the causes of packet failures and the amount of consequent energy consumption due to them. It is concluded that resilience to location error is imperative, but attention to node placement is also necessary.

4.1.1 Simulation setup

The simulation results present the total energy consumption per network as well as the energy spent on both successful and unsuccessful transmissions in relation to the average number of hops of their routes. Because failure can occur due to multiple causes: connectivity loss, lack of neighbours which offer advance towards D , location error and traffic congestion, the analysis reveals the percentage of failures and the average energy consumption per network due to each cause. To offer more insight an investigation of the route length of packets lost due to location error is also provided.

Findings show that an assumption of correct location leads to an unrealistic view of geographic routing behaviour. In comparison with networks with accurate location information, energy expenditure is higher for both failed transmissions, which are more numerous, as well as for successful ones, which have longer routes. Energy consumption is high even if node density is increased. Failure percentages indicate that connectivity loss is related to network density as well as node placement.

The simulation uses a static network scenario and the parameter values are specified in Table 4.1. It is assumed that the nodes are randomly and uniformly distributed, as in [29, 30, 110, 114, 116] and considered that each time a sensor node measures a parameter and wants to transmit the information to a destination D , an event takes place in the network. The number of sensed events SE [120] and the positions of the sources S are random in each trial [5] and D is placed in the right upper corner of the network as in [114]. As previously, the failure probability at node level is proportional to SE . The simulation includes the use of the MAC layer.

The network size is now smaller than in chapter 3, to improve the time of the simulations, but it is still appropriately chosen for a network of large scale. The number of nodes N is chosen in relation to the range R , to provide sufficient connectivity; the increase in node density is analysed in Table 4.2. Network density is discussed in several references: in [83] the density is varied between 25 to 200 nodes/range, in [8] the considered mean neighbour density is 15, in [106] the density is varied between 6 to 20 nodes per neighbour, in [30] it is varied between 5 to 20 nodes per range, and in [5] it is decreased even further being varied between 4.7 to 8.8 neighbours per node. The density here is varied in a similar way as in [5] which has a more realistic approach being dedicated to practical geographic routing.

Network performance is examined for different network sizes. The network surface is kept constant, while the node density (calculated as number of in-range neigh-

Simulator parameters (unit)	Symbol	Value
Transmission range (m) [96, 121]	R	100
Transmission power (W) [110]	P_t	1.778
Distance of reference (m) [92]	d_0	1
Path loss exponent [92]	α	4
Standard deviation for shadowing model (dB) [92]	σ_{sh}	5.6
Sensitivity threshold (dBm) [122]	rv_{th}	-95
Packet size (bits) [95]	p_{size}	1024
Data rate (Kbits/s) [86]	dr	250
Number of packets/source [5]	p_{kts}	10
Energy per bit spent on transmission (J/bit) [96]	e_{tx}	2.5e-07
Energy per bit spent for reception (J/bit) [96]	e_{rx}	1.5e-0.7
Initial node energy (J) [95]	E_i	1
Network side length (m) [19, 121, 123]	l	400
Number of trials [124]	η	300
Number of sensed events [120]	SE	15
Number of nodes	N	20-65
Standard Deviation of location errors (m) [30]	σ	0-30

Table 4.1: Simulation parameters

bours per node) is gradually increased. Network routing is achieved with the MFR forwarding algorithm, explained in subchapter 3.3. Each simulation (trial) consists in generating the following:

- a network with accurate location information and
- 5 networks for which the position information is inaccurate and whose location error is varied.

The process is repeated for each network size and results are averaged. To be able to calculate the network density, it is computed for each trial at a time and then the results are averaged over η , as in Table 4.2.

Nodes	20	25	30	35	40	45	50	55	60	65
Density	2.7	3.5	4.4	5.1	5.8	6.6	7.4	8.2	9.0	9.8

Table 4.2: Network density (neighbours/node)

4.1.2 Simulation results

PDR and hop count analysis

The PDR of the simulated networks is shown in Figure 4.1. As expected, routing performance improves when the number of nodes and connectivity increase. When $\sigma = 0$ (i.e. there is no error in the location information) the routing algorithm leads to the highest results. However, as location information degrades, network performance changes dramatically. For $\sigma = 10$, the PDR is less than 50%, while for larger values, the network PDR decreases reaching just 13% for the highest density tested here.

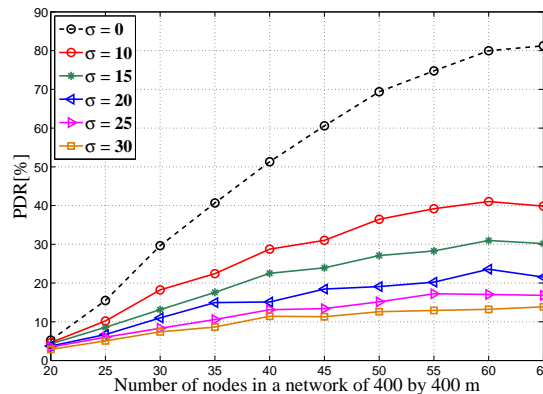


Figure 4.1: Packet delivery ratio (Gaussian location error)

As it can be seen in Figure 4.2, the higher the PDR, the more energy is consumed by the network. When analysing energy consumption, it is found that for $\sigma > 0$ power consumption values are unsatisfactory for both received and lost packets. Figure 4.3 presents the energy consumed to route the same delivered packets over networks with different positioning accuracy. It is reduced for the network with $\sigma = 0$ in comparison with other networks because of the path length of the successful packets. The results in Figure 4.2 are not contradicted by Figure 4.3 because the surplus of energy consumed for $\sigma = 0$ results from a higher PDR.

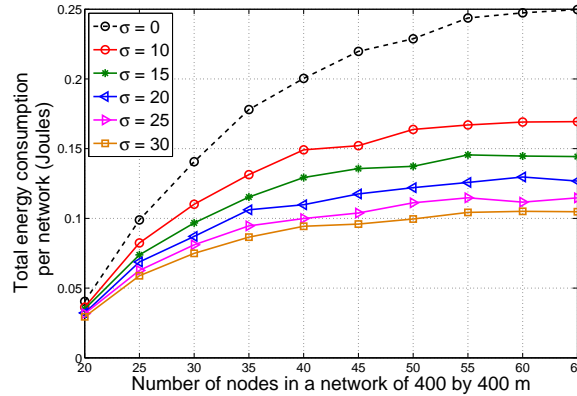


Figure 4.2: The total energy consumed in the network

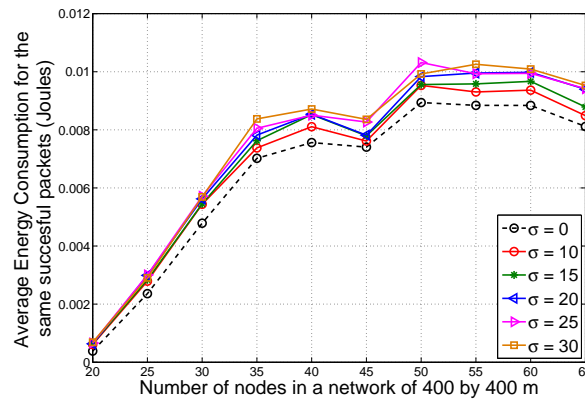


Figure 4.3: Average energy consumption for successful transmissions

Figure 4.4 displays the number of hops per successful packet, when the same packet is received in all the networks (with or without error); the networks with $\sigma = 0$ have the fewest hops. As the location error increases, so do the lengths of the routes taken. Because of the relatively high R in comparison with the network size, the routes do not have a very high number of hops. As a result, the difference in route length between the networks is not big, but exists nonetheless.

However, for $\sigma > 0$ the successful transmissions are not the only cause of energy expenditure. Figure 4.5 shows that energy spent routing packets which are eventually lost is greater when networks suffer from location error, but only for networks with a density higher than 5 (with $N \geq 35$ nodes and a $PDR = 50\%$).

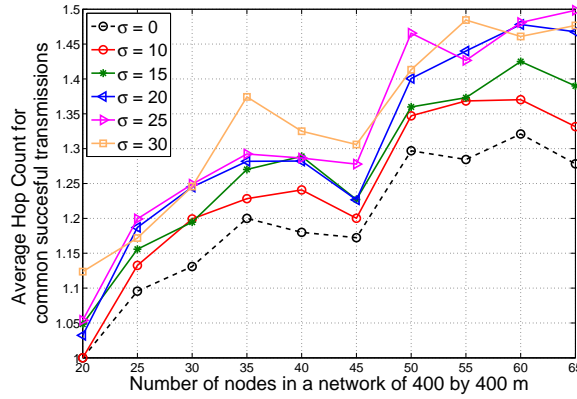


Figure 4.4: Average number of hops per received packet

For any σ , the energy spent on lost packets is very little in low density networks, due to a lack of connectivity. The packets are lost by the S or close to it, without travelling in the network and without consuming extra energy. As density increases, the routing algorithm finds routing alternatives, so the failed attempts consume more energy. After reaching a density threshold, the energy spent on failures decreases quickly as fewer packets are lost. For the other networks, the amount of energy spent on failed transmissions is low when connectivity is poor, but increases and remains constant when node density is high. Although good connectivity ensures more routing alternatives, most failures are due to location errors.

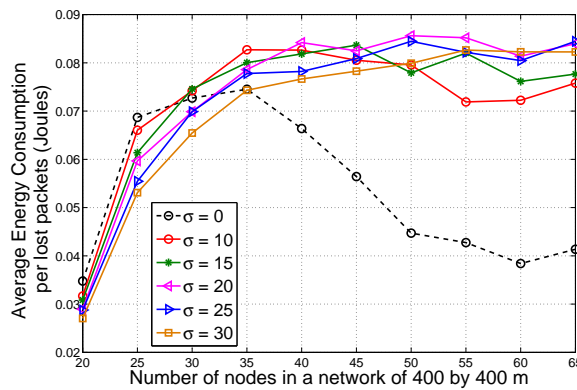


Figure 4.5: Average energy consumption for all lost packets

The same density threshold makes itself noticed in Figure 4.6, for $\sigma > 0$, as the num-

ber of hops remains relatively constant, leading to the constant energy consumption from Figure 4.5. Even with an increase in node density, the routes are shorter for a higher σ and longer for $\sigma = 0$ because failures occur “faster” (near S) in the first case and “slower” (further away from S) in the accurate location case.

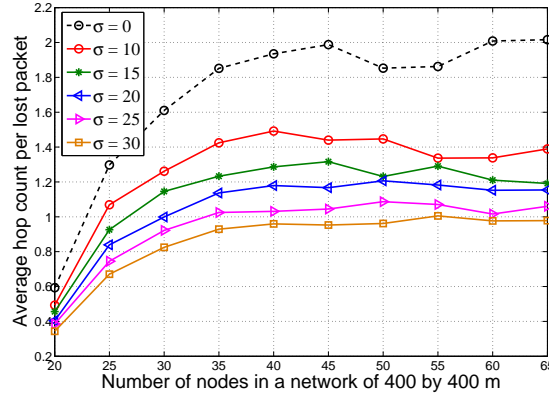


Figure 4.6: Average hop count per lost packet

Figure 4.7 is relevant for packets lost strictly because of location error. The number of hops for these packets increases proportionally with node density. This shows that, due to location error, packets travel in the network more, taking longer routes until they are finally lost. It is also observable that failure also occurs closer to S for larger σ resulting in a smaller number of hops for bigger σ . As failure due to location error is not possible when $\sigma = 0$ the number of hops is zero and the corresponding curve can be ignored.

Sources of packet failure and their quantification

Energy consumption values are of concern when energy is spent without a successful delivery. Packet delivery failure can take place for various reasons as listed in Table 3.3, but the battery exhaustion option is not considered here. Also, the connectivity failure is now re-defined using the Partial Progress Failure definition.

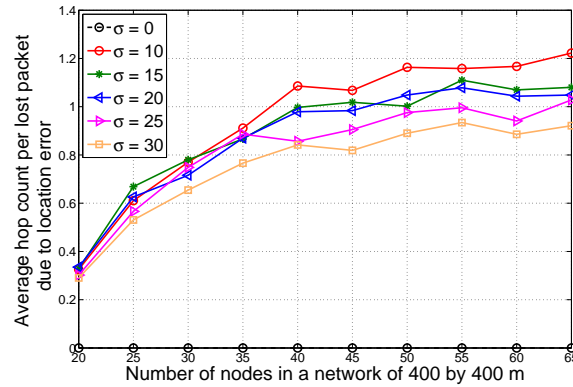


Figure 4.7: Average hop count per lost packet (cause: location error)

Therefore, a failure due to connectivity takes place when there are no neighbours, except S or previous hops of the same packet, which are not considered because of the possibility of backward progress and routing loops. With progress failure it can be implied that routing voids are encountered and a recovery method could increase the PDR. However, a recovery option has not been included in the simulation because of the aim to study the behavior of basic geographic routing, greedily forwarding packets.

Figure 4.8 confirms the previous explanations related to the average energy consumption per lost packet. The percentage of failures which occur due to location error is higher with the increase of σ . The rising shape of the curves when density increases might seem unexpected as one is tempted to believe that more routing options should lead to less failure (as illustrated by Figure 4.1), but the curves represent the percentage of failures out of the total number of failures, not out of the overall number of transmissions. This means that from the number of the failures that occur in the networks with $\sigma > 0$ there are increasingly more due to location error. Figure 4.9, Figure 4.10 and Figure 4.11 confirm this through their complementary decreasing slopes.

For the networks with $\sigma = 0$, the failure percentages are divided between connectiv-

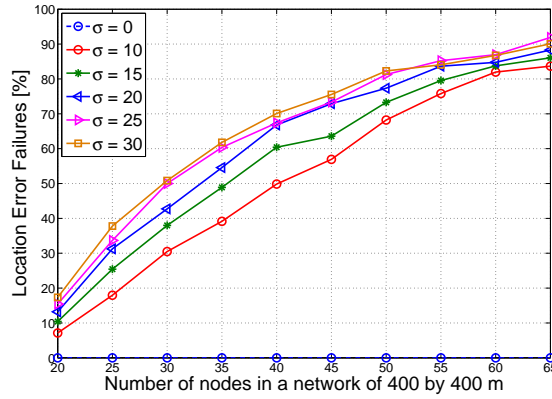


Figure 4.8: Percentage of failures due to location error

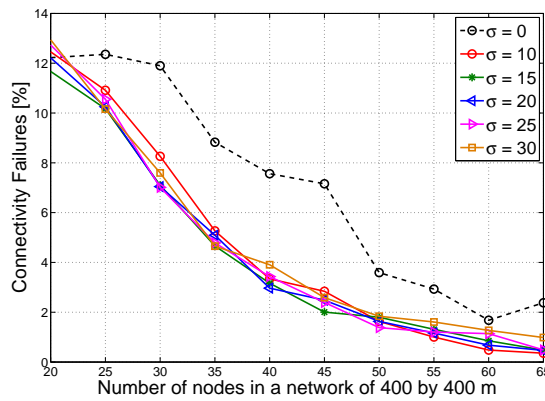


Figure 4.9: Percentage of failures due to connectivity failures

ity, progress and congestion, but the greatest percentage belongs to progress failure for lower densities and to congestion failures for higher ones. For all 3 causes, the values when $\sigma > 0$ are surpassed by values of $\sigma = 0$ because most of the failures in those networks take place due to location error. As expected, all types of failures decrease when connectivity is improved through a higher number of nodes.

Energy consumption analysis

The energy consumption is studied here based on the simulation output, as described in subchapter 3.2.2. For each failure cause, the energy spent in the network up to

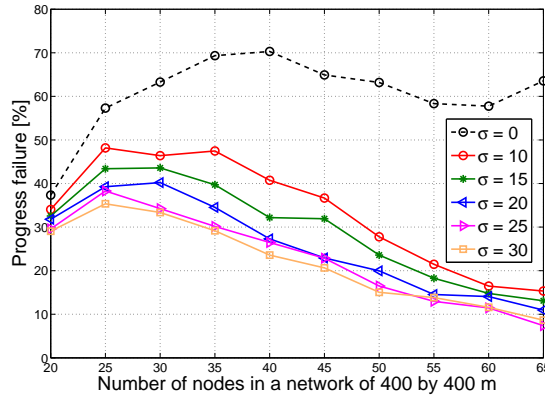


Figure 4.10: Percentage of failures due to progress failure

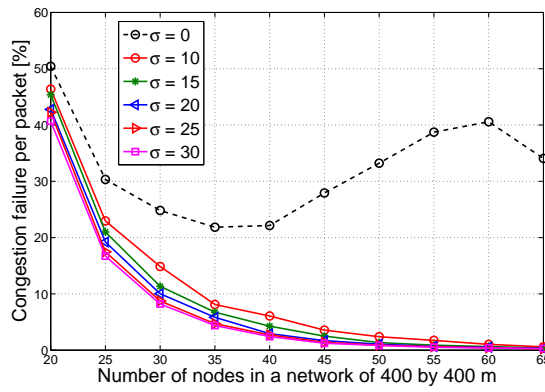


Figure 4.11: Percentage of failures due to congestion

the point until the packets are lost is recorded. The information is averaged over the number of trials in which that particular type of failure occurred. If a trial does not have a particular type of failure, it is not considered for averaging. The values in the graphs are obtained by considering that each node spends energy on channel assessment, transmission to and reception from other nodes. For each operation the energy is added and recorded for each packet and at each node. The simulation performs calculations and averaging.

For $\sigma > 0$, energy expenditure has the highest values for failures due to location errors (see Figure 4.12). In this case, the energy consumption for the lost packets depends on two factors, as previously shown: number of lost packets and number of

hops until they are lost. Figure 4.12 shows that for higher σ there is more energy consumed and this is mostly due to the number of lost packets, not due to the route length (as shown previously in Figure 4.7, the routes are shorter when σ is high so less energy should be spent on them). In regard to density, the networks consume more energy when there are more forwarding options because of longer routes, while for sparse cases, they spend less, failing early.

For all networks, the power lost on routing, when failure is caused by loss of connectivity (as defined here), is random in nature reflecting the randomness of the moment when network connectivity failure occurs (see Figure 4.13). While fewer failures take place when the network density increases, the moment at which nodes detect the lack of forwarding options seems random in nature, most likely depending on the node placement.

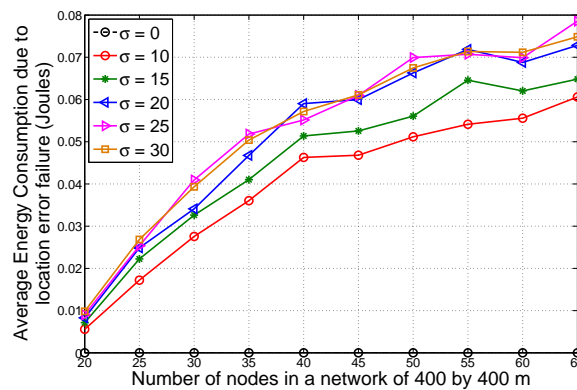


Figure 4.12: Average energy consumption per network due to location error failure

Failures due to lack of neighbours with progress take place more often for networks with $\sigma = 0$ than for the ones with $\sigma > 0$, but energy consumption is at its lowest for them (see Figure 4.14). The explanation is that the LR is at its lowest for $\sigma = 0$.

Because of this particular reason, the networks with correct node coordinates are not really comparable in terms of energy consumption with the networks with inaccurate

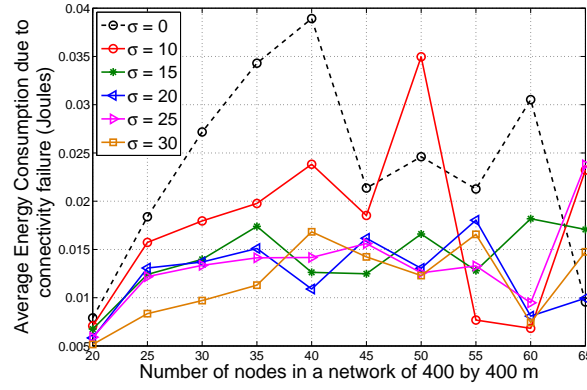


Figure 4.13: Average energy consumption per network due to connectivity failure

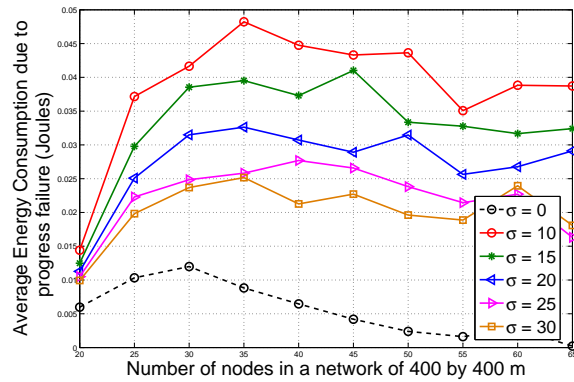


Figure 4.14: Average energy consumption per network due to progress failure

localisation. Nevertheless, they are useful in observing the tendencies. For $\sigma > 0$, when more failures take place because of no neighbours with progress to D , it is observable that the energy consumption is inversely proportional to σ . This also proves that progress failures take place closer to S as σ is increased (as in Figure 4.6 and Figure 4.7). The energy consumption is rather constant for all densities higher than 5, but under this value, it is very low showing abrupt packet loss.

When analysing the energy spent due to failures because of congestion (see Figure 4.15), it is necessary to keep in mind that the probability of congestion in the current simulation is constant for all network densities. Although the percentage of congestion failures decreases for all networks with the increase of node density (because of an

increase in PDR), the values of the energy consumption are high for lower densities because of the number of hops the packets go through before they are dropped (due to the detection of a busy channel).

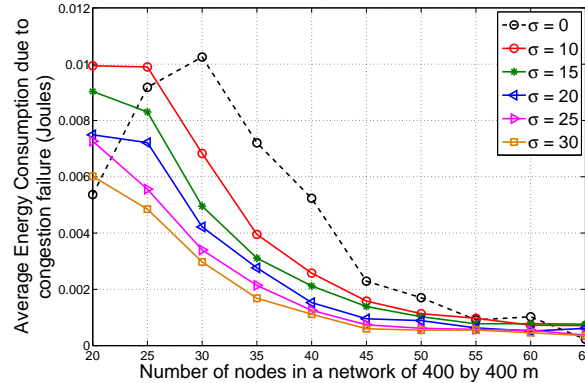


Figure 4.15: Average energy consumption per network due to congestion failure

For higher σ , the number of hops per lost packet has been determined to be lower and thus the energy consumption is lower. For $\sigma = 0$, the energy values are lower than for the rest of the networks up until the number of nodes per network is 30. The explanation is the same as for Figure 4.5: the percentage of failures due to congestion though higher than for $\sigma > 0$ (see Figure 4.11), take place at S or near it, leading to less power consumption. For all the rest of the $\sigma = 0$ networks with more than 30 nodes, the higher the density, the more forwarding options there are, the fewer the failures and the more constant the number of hops per lost packet.

The performance of geographic routing (without a recovery method for network voids) is considerably influenced by location error. Networks with location error above 10% are seriously affected in terms of PDR which is below 50%, even for the highest node density considered here. The percentage of packets that are lost in networks with location error is higher than the percentage of lost packets due to other causes. Also, the energy consumption figures regarding all received and lost packets alike is not satisfactory for the networks with poor location information in

comparison with the case of accurate location information.

While networks with accurate location information owe their energy consumption to other types of failure, for networks with poor localisation, it is the main cause for energy wastage. The expectation that more power is wasted (on unsuccessful packets) in networks with $\sigma > 0$ is confirmed, but the novel findings show that more power is spent on both the successful and the less successful transmissions alike. This study indicates that although energy consumption is higher for networks with $\sigma = 0$ because of its use for more successful routing, looking at the networks with $\sigma > 0$, the energy is used to route fewer successful packets on longer routes and more unsuccessful packets on shorter routes. For $\sigma > 0$ the packets which fail to reach D are lost quickly in sparse networks. In dense networks they take longer routes, only to waste more energy before failure occurs.

The network density is very important for the outcome of the failure percentages, but even more important for the energy spent in the network. When networks are sparse, the routing behavior for $\sigma = 0$ is unrealistic and consistently different than for the $\sigma > 0$. When less than 35 nodes are deployed, the energy consumed is higher because more packets are lost mostly due to poor connectivity and congestion, which have the highest percentage of occurrence. When density is high, energy wastage is minimized for $\sigma = 0$. Even though routes become longer for the failed deliveries, they are fewer in number. When $\sigma > 0$, most of the failures which are not due to location error are the result of no neighbour options with progress towards D , especially when node density is low. This implies that in a realistic network, not only is resilience to location error necessary, but the node distribution has to be carefully chosen as well.

As the study indicates, geographic routing can be studied further with more realistic errors. Though [29] attempted to include the localisation process into the simula-

tions, there are aspects omitted by his work which still need to be investigated: the degree of localisation error obtained through different ranging methods such as received signal strength (RSS) or time of arrival (TOA) and its realistic impact on large scale networks. Subchapter 4.2 considers the different error characteristics of various ranging techniques [11] and the use of anchor nodes needed for accurate localisation and investigate their influence on geographic routing.

4.2 Routing performance with RSS and ToA ranging

This subchapter presents a study of geographic routing with received signal strength (RSS) and time of arrival (ToA) localisation. ToA and RSS are chosen over other localisation methods because they have gained a lot of popularity over the years being based on inter-nodal ranges and not requiring costly equipment. Both techniques are simulated using the linear least square method (LLS) and maximum likelihood (ML) based Levenberg Marquardt (LM) method. The two methods are explained in the following section of this chapter. The routing behaviour is investigated in terms of Loss Rate (LR) and energy spent on unsuccessful routing. As in subchapter 4.1, simulations shed light on the failure percentages and the consequent power wasted due to loss of connectivity, lack of forwarding options with progress, traffic congestion and location error. Furthermore, it is attempted to determine which localisation technique leads to more energy consumption and thus a shorter network life. As expected, it is found that geographic routing throughput depends on the level of accuracy of the localisation method. It is confirmed that for ToA there is higher location accuracy and a smaller loss rate than for the RSS technique. It is also observed that although with ToA the network wastes less energy on lost packets, the extra energy consumption figures are higher than for RSS because of the localisation

method which is more energy costly. The findings indicate that a general model for location errors is not sufficient for a correct algorithmic design as each localisation technique yields errors of a different degree, with a different impact on the routing performance.

4.2.1 Simulations setup

To provide more insight into the performance of geographic routing with realistic localisation and with position inaccuracy of various degrees, the MATLAB simulator makes use of the following signal models and assumptions.

The estimated distance between an anchor node and a target node can be expressed as a circle, centred in the anchor and with a radius equal to the distance. 2D localisation can be completed only if three such distances are made available for each target node. As in Figure 4.16, the intersection of the three existing circles reveals the position of the target. Its coordinates are calculated from the distance equations: $\hat{d}_i = \sqrt{(x - x_i)^2 + (y - y_i)^2}$, where $i = 1, \dots, M$. M being the number of anchor nodes. Distances can be estimated through ToA or RSS [28], both of which have been briefly discussed in subchapter 3.4.1.

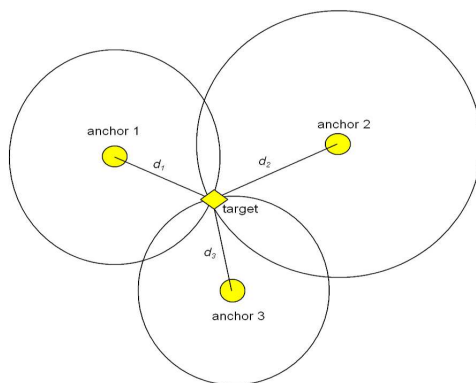


Figure 4.16: Localisation process

A 2-dimensional (2-D) network is considered, which consists of M anchor nodes with

known locations, situated at $\boldsymbol{\theta}_i = [x_i, y_i]^T$ for $i = 1, \dots, M$. The network also consists of N target nodes, such that their location coordinates are given by $\boldsymbol{\theta}_j = [x_j, y_j]^T$ for $j = 1, \dots, N$. It is considered here that the localisation of target nodes is made in a non-cooperative fashion, i.e every target node is localised individually by the anchor nodes.

Signal model for ToA

The distance estimate of the j^{th} target node at the i^{th} anchor \hat{d}_{ij} is given by

$$\hat{d}_{ij} = d_{ij}(\boldsymbol{\theta}_j) + n_{ij}, \quad (4.1)$$

where $d_{ij}(\boldsymbol{\theta}_j)$ is the actual distance given by $d_{ij}(\boldsymbol{\theta}_j) = \sqrt{(x_j - x_i)^2 + (y_j - y_i)^2}$ and n_{ij} is the additive noise that has Gaussian distribution with zero mean i.e $n_{ij} \sim (\mathcal{N}(0, \sigma_{ij}^2))$. An alternative multiplicative noise model is discussed in [11]. In matrix form equation 4.1 is written as

$$\hat{\mathbf{d}}_j = \mathbf{d}(\boldsymbol{\theta}_j) + \mathbf{n}_j, \quad (4.2)$$

for $\mathbf{d}(\boldsymbol{\theta}_j) = [d_{1j}, \dots, d_{Mj}]^T$, $\hat{\mathbf{d}}_j = [\hat{d}_{1j}, \dots, \hat{d}_{Mj}]^T$ and $\mathbf{n}_j = [n_{1j}, \dots, n_{Mj}]^T$.

Signal model for RSS

The distance $d_{ij}(\boldsymbol{\theta}_j)$ is related to the path-loss at the i^{th} anchor, L_{ij} as

$$L_{ij} = L_0 + 10\alpha \log d_{ij}(\boldsymbol{\theta}_j) + w_{ij}, \quad (4.3)$$

where L_0 is the path-loss at the reference distance d_0 ($d_0 < d_i$, and is taken as 1 m) and w_{ij} represents the log-normal shadowing effect, i.e. $w_{ij} \sim (\mathcal{N}(0, \sigma_{ij}^2))$. α represents the path loss exponent (PLE) which is assumed to be known. A discussion

on localisation with unknown PLE is given in [125]. The path-loss is given by:

$$L_{ij} = 10 \log_{10} P_j - 10 \log_{10} P_{ij}, \quad (4.4)$$

where P_j represents transmit power at the j^{th} target node and P_{ij} is the received power at the i^{th} anchor node. Equation 4.4 can also be written in the form,

$$\hat{f}_{ij} = f_{ij}(\boldsymbol{\theta}_j) + w_{ij} \quad (4.5)$$

where $\hat{f}_{ij} = L_{ij} - L_0$ is the observed path loss (in dB) from d_0 to $d_{ij}(\boldsymbol{\theta}_j)$ and $f_{ij}(\boldsymbol{\theta}) = \kappa \alpha \ln d_{ij}(\boldsymbol{\theta}_j)$, $\kappa = \frac{10}{\ln 10}$. In a vector form,

$$\hat{\mathbf{f}}_j = \mathbf{f}(\boldsymbol{\theta}_j) + \mathbf{w}_j, \quad (4.6)$$

where $\hat{\mathbf{f}}_j = [\hat{f}_{1j}, \dots, \hat{f}_{Mj}]^T$ is the vector of the observed path loss.

$\mathbf{f}(\boldsymbol{\theta}_j) = [f_{1j}(\boldsymbol{\theta}), \dots, f_{Mj}(\boldsymbol{\theta})]^T$ is the actual path-loss vector and $\mathbf{w}_j = [w_{1j}, \dots, w_{Mj}]^T$ is the noise vector.

It is evident from equations 4.2 and 4.6 that they are non-linear, hence can be solved via an iterative algorithm. However a linear model can also be developed and the solution can be obtained in a non iterative fashion. Both methods are discussed next.

The MATLAB simulator in subchapter 3.2.2 is modified to include the following localisation algorithms:

1. Iterative algorithm

In order to estimate the location coordinates iteratively the Lavenberg-Marquardt (LM) method [125] is used, which is a modification to the Gauss-Newton (GN)

method. The solution at the $k + 1^{th}$ iteration is given by

$$\boldsymbol{\theta}_j^{k+1} = \boldsymbol{\theta}_j^k + \left((\mathbf{J}_j^k)^T \mathbf{J}_j^k + \lambda^k \mathbf{I} \right)^{-1} (\mathbf{J}_j^k)^T (\hat{\mathbf{s}}_j - \mathbf{s}^k(\boldsymbol{\theta}_j)), \quad (4.7)$$

where \mathbf{I} is the 2×2 identity matrix, λ is the step size ($\lambda = 0.5$), \mathbf{J}_j^k is the Jacobian matrix at the k^{th} step, $\hat{\mathbf{s}}_j$ is the observed signal, while $\mathbf{s}^k(\boldsymbol{\theta}_j)$ refers to the value of the actual signal at the k^{th} step. These values are defined for both models. It should be noted that as with any iterative algorithm, equation 4.7 requires a close initial guess to the true coordinates for convergence. This close initial guess is given inside the network randomly and the convergence takes place.

ToA For ToA $\hat{\mathbf{s}}_j = \hat{\mathbf{d}}_j$ and $\mathbf{s}^k(\boldsymbol{\theta}_j) = \mathbf{d}^k(\boldsymbol{\theta}_j)$ while \mathbf{J}_j^k is given by

$$\mathbf{J}_{\text{ToA}j}^k = \begin{bmatrix} \left(\frac{x_j - x_1}{d_{1j}} \right) & \left(\frac{y_j - y_1}{d_{1j}} \right) \\ \left(\frac{x_j - x_2}{d_{1j}} \right) & \left(\frac{y_j - y_2}{d_{1j}} \right) \\ \vdots & \vdots \\ \left(\frac{x_j - x_M}{d_{Mj}} \right) & \left(\frac{y_j - y_M}{d_{Mj}} \right) \end{bmatrix}.$$

RSS For RSS $\hat{\mathbf{s}}_j = \hat{\mathbf{f}}_j$ and $\mathbf{s}^k(\boldsymbol{\theta}_j) = \mathbf{f}^k(\boldsymbol{\theta}_j)$ while \mathbf{J}_j^k is given by:

$$\mathbf{J}_{\text{RSS}j}^k = \begin{bmatrix} \kappa\alpha \left(\frac{x_j - x_1}{d_{1j}^2} \right) & \kappa\alpha \left(\frac{y_j - y_1}{d_{1j}^2} \right) \\ \kappa\alpha \left(\frac{x_j - x_2}{d_{1j}^2} \right) & \kappa\alpha \left(\frac{y_j - y_2}{d_{1j}^2} \right) \\ \vdots & \vdots \\ \kappa\alpha \left(\frac{x_j - x_M}{d_{Mj}^2} \right) & \kappa\alpha \left(\frac{y_j - y_M}{d_{Mj}^2} \right) \end{bmatrix}.$$

2. Linear least square formulation

The non-linear equations can be linearized by subtracting the signal of a reference anchor from all anchors [126]. The obtained linear system can be solved via classical

least square method, the solution to which is given by [127]:

$$\hat{\theta}_j = \mathbf{0.5A}^\dagger \mathbf{b},$$

where $\mathbf{A}^\dagger = (\mathbf{A}^T \mathbf{A})^{-1} \mathbf{A}^T$ is the Moore–Penrose pseudoinverse, where \mathbf{A}^T is the transpose matrix of \mathbf{A} and \mathbf{A} is given by:

$$\mathbf{A} = \begin{bmatrix} x_1 - x_r & y_1 - y_r \\ x_2 - x_r & y_2 - y_r \\ \vdots & \vdots \\ x_M - x_r & y_M - y_r \end{bmatrix}.$$

For ToA, \mathbf{b}_{ToA} is given by:

$$\mathbf{b}_{ToA} = \begin{bmatrix} (\hat{d}_r)^2 - (\hat{d}_1)^2 - \Xi_r + \Xi_1 \\ (\hat{d}_r)^2 - (\hat{d}_2)^2 - \Xi_r + \Xi_2 \\ \vdots \\ (\hat{d}_r)^2 - (\hat{d}_M)^2 - \Xi_r + \Xi_M \end{bmatrix},$$

and for RSS, \mathbf{b}_{RSS} is given by:

$$\mathbf{b}_{RSS} = \begin{bmatrix} \left(\exp \frac{\hat{f}_r}{\kappa\alpha}\right)^2 - \left(\exp \frac{\hat{f}_1}{\kappa\alpha}\right)^2 - \Xi_r + \Xi_1 \\ \left(\exp \frac{\hat{f}_r}{\kappa\alpha}\right)^2 - \left(\exp \frac{\hat{f}_2}{\kappa\alpha}\right)^2 - \Xi_r + \Xi_2 \\ \vdots \\ \left(\exp \frac{\hat{f}_r}{\kappa\alpha}\right)^2 - \left(\exp \frac{\hat{f}_M}{\kappa\alpha}\right)^2 - \Xi_r + \Xi_M \end{bmatrix},$$

where $\Xi_i = x_i^2 + y_i^2$ and $\Xi_r = x_r^2 + y_r^2$.

The simulator is also adjusted in the following ways: Because geographic routing depends on knowledge of location which is itself derived from measured distance

estimates either by RSS or TOA, the inclusion of anchor nodes is needed. The following simulation evaluation is based on 8 anchor nodes, situated 20 m outside the network, in the corners and on the edges of the routing surface, while the 9th is placed in the centre. Anchors do not participate in the routing process and their transmission range R_a is calculated to provide complete network coverage. Different network densities are simulated, as in Table 4.4 similar to [5], so N and R are chosen in correlation to provide network coverage. The variance (σ^2) of the estimated distance (m) (for ToA) and path-loss (dB) (for RSS) is varied at the same pace. The simulation uses the parameter values specified in Table 4.3 and makes use of the MAC layer. The destination D is placed in the right upper corner of the square network. The number of sensed events SE [120] determines the congestion level in the networks. The networks are assumed static, with randomly and uniformly distributed nodes, as in [7, 29, 30, 85, 110, 114, 116]. The forwarding is achieved with the MFR algorithm, explained and illustrated in subchapter 3.3.

Each simulation consists in generating:

- a network with accurate location information and
- 5 networks with inaccurate location information, for TOA and RSS ranging.

This process is repeated for each network size and results are averaged over η .

4.2.2 Simulation results

This subchapter refers to routing performance. The simulation results using the same localisation technique, but which are obtained for the two different algorithms (ML and LLS), are presented in the same figure. It is expected that ML simulations provide better localisation results, thus improving the routing process. ML localisation offers better accuracy at higher computational costs and is sometimes unfeasible

Simulator parameters (unit)	Symbol	Value
Transmission range of Target Nodes (m) [96,121]	R	100
Transmission range of Anchor Nodes (m)	R_a	623
Transmission power (mW) [110]	P_t	1.778
Path Loss Exponent [88,92]	α	3
Standard Deviation for Shadowing in ToA (dB) [88,92]	σ_{sh}	3.5
Sensitivity Threshold (dBm) [122]	rv_{th}	-95
Packet Size (bits) [95]	p_{size}	1024
Data rate (kbits/s) [86]	dr	250
Energy spent on Transmission (J/bit) [96]	e_{tx}	2.5e-07
Energy spent on Reception (J/bit) [96]	e_{rx}	1.5e-07
Network side length (m) [19,121,123]	l	400
Number of trials [124]	η	300
Number of packets/source [5]	$pkts$	10
Number of sources (events) [120]	SE	15
Number of target nodes	N	25-65
Number of anchor nodes [11,29]	M	9
Variance σ^2 of ToA location error (m) [30]	\mathbf{n}_j	0-10
Variance σ^2 of RSS location error (dB) [30]	\mathbf{w}_j	0-10

Table 4.3: Simulation parameters

Nodes	25	35	45	55	65
Density	3.5	5.2	6.7	8.2	9.8

Table 4.4: Network density (neighbours/node)

because it requires a good, but sometimes unachievable, initial estimation.

Performance comparison for ToA and RSS

The Loss Rate (LR) is shown in Figure 4.17. For lower densities, routing performance is unsatisfactory in all cases and this is more pronounced as σ^2 increases. For ML localisation with RSS ranging (ML-RSS), even for the smallest $\sigma^2 > 0$, the LR reaches 89%, worse than for ML localisation with ToA ranging (ML-ToA) where the value is 81%. Although the LR for RSS ranging decreases with the increase in density, the figures show how the best value, with the smallest σ^2 reach 64% so, more than half of the sent information is lost. However, for both LLS- and ML-ToA,

the performance improves considerably when node density increases, reaching a LR of 26% for the worst case scenario of $\sigma^2 = 10$ of the LLS-ToA.

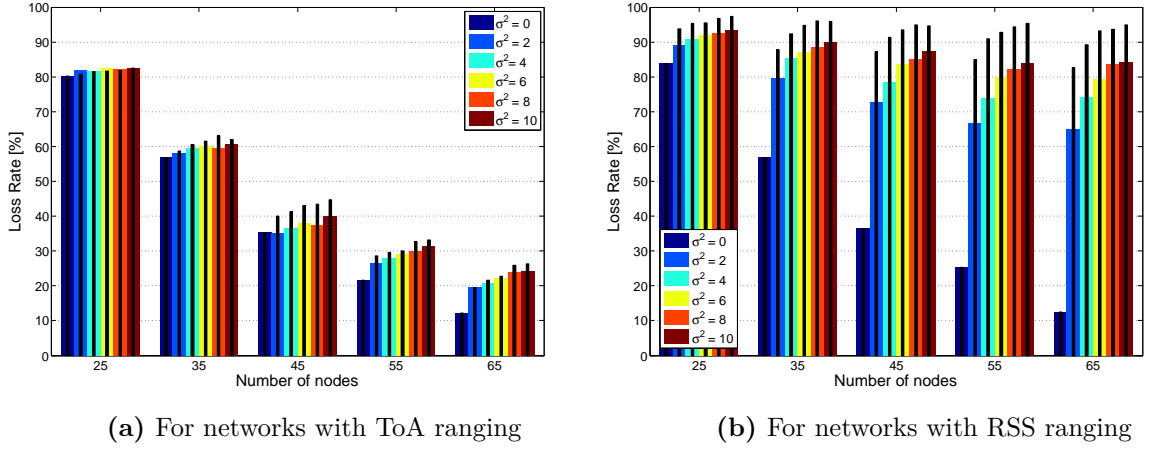


Figure 4.17: Loss Rate (black: LLS; colour: ML)

The fewer the packets lost, the higher is the overall energy consumed by the network. However energy consumption is of interest when routing is unsuccessful and energy is wasted. The energy values are based on the number of lost packets as well as to the number of hops these packets travel before they are lost. Analysing both aspects, it is found that the highest values for energy consumption are attained by networks using ML-RSS, while the smallest values are attained with ML-ToA. The energy consumed on the total number of lost packets is illustrated in Figure 4.18.

For the networks with ToA (ML or LLS), the total energy consumption for lost packets decreases with an increase in connectivity as in Figure 4.18a (this is not the case with RSS ranging). The LLS figures are higher than for the ML case because of more inaccurate localisation. However, as the node density increases reaching a value of 8 or 10 neighbours per node (55 and 65 nodes in the network), the connectivity is improved and the energy loss decreases. Also, the results for higher densities are similar for both ML and LLS ToA. Looking at the increase in σ^2 for a particular number of nodes, the bars indicate that the higher the error

variation, the more power is consumed.

When RSS is employed, the energy wasted is higher than for ToA, especially for the ML case. For all networks of above 35 nodes (density of 5.1), the energy consumption figures of the networks with ML-RSS are higher and relatively constant for more than 35 nodes (Figure 4.18b). The cause of this is the number of lost packets and not their number of hops. As can be seen in Figure 4.19b, most of the packets are lost by the S or close to it, without traveling in the network for a long time. Because RSS ranging is not as accurate as that of ToA, the LR is high and the paths are shorter.

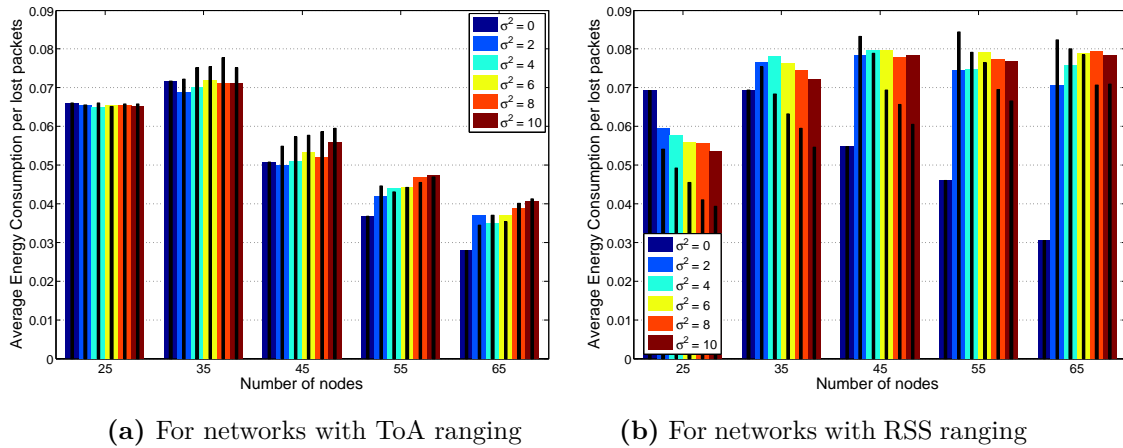


Figure 4.18: Average energy consumption for all lost packets [Joules] (black: LLS; colour: ML)

Comparing Figures 4.19a and 4.19b, it is easily observable that for RSS, the routes of the abandoned packets are short. Looking at the trend of the routing with the increasing σ^2 , it is noticeable that both ML- and LLS-RSS networks decrease the number of traveled hops for the lost packets. However, the energy consumption results maintain their relatively constant level because of the increase in number of lost packets. For the networks with ToA, the route lengths of the lost packets are longer (as seen in Figure 4.19a). The average energy wasted on lost packets is not

high because of fewer lost packets.

Looking strictly at the failures due to location error (Figures 4.19c and 4.19d), (when $\sigma^2 > 0$), the number of hops for these packets increases with node density. This shows that, as a result of location error, packets travel in the network further until they are finally lost. It is also observable that RSS and ToA failures differ with increase of σ^2 . For RSS, the more erroneous the position knowledge, the closer to S the failures take place. For ToA, the number of hops for packets lost due to location error does not grow proportionally to σ^2 and is more dependent on the connectivity.

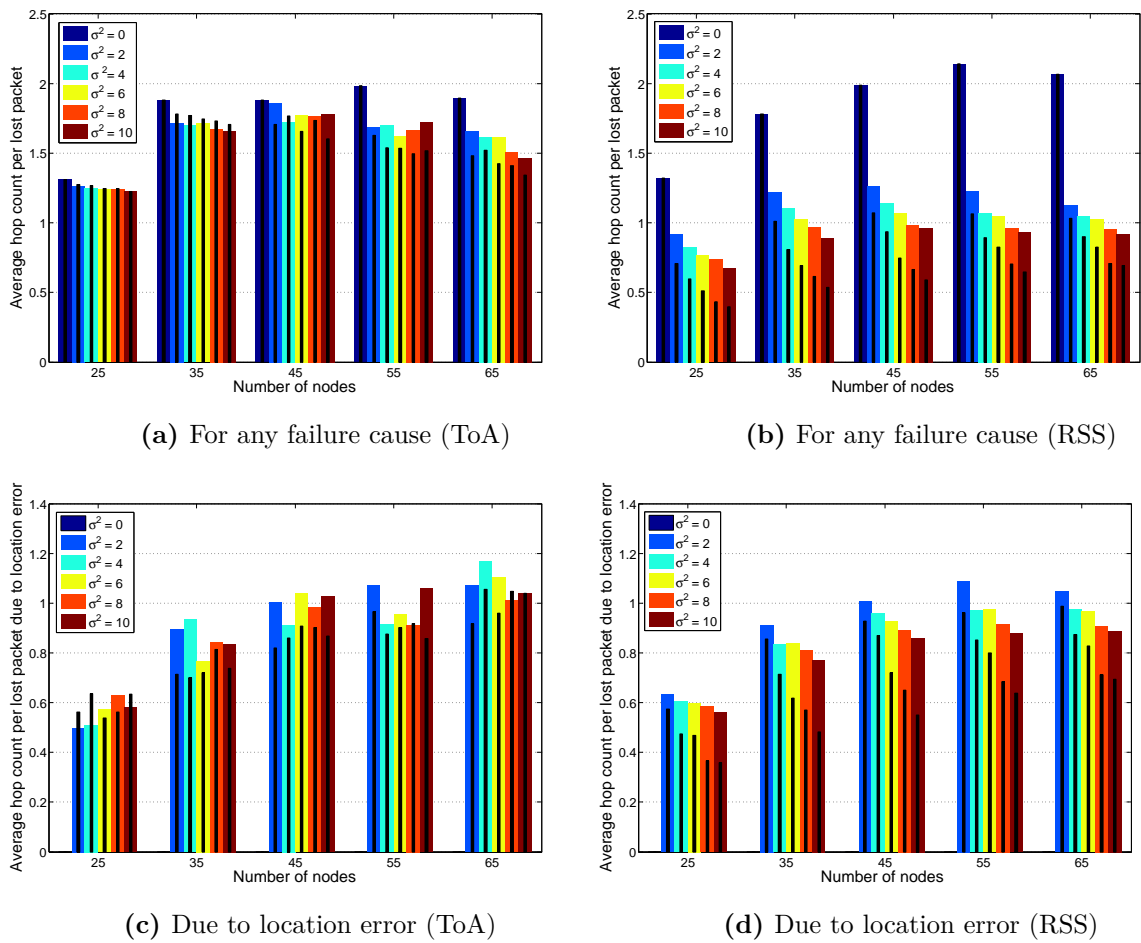


Figure 4.19: Average hop count per lost packet (black: LLS; colour: ML)

Because energy wastage has to be examined when packets are lost, the possible causes for increase in LR are also inspected (see Table 3.3). The following discussion

and figures present the percentage of failures of a certain type out of the total number of failures, not out of the overall number of communication attempts. The failures occurring due to location error increase with σ^2 and with network density for both ToA and RSS cases. Though better connectivity would be expected to lead to reduced failure, the values in the Figures 4.20a and 4.20b show a rise. This means that out of the number of occurring failures, the more routing options there are, the more the chances are to abandon packets at a certain point, due to location error. Figures 4.20c and 4.20d confirm this through the complementary decreasing percentage in connectivity failures.

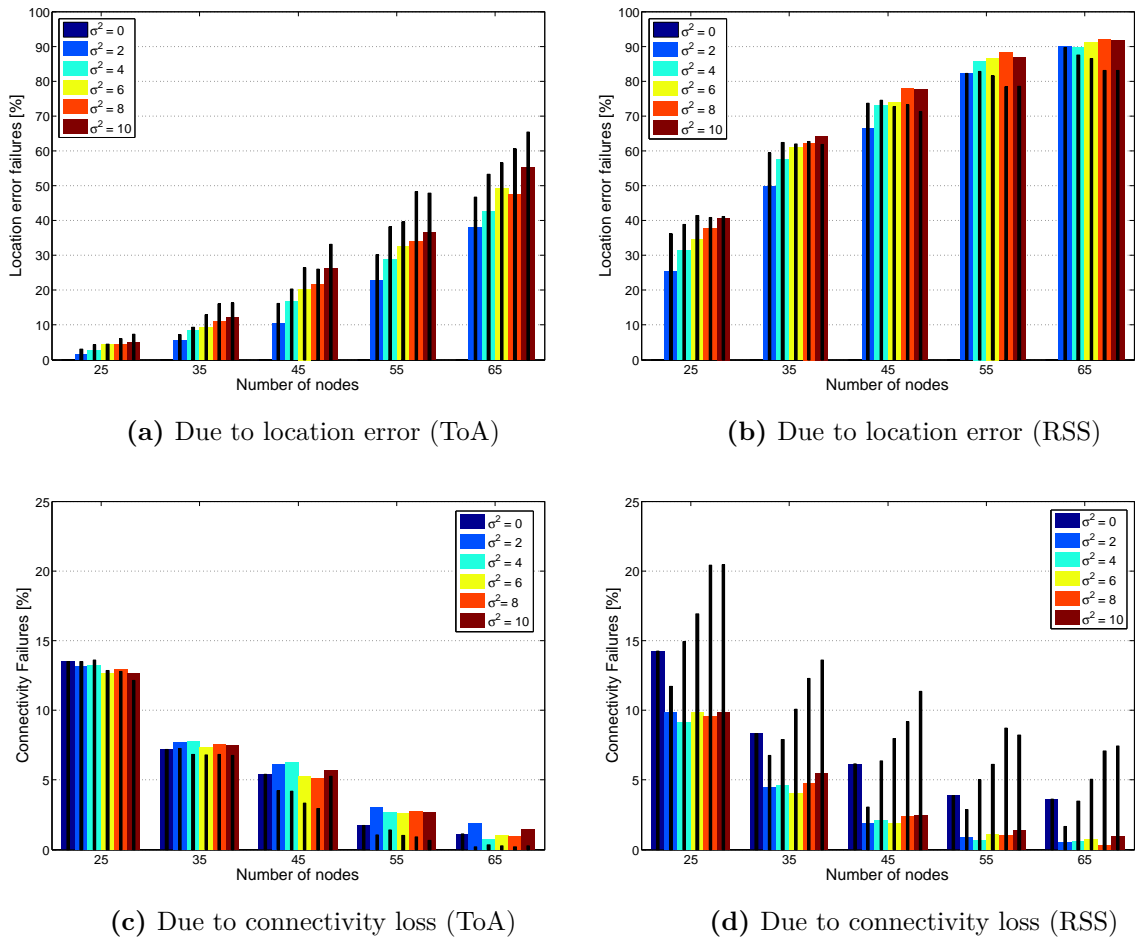


Figure 4.20: Percentage of failures due to location error and connectivity loss (black: LLS; colour: ML)

Analysing the differences between ToA and RSS, it is noticeable that RSS results in the biggest losses. Location error failures reach 55.1% for ML-ToA and 65.4% for LLS-ToA in comparison with 83% for the LLS-RSS and 91.7% for ML-RSS. Also, the increase in network connectivity benefits the LLS-RSS case more.

By avoiding the forwarding options with backward progress, there is an increased possibility of abandoning packets which have reached a local maximum. The corresponding unsuccessful transmissions are named progress failures (Figures 4.21a and 4.21b).

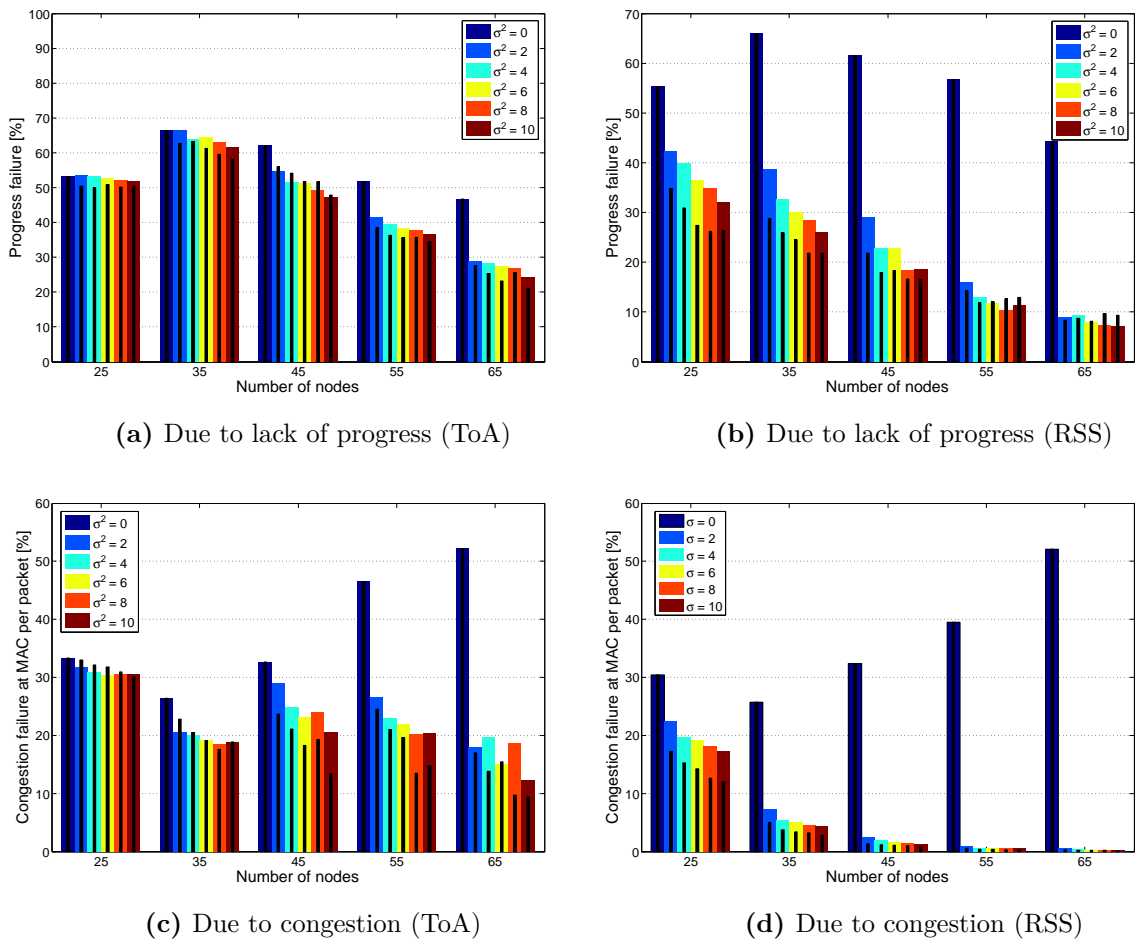


Figure 4.21: Percentage of failures due to lack of progress and congestion (black: LLS; colour: ML)

For all the networks with $\sigma^2 = 0$, the failure percentages are divided only amongst

three causes, but the greatest percentage belongs to progress failure for lower densities (66% for 35 nodes) (Figures 4.21a and 4.21b) and to congestion failures when networks are larger (52% for 65 nodes) (Figures 4.21c and 4.21d). For all location methods, when $\sigma^2 > 0$, the percentage of the other three types of failures decreases in the detriment of the location error failures, especially for the ML cases (Figures 4.20a and 4.20b). As expected, all failures decrease when network size increases. For the networks with RSS ranging and high network density, connectivity or congestion failures preponderate (Figures 4.20d and 4.21d).

ToA and RSS energy consumption

Localisation power consumption is inflicted by initial network measurements. For RSS, it is assumed that the size of a ranging package (RP) is 11 bytes, as big as the ACK message in [15], and the energy consumption values for reception and transmission per bit are considered as in Table 4.3. The energy spent for a single RSS ranging measurement between a target and an anchor node can be calculated as:

$$\hat{e}_{RSS} = 8 \times RP \times (e_{tx} + e_{rx}), \quad (4.8)$$

and approximated to

$$\hat{e}_{RSS} = 35.2\mu J.$$

TW-ToA measurements require more resources because the method relies on more than one communication connection between two devices. Even while using the same clock, as with the Jennic Evaluation Kit JN5139 [122], its energy consumption is increased. The calculations here represent an approximation based on the documentation in [122]. The specific sequence of packets transacted between

an anchor and a target node involves the transmission and reception of at least 3 command packets (CMD) of 19 bytes, 3 acknowledgements (ACK) of 11 bytes and 1 data transmission (DATA) of 31 bytes. The energy and delay of the ToA communication cycle is variable because of the use of the Carrier Sense Multiple Access-Collision Avoidance (CSMA-CA). It can be estimated for one operation, in a best case scenario of 4 channel assessments which result in an idle channel each time. The energy spent on processing and memory access has not been considered but the values are expected to be directly proportional to the number of operations of each localisation method (this implies more expenses for ToA). The energy spent on CCA has been referred to [15]. By using the energy consumption values in Table 4.3 and the following mathematical expression:

$$\hat{e}_{TOA} = (3 \times 8 \times (CMD + ACK) + 8 \times DATA) \times (e_{tx} + e_{rx}), \quad (4.9)$$

the energy consumed on the ranging between 2 nodes using ToA is estimated as:

$$\hat{e}_{TOA} = 553\mu J.$$

The total estimated energy consumption over an entire network (\hat{E}) is proportional to the number of target nodes in the network (N) and of anchor nodes (M):

$$\hat{E} = \hat{e} \times N \times M, \quad (4.10)$$

where \hat{e} is either \hat{e}_{TOA} or \hat{e}_{RSS} . \hat{E} is calculated for both TOA and RSS in Table 4.5:

Nodes	25	35	45	55	65
$\hat{E}_{RSS}[J]$	0.007	0.009	0.012	0.015	0.018
$\hat{E}_{TOA}[J]$	0.11	0.15	0.19	0.24	0.28

Table 4.5: Energy consumption for ToA and RSS, with 9 anchor nodes

Figure 4.22 shows the overall energy wasted on unsuccessful routing and on localisation by the networks using ML-ToA and ML-RSS. By looking at the values of the erroneous networks of highest node density, the energy figures for TOA are between 0.35-0.040 (J) on lost packets, while the more wasteful networks with RSS spend 0.75-0.78 (J). However, when adding the extra energy of the localisation process, the networks with ToA become the most wasteful, reaching values of 0.31-0.32 (J) for the highest network density. That is 3 times more than for RSS which remains with its highest at 0.088-0.096 (J).

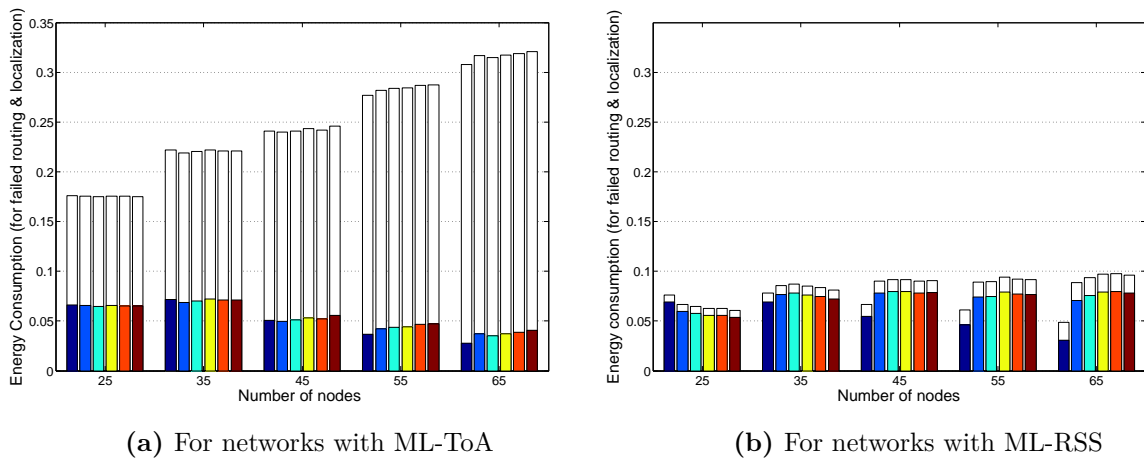


Figure 4.22: Energy consumed by the network (in colour - the energy spent on failed routing; in white - energy spent on localisation)

4.3 Conclusions

In this chapter, the performance of basic greedy geographic routing is analysed when the coordinates of the sensor nodes are not known with accuracy. Two cases are studied. Firstly, the location error is random and modelled with a Gaussian distribution. Secondly the positioning process is simulated and the location error is estimated by anchor nodes based on distance and power measurements. In both cases, the routing behaviour changes considerably being influenced by the magnitude

of the location error.

In subchapter 4.1, which considers the case of normally distributed location errors, it is concluded that if the errors are higher than 10% of the R , the PDR decreases to less than 50%, even in high density scenarios. The energy consumption is also consequently affected. When the coordinates of the nodes are accurately known, the energy is used for successful packet routing mostly; the few losses that do take place are owed to congestion and bad network connectivity. When a random location error intervenes, the battery power is wasted on lost packets which either get lost quickly in large numbers, either travel on longer routes to be lost further away from the source of the sensed event. It is observed that the denser the networks, the longer the paths of the lost packets are contributing to an undesired power consumption.

The design of new energy efficient algorithms as well as the analysis of the existing ones has to be made with realistic considerations of location errors, given by localisation techniques employed in real network design. In subchapter 4.2, it is found that the performance of networks employing geographic routing, under the same relaxed traffic load, is considerably different for the positioning errors induced by ToA and RSS. Good connectivity is necessary for large scale networks, but even if this is ensured, the routing outcome is seriously affected in terms of throughput when RSS is employed. If networks are sparse, the loss ratio can reach 80-90% regardless of the localisation method used. Also, even if the right density is ensured, the localisation process is the most important cause for failure.

It has been noticed that RSS is not suitable for large networks as it results in less than 20% delivery. In addition, the energy consumed on the lost packets is higher and although the energy consumption of the RSS localisation process is attractive, the main objective of the routing is not accomplished to a satisfactory level. ToA seems to be a better option in terms of throughput. However, in terms of power

consumption, it is not very efficient. The energy values spent for localisation are at least three times higher than what is spent for routing. As the number of nodes increases in the network, so does the energy spent on localisation.

This chapter has provided proof as to how realistic location errors impacts geographic routing in large scale WSNs. It has been shown that the performance of the forwarding algorithms, which would otherwise provide 100% PDR, is severely affected by large errors to the point that they become inefficient and the network is not functional anymore. In addition, the localisation process results in errors of different magnitude, depending on the employed ranging technique and thus, impacts the routing component in a different way than anticipated through theoretical error modelling. It is therefore concluded that new geographic routing algorithms need to be proposed, which can cope with the effects of inaccurate localisation.

Chapter 5 provides two such solutions, explains their approaches and compares their performance in similar conditions. The novel approaches aim to make geographic routing practical for real-life applications and to provide a better performance when compared with similar algorithms in the literature.

5 Solutions for geographic routing resilient to location errors

As previously underlined, geographic routing is an attractive option for large scale WSNs because of its low overhead and energy expenditure, but is inefficient in realistic localisation conditions which are inevitably imprecise. Inexact range measurements and location errors can lead to low PDR and to node power being wasted.

In this chapter a novel, low-complexity, error-resilient geographic routing method is proposed: the Conditioned Mean Square Error Ratio (CMSER) routing algorithm, intended to efficiently make use of existing network information and to successfully route packets when localisation is inaccurate. Next hop selection is based on the largest distance to D (minimizing the number of forwarding hops) and on the smallest estimated error figure associated with the measured neighbour coordinates. It is found that CMSER outperforms other basic greedy forwarding techniques. Simulation results show that the throughput for CMSER is higher than for other methods, also reducing the energy consumption on lost packets by keeping their routing paths shorter than other algorithms with similar goals.

5.1 Previous works

Three of the geographic forwarding techniques which have been studied with imprecise location measurements are given more attention because of their approach on the forwarding [3,7,8,85]. They target either the optimization of the throughput or of the energy consumption. While [3] and [8] focus on increasing the throughput and make use of the notion of advance towards the destination, the algorithm in [7,85] aims to optimize power consumption.

The Maximum Expectation within Transmission Range (MER) proposed in [3] considers the error probability when making forwarding decisions, determines the goodness of routing candidates and penalizes those whose inaccurate location can lead to packet failure. The routing decision requires knowledge about the furthest neighbor from the transmitting node, but also of the probability that its actual coordinates are within the transmission range (R). It then dismisses those forwarding options with either excessive distance or possibility of backward progress and is prone to choosing the node situated midway between the relays. MER does not cope well with large errors (31.5% of R). [8] proposes the objective function named Maximum Expectation Progress (MEP) for greedy routing, while backward progress is differently treated. MEP penalizes neighbors only for excessive distance thus managing larger location errors through the availability of more forwarding options. The forwarding technique in [8] is used for further improvement by the geographic routing proposal CMSER.

The least expected distance (LED) algorithm is first proposed in [85] and is elaborated in [7]. It is presented as a novel, error-robust routing scheme, whose main aim is to preserve the power saving features of basic geographic forwarding. It is proven in [7] that whichever approach the position-based routing may have, either

to optimize the energy spent per hop or for the overall chosen path, the energy-optimal forwarding position is the same. LED determines this theoretical optimum and subsequently chooses as the next hop the neighbor whose real position is closest to it. The algorithm strategically incorporates location error into the forwarding objective function. It is assumed that the estimated coordinates of each node are affected by a Gaussian error of a given variance. As a consequence the erroneous distances between nodes are random variables characterized by the Rice distribution. LED calculates the expectation of the considered distances and chooses the node with the minimum expectation.

Although the forwarding techniques in [3, 7, 8] provide solutions in realistic localisation scenarios, performance degradation can still be considered severe and can be further reduced. As a consequence, the basic forwarding methods of their algorithms have been comparatively studied and the conditioned mean square error ratio (CMSE) algorithm has been proposed as an alternative method to improve the overall routing performance while still coping with location errors. To be able to compare the routing techniques, all the algorithms are modified to forward based on positive advance to destination, dismissing the possibility of backward progress. The MFR algorithm [34], explained in the previous chapters, is also used in the comparison, as a geographic routing algorithm which does not cope with location errors. Its distance metric is used for all the simulated algorithms in this study. MFR is considered an energy efficient forwarding strategy when using a fixed transmission power because it minimizes the hop count [3].

Simulations have shown that, under identical circumstances, the PDR of the proposed forwarding method increases and the energy wasted on lost packets is limited. The CMSE throughput grows higher without the lost packets having a large number of hops, thus reducing the overall power consumption of the network.

5.2 Error model

Network nodes may be localised through positioning techniques such as time-of-arrival (ToA) or received signal strength (RSS) [11, 13, 87], but in this subchapter the errors are modelled in a simplistic way, similar to that explained in chapter 3. It is considered that the location errors are independent Gaussian random variables and that the error variance of each node is different. Let there be a relay node S_i , with $i = 1, \dots, I$, where I is the number of transmitting nodes along a routing path. Let F_j be a forwarding candidate of S_i , with $j = 1, \dots, J$, where J is the number of neighbors of S_i with positive progress to destination D (so $d_{jD} < d_{iD}$). In the two dimensional plane, S_i and F_j have the real coordinates $S_i(x_i, y_i)$ and $F_j(x_j, y_j)$ and the estimated locations $S'_i(\hat{x}_i, \hat{y}_i)$ and $F'_j(\hat{x}_j, \hat{y}_j)$, where $\hat{x}_i = x_i + W_i$, $\hat{y}_i = y_i + W_i$, $\hat{x}_j = x_j + W_j$ and $\hat{y}_j = y_j + W_j$. $W_i \sim N(0, \sigma_i^2)$ and $W_j \sim N(0, \sigma_j^2)$ are independent Gaussian random variables with zero mean with standard deviation σ_i and σ_j . For each node, it is considered that the error variance is equal on the x and y axes. The probability density function of the measured distance \hat{d}_{ij} between 2 nodes (S'_i and F'_j) follows a Rice distribution [7] (if W_i and W_j are independent):

$$f(\hat{d}_{ij}) = \left(\frac{\hat{d}_{ij}}{\sigma_{ij}^2} \right) \exp\left(-\frac{\hat{d}_{ij}^2 + d_{ij}^2}{2\sigma_{ij}^2} \right) I_0\left(\frac{\hat{d}_{ij}d_{ij}}{\sigma_{ij}^2} \right). \quad (5.1)$$

The estimated distance \hat{d}_{ij} is a Rician random variable (see equation 5.2) and d_{ij} is the accurate distance between S_i and F_j (see equation 5.3):

$$\hat{d}_{ij} = \sqrt{(\hat{x}_i - \hat{x}_j)^2 + (\hat{y}_i - \hat{y}_j)^2}, \quad (5.2)$$

$$d_{ij} = \sqrt{(x_i - x_j)^2 + (y_i - y_j)^2}. \quad (5.3)$$

I_0 is the modified Bessel function of the first kind and order zero and σ_{ij} is the scale parameter of the Rician distribution:

$$\sigma_{ij} = \sqrt{\sigma_i^2 + \sigma_j^2} \quad (5.4)$$

The mean (expectation) of the estimated distance \hat{d}_{ij} is

$$E(\hat{d}_{ij}) = \sigma_{ij} \sqrt{\frac{\pi}{2}} L_{\frac{1}{2}} \left(-\frac{d_{ij}^2}{2\sigma_{ij}^2} \right), \quad (5.5)$$

where $L_{\frac{1}{2}}(x)$ denotes the Laguerre polynomial with equation 5.6 and I_1 is the modified Bessel function of the first kind and first order.

$$L_{\frac{1}{2}}(x) = \exp\left(\frac{x}{2}\right) \left[(1-x) I_0\left(-\frac{x}{2}\right) - x I_1\left(-\frac{x}{2}\right) \right]. \quad (5.6)$$

The variance of the estimated distance \hat{d}_{ij} is

$$Var(\hat{d}_{ij}) = 2\sigma_{ij}^2 + d_{ij}^2 - \left(\frac{\pi\sigma_{ij}^2}{2}\right) L_{\frac{1}{2}}^2\left(-\frac{d_{ij}^2}{2\sigma_{ij}^2}\right). \quad (5.7)$$

5.3 CMSER routing algorithm

As it has been proven in the previous chapters, location errors have a significant impact on geographic routing performance. The forwarding techniques from [3, 7, 8], presented in subchapter 5.1, are further discussed below and a novel routing algorithm to address the presence of location errors is proposed. The aim is to

minimize the effect of inherent positioning errors on the network throughput, when nodes use a fixed transmission power. To be able to analyze strictly the forwarding techniques, it is assumed that the communication is not affected by the environment. According to a simple forwarding algorithm like MFR, when a node S_i has to choose among the available forwarding candidates with positive advance, the next hop F_j will be the one closest to the destination D , so the node with the largest distance d_{ij} . However, as underlined in [3], it is likely that the furthest node from S_i will also be the nearest to the edge of R . Because all choices are made based on the estimated distances, the transmission is susceptible to failure and energy wastage. If a statistical error characteristic associated with the measured location of each node (a mean and error variance) is known and communicated along with the coordinates, then the forwarding decision can make use of this data.

The objective functions of MER and MEP compute the expectation of a successful transmission for F_j , based on their statistical error characteristics. To determine the neighbor with the highest expectation within R , both MER and MEP policies use statistics related to point and area coverage, similar to those used in target destruction applications within circular areas [128]. Thus, the probability of the real coordinates of a node to be found within a circle centered at its estimated coordinates is detected. MEP's decision is based on the measured progress to D , expressed as P_{ij} , and on the probability of node F_j to be out of the R of S_i . The neighbor goodness is determined by calculating its probability to be found within a circular area of a radius $u_{ij} = M_{ij}$, using the Rayleigh cumulative distribution function $F_{ij} = 1 - \exp\left(-\frac{u_{ij}^2}{2\sigma_{ij}^2}\right)$, where

$$M_{ij} = R + \sigma_{ij} - \hat{d}_{ij}. \quad (5.8)$$

The MEP objective function, $MEP_{ij} = P_{ij} * F_{ij}$, favours the choice of the most useful forwarding option, in terms of distance (choosing the closest to D), and in terms of location error magnitude (choosing the one with smaller error) (see Figure 5.1). So the algorithm calculates $F_j = \text{argmax} (MEP_{ij})$ for each node before deciding.

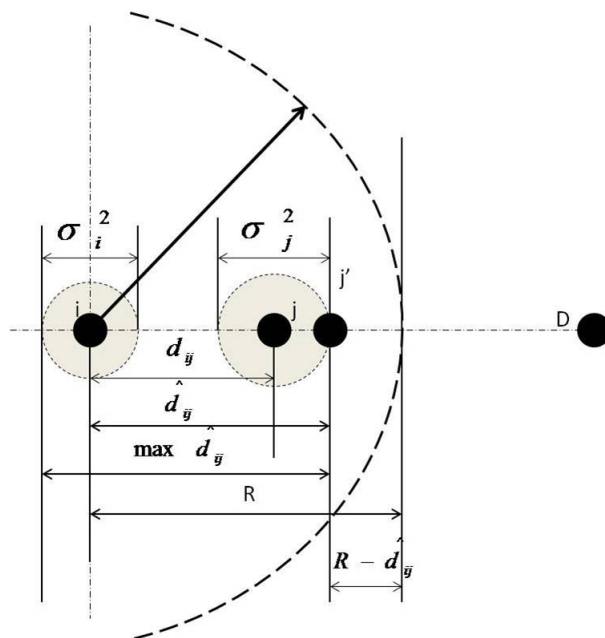


Figure 5.1: COND approach

The underlying idea of MEP is used in the algorithm proposed in this chapter, but the mathematical approach is different.

Let S_i first calculate the mean square error (MSE) associated with all F_j with

$$MSE_{ij} = E(\hat{d}_{ij} - d_{ij})^2 = E(\hat{d}_{ij}^2) - 2d_{ij}E(\hat{d}_{ij}) + d_{ij}^2, \quad (5.9)$$

where $E(\hat{d}_{ij})$ is calculated with equation 5.5 and $E(\hat{d}_{ij}^2)$ is calculated as follows:

$$E(\hat{d}_{ij}^2) = E(\hat{x}_i^2 - 2\hat{x}_i\hat{x}_j + \hat{x}_j^2) + E(\hat{y}_i^2 - 2\hat{y}_i\hat{y}_j + \hat{y}_j^2) \quad (5.10)$$

Using the second moments in equation 5.10, i.e. $E(\hat{x}_i^2) = x_i^2 + \sigma_i^2$, $E(\hat{y}_i^2) = y_i^2 + \sigma_i^2$,

$E(\hat{x}_j^2) = x_j^2 + \sigma_j^2$ and $E(\hat{y}_j^2) = y_j^2 + \sigma_j^2$, the equation 5.11 is obtained as follows:

$$E\left(\hat{d}_{ij}^2\right) = 2\sigma_i^2 + 2\sigma_j^2 + x_i^2 + x_j^2 + y_i^2 + y_j^2 - 2x_i x_j - 2y_i y_j. \quad (5.11)$$

The actual distance d_{ij} is not available as the accurate locations are unknown, hence the calculations are made using the estimated coordinates instead.

The next step is to calculate the mean square error ratio (MSER) associated with each forwarding candidate F_j and to detect the best choice as follows:

$$MSER_{ij} = MSE_{ij} / \hat{d}_{ij}. \quad (5.12)$$

The forwarding candidate F_j is selected using:

$$F_j = \arg \min (MSER_{ij}). \quad (5.13)$$

By choosing the neighbor F_j with the minimum value for MSER as in equation 5.13, a balance is obtained between the shortest distance to D and the smallest error of the next hop. In the special case of two forwarding options equally far from S_i , the next hop will be the node with the smallest error. If the error characteristics are the same, the next hop will be the furthest one from S_i . So, F_j is chosen depending on the scale of the error in comparison with the distance \hat{d}_{ij} .

The algorithm can be further improved by considering that F_j , although optimal from the MSE point of view, can still be close to the edge of R , especially when few routing options are available. The routing selection can be refined by considering a condition similar to that of MEP, but redefined as follows: that the squared difference between R and the estimated distance to the neighbor node should be greater than the variance of the erroneous distance (see equation 5.14). The quadratic form

is used to have the same unit of measurement. The inequality in equation 5.14 contains the variance of the erroneous distance (as in equation 5.7) instead of using the standard deviation of each of the nodes (sender and receiver) as in MEP, because the entire algorithm is based on considering the distance between nodes as a random variable,

$$\left(R - \hat{d}_{ij}\right)^2 > Var\left(\hat{d}_{ij}\right). \quad (5.14)$$

This algorithm is named as conditioned mean square error ratio (CMSER).

For a complete comparison and a more appropriate evaluation, the basic forwarding ideas of MEP and LED are simulated, but with alterations: MEP is simulated with the expression in equation 5.14 instead of that in equation 5.8 and it is thus referred to as the condition (COND) in the graphs. LED is now based on the maximum $E\left(\hat{d}_{ij}\right)$ used to determine the F_j closest to D , instead of that used for the F_j closest to a predetermined energy-optimal forwarding position, and it is thus referred to as most expected distance (MED).

5.3.1 Simulation setup

The PDR, hop count of lost and received packets, as well as consequent energy consumption figures are analysed for the forwarding methods referred to as MFR, MED, COND, MSER and CMSEr. The network area is considered smaller in comparison with those in chapter 3 because of two practical reasons: the simulation speed and the fact that the MATLAB Bessel function of zero order (necessary in some of the calculations in the algorithms of this chapter) is not operational for large values (of the distance) and causes a stack overflow.

The nodes are erroneously localised with $\sigma_i, \sigma_j \in [0, \sigma_{max}]$. The MATLAB simulation

Simulator parameters (unit)	Symbol	Value
Transmission power (W) [110]	P_t	1.778
Distance of reference (m) [88, 92]	d_0	1
Path loss exponent [88, 92]	α	3
Packet size (bits) [95]	p_{size}	1024
Data rate (Kbits/s) [86]	dr	250
Number of packets/source [30]	$pkts$	1
Energy per bit spent on transmission(J/bit) [96]	e_{tx}	2.5e-07
Energy per bit spent for reception (J/bit) [96]	e_{rx}	1.5e-0.7
Network side length (m) [105]	l	200

Table 5.1: Simulation parameters

parameters are listed in Table 5.1. The MAC layer is not active here, as it is not in [7]. Nodes are randomly distributed and several scenarios are studied, as described in Table 5.2, where SE random sensing events take place [3, 53, 83]. The probability of correctly receiving any packet within R is 1, and 0 outside R . Performance is studied for different network densities (the number of nodes N is varied), for different values of the maximum standard deviation of errors (σ_{max}) or different R . Each scenario consists of a node distribution with accurate coordinates, where packet forwarding is made with MFR, and a number of η distributions with inaccurate locations (η being the number of trials/iterations), where the errors have been modelled as in subchapter 5.2. The figures are obtained through averaging over η .

The analysis covers several scenarios, similarly to [3, 7]. The purpose of each scenario is to analyse the PDR in different conditions: for different network densities, location errors of various magnitude, different communication ranges, when the number of triggered events are different or the number of iterations is varied to 100 [83] and 300 [124]. Just as in the previous chapters, the number of SE only impacts the amount of network traffic and congestion levels, but does not affect the evaluation of geographic routing in terms of throughput.

Scenario	N	$R(m)$	$\sigma_{max}(m)$ (% of R)	η	SE
1	50-600	40 [83]	8 (20%) [3]	100 [7, 83]	50
2	350	40 [83]	4-20 (10-50%) [7]	100 [7, 83]	50
3	200	10-100 [3, 7, 96]	5 (50-5%) [7]	300 [124]	30

Table 5.2: Simulation scenarios

5.3.2 Simulation results

Figure 5.2 presents the forwarding performance for different network densities. For an optimal density of more than 200 network nodes, CMSER has a PDR between 70% to 80%. The MFR performs worst with approximately 10% PDR for all network densities. MSER and MED have a similar throughput with PDR values between 20% and 40%. It is however noticeable that MSER has a slightly better performance than MED. Looking strictly at COND, it is noticeable that it offers an obvious improvement over the other methods, that is has a parallel behavior to that of CMSER, but has a PDR below 50%. To indicate the reliability of the estimations, Figure 5.2 illustrates the PDR with a 95% confidence level.

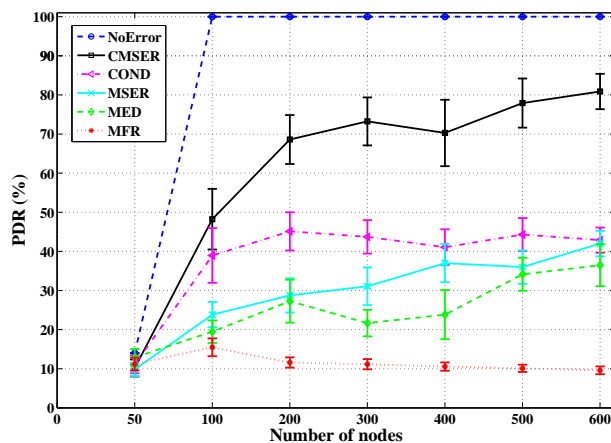


Figure 5.2: Routing performance for scenario 1.

Looking at the PDR when σ_{max} is increased Figure 5.3, the performance degrades, as expected. The most severe performance degradation is that of MED, which for large errors behaves worse than MFR. In this scenario with an optimal network density,

MSER outperforms MED, but this is mainly because of the severe degradation of MED. COND has the second best performance maintaining a PDR of above 50% only for errors with σ_{max} up to 10% of R . CMSER is the best forwarding method here because its performance has the least abrupt degradation slope with the increase of errors. Although the PDR for CMSER drops below 50% when $\sigma_{max} \geq 45\%$ of R , it still maintains a significantly superior performance than for the other methods.

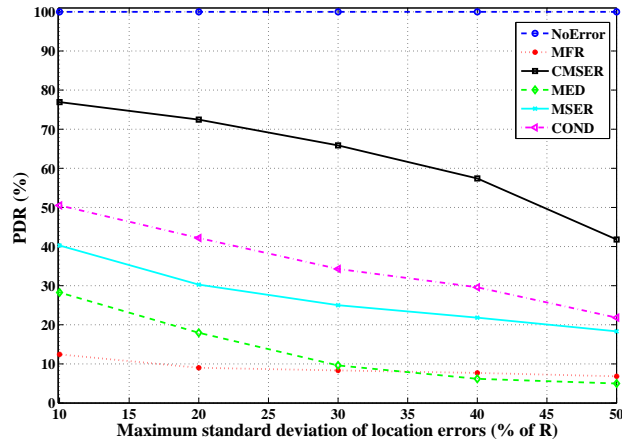


Figure 5.3: Routing performance for scenario 2.

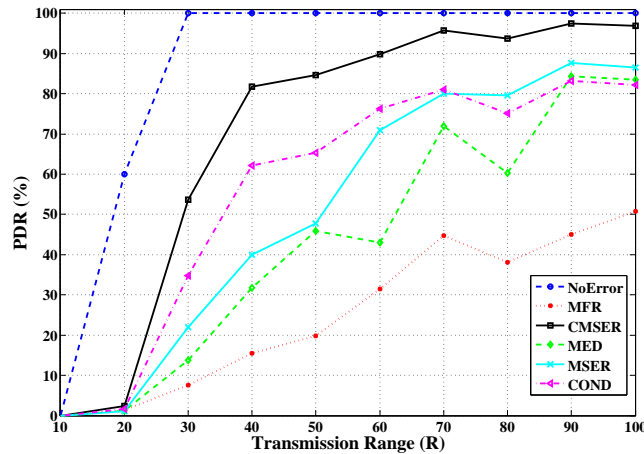


Figure 5.4: Routing performance for scenario 3.

Varying the R within a reasonably dense network increases the potential forwarding options for each node (see Figure 5.4). With more neighbors to choose from, the throughput also increases. For $R \leq 20$, all the considered forwarding methods fail

to find neighbors to forward to and the routing fails. While for $R > 30$ CMSEER increases its throughput progressively from 60% to almost 100% PDR, none of the other algorithms perform as well. The PDR curve for MFR remains detached below the rest of the algorithms for all values of R . The performance of MSER, COND and MED is similar, but lower than for CMSEER whose behaviour is constantly superior. The novel geographic routing algorithm, CMSEER, proposed in this subchapter has been proven to be resilient to location errors and to outperform other basic greedy routing techniques (MFR, MSER, COND, MED). The results of the three scenarios simulated in MATLAB confirm that CMSEER is superior in terms of PDR, while minimizing energy losses on packets that are lost. Its main objective is to maximize throughput with as few energy costs as possible. However, the literature provides a geographic routing solution in [7], by presenting LED as mainly focused on minimizing energy efficiency instead. Subchapter 5.4 studies the design of LED and presents an improvement of the CMSEER algorithm, by adopting a similar energy-efficient technique. The update does not affect the routing principle of CMSEER and makes it possible to compare its performance with that of LED.

5.4 Modified version of CMSEER routing algorithm

Subchapter 5.3 analyzes geographic routing algorithms resilient to location error looking at the basic forwarding methods based on: the MSE (for CMSEER), Rician expectation (for MED, which is a modified version of LED) and Rician variance (for COND, which is a modified version of MEP). However, the design of the LED protocol (as proposed in [7]) indicates that the routing performance is improved through the selection of the forwarding neighbour based on its proximity to an energy optimal forwarding position. The calculation of such a position would thus

increase not only the PDR, but also presumably make the routing process more energy efficient. The following subchapters present how this is achieved for LED and how this improvement is used in the modified CMSEER algorithm (M-CMSEER) by considering a similar energy-optimal forwarding choice.

5.4.1 Energy saving feature

The scope of LED is to preserve the power saving features of basic geographic forwarding. It is stated in [7] that whether the approach of the position-based routing may be to optimize the energy spent per hop or that of the overall chosen path, the energy-optimal forwarding position is the same. LED determines this theoretical optimum and chooses to forward to the neighbour closest to it. The forwarding objective function considers the location error of nodes as well and the assumption is that the coordinates are affected by a Gaussian error of a given variance. Consequently the \hat{d}_{ij} are random variables characterized by the Rice distribution. LED calculates the expectation of the considered distances and chooses the node with the minimum expectation.

A general energy model per bit is presented in [7] and assumes that the total energy consumed per bit at the physical layer is the sum of the energy dissipated for the transmission (e_{tx}) and for the reception (e_{rx}) of that bit, $e_t = e_{tx} + e_{rx}$. The energy consumption of the transmission process consists in the energy spent on the radio electronics and that spent on the amplification of the signal. Therefore $e_t = e_{tx-elec} + e_{tx-amp} + e_{rx-elec}$. The simplifying assumption is that the energy spent to operate the radio electronics is equal for both the transmission and the reception, $e_{tx-elec} = e_{rx-elec} = e_{elec}$, so $e_t = e_{tx-amp} + 2e_{elec}$. The energy spent on the amplification can be further expressed as $e_{tx-amp} = \beta d^\alpha$, where α is the path loss index and β is a constant [*Joule/bit/m $^\alpha$*]. Thus, the total energy consumed per

bit can be written:

$$e_t = \beta d^\alpha + c, \quad (5.15)$$

where $c = 2 * e_{elec}$. The expression changes for free space or multipath, but for simplicity free space is the only case considered here.

The distance between the node i and the theoretical energy optimal position M is calculated as in [7] or [129]:

$$d_{iM} = \sqrt[\alpha]{\frac{c}{(\beta(1 - 2^{1-\alpha}))}}. \quad (5.16)$$

The energy-optimal position M is located on the line connecting the current sending node i and the destination D . Using this information, the slope m of the line can be calculated with $(y_i - y_D) = m(x_i - x_D)$. Its value is the same for all the points on the line, including for M , so the coordinates x_M and y_M are found using the following system of two equations: the point-slope formula for $(y_i - y_M) = m(x_i - x_M)$ and the equation of the Euclidean distance $d_{iM} = \sqrt{(x_i - x_M)^2 + (y_i - y_M)^2}$, where d_{iM} value is obtained with equation 5.16 and m , x_i , y_i are known. Depending on where M is found in reference to node i (on its right or left side), x_M and y_M are:

$$x_M = x_i \pm \frac{d_{iM}}{\sqrt{1 + m^2}},$$

$$y_M = y_i \pm \frac{m d_{iM}}{\sqrt{1 + m^2}}.$$

With the known coordinates of M , LED can calculate the mean (expectation) of the measured distance \hat{d}_{jM} between M and the neighbours j of node i using equation 5.5 and selects the option closest to M . The forwarding is made based on the objective

function of LED, which minimizes the expectation:

$$F_j = \arg \min \left(E \left(\hat{d}_{jM} \right) \right). \quad (5.17)$$

In subchapter 5.3, to be able to compare the routing performance from a similar point of view, instead of using the LED algorithm for comparison, a basic form of it was employed, the maximum expected distance (MED). MED forwards based on the maximum $E \left(\hat{d}_{ij} \right)$ used to determine the F_j closest to D , instead of $E \left(\hat{d}_{jM} \right)$ used by LED to determine the F_j closest to an energy-optimal forwarding position M . The basic forwarding method of MED relays similarly to MFR, considering the notion of maximum advance to D , and its objective function is:

$$F_j = \arg \max \left(E \left(\hat{d}_{ij} \right) \right). \quad (5.18)$$

The novel solution proposed in this chapter is the modified conditioned mean square error ratio algorithm, M-CMSEER. It adopts the theoretical and energy optimal point M as used in [7]. Instead of using the MSEER in equation 5.12, the algorithm minimizes the MSE obtained in equation 5.9 (because its aim is to select the neighbour j with the smallest error) and makes its choice considering the option closest to M , so minimizing the distance between j and M . The objective function is:

$$F_j = \arg \min \left(MSE_{ij} * \hat{d}_{jM} \right). \quad (5.19)$$

M-CMSEER then makes use of the condition explained in equation 5.14.

5.4.2 Simulation setup

As CMSER has already been proven to be robust against location errors and to have a better throughput than that of MED, the performance of M-CMSER is the one which remains to be studied. Hence, M-CMSER, CMSER and LED are first compared based on the throughput. Then, the energy consumption is analysed, considering the realistic case in which the routing benefits from transmission acknowledgement. The energy spent in the routing process is influenced by the number of successful transmissions and by the efforts of resending the data to achieve this. Both aspects are studied for networks which are dense enough to ensure the highest PDR possible (of almost always 100%).

The nodes are erroneously localised with $\sigma_i^2, \sigma_j^2 \in [0, \sigma_{max}^2]$. The MATLAB simulation parameters are listed in Table 5.3 and no MAC layer is assumed [7]. Nodes are randomly distributed and several scenarios are studied, as described in Table 5.4, where SE random sensing events take place. Performance is studied for different network densities (the number of nodes N is varied), for different values of the maximum standard deviation of errors (σ_{max}) or different R . Similarly to subchapter 5.3, each scenario consists of a node distribution with accurate coordinates, where packet forwarding is made with MFR. During the same simulation, a number of η distributions with inaccurate locations (η being the number of trials/iterations) takes place, where the errors have been modeled as in subchapter 5.2. The figures are obtained through averaging over η .

The analysis covers several scenarios, similarly to [3,7]. The purpose of each scenario is to analyse the PDR in different conditions: for various network densities when the standard deviation of the location error is kept constant, when the network density and R are kept constant but the location error is increased, when the network density and location errors are kept constant and R is varied, when the number of sources

Simulator parameters (unit)	Symbol	Value
Transmission power (W) [110]	P_t	1.778
Distance of reference (m) [88, 92]	d_0	1
Path loss exponent [88, 92]	α	3
Packet size (bits) [95]	p_{size}	1024
Data rate (Kbits/s) [86]	dr	250
Number of packets/source [30]	$pkts$	1
Energy spent to operate the radio electronics (nJ/bit) [7]	e_{elec}	50
Energy per bit spent on transmission(J/bit) [96]	e_{tx}	2.5e-07
Energy per bit spent for reception (J/bit) [96]	e_{rx}	1.5e-0.7
Constant (pJ/bit/m ²) [7]	β	100
Network side length (m) [7, 82]	l	50

Table 5.3: Simulation parameters

is varied to 10 [30], 1 [53] or 50 or the number of iterations is varied to 100 [83], 1000 [7, 30], 300 [124]. As previously, the number of SE only impacts the amount of network traffic and congestion levels, but does not affect the evaluation of geographic routing in terms of throughput.

While the first three scenarios listed in Table 5.4 do not consider the use of any reception acknowledgement (ACK), in the fourth and fifth ones the performance of the algorithms is analysed for a best-effort type of packet forwarding [53]. The use of the ACK messages sent by receiving nodes increases the overhead of the network and influences the energy consumption mainly through the number of necessary retransmissions. Each forwarding node tries to transmit to each of its detected neighbours, until either the packet is received or all forwarding options are exhausted. Routing with reception confirmation does not imply a guaranteed delivery of the sent data packets; it is only a way of improving the reception chances and finding the path to D when one exists. Hence, when the networks have a good node density, the PDR is always above 98% for all algorithms. For sparse networks, the PDR changes depending on node topology and magnitude of the location errors.

The simulations using a realistic acknowledgement assumption have the purpose of

facilitating the energy consumption analysis of the algorithms by maintaining the same PDR for all algorithms. The differences in the design of the algorithms results in a different number of hops for the received packets, of retransmissions at each node and consequently in different levels of energy losses and network lifetime for each. The total energy consumed in a network (E_{total}) represents the sum of the energy spent on all packet transmissions (including the re-transmissions when no ACK is received) and of the energy spent receiving. The total number of transmissions is $TrNo$ and the energy spent on receiving is calculated based on the average number of hops in the path of each received packet, $HopNo$. Thus, the total energy consumed in a network is calculated as:

$$E_{total} = E_{trans} + E_{rcv},$$

$$E_{trans} = TrNo * e_{tx} * pkts * SE * p_{size},$$

$$E_{rcv} = HopNo * e_{rx} * pkts * SE * p_{size}.$$

For simplicity, the results for scenarios 4 and 5 and presented in parallel - all their parameters are the same, except the total number of transmitted data packets.

Scenario	N	R (m)	σ_{max} (m) (% of R)	η	SE	ACK
1	50-400	40 [83]	8 (20%) [3]	100 [83]	10	No
2	200	10 [7]	1-25 (10-50%) [7]	100 [83]	10	No
3	200	5-25 [7]	1 (20-4%) [3]	100 [83]	10	No
4	100-500	10 [7]	1.5 (15%) [3]	1000 [7, 30]	1	Yes
5	100-500	10 [7]	1.5 (15%) [7, 30]	300 [124]	50	Yes

Table 5.4: Simulation scenarios

5.4.3 Simulation results

Under all the scenarios, the PDR of the M-CMSER algorithm is higher than that of CMSER or LED. In Figure 5.5 the number of nodes is increased gradually from 50 to 400 nodes. As expected LED has a better performance than CMSER, but its PDR is not as good as that of M-CMSER, which uses the same distance-energy metric as LED. Because of the speed of the simulation, only 10 sensing events were chosen to take place in these networks, generating 10 traffic connections. If more were used, the PDR values would also be influenced.

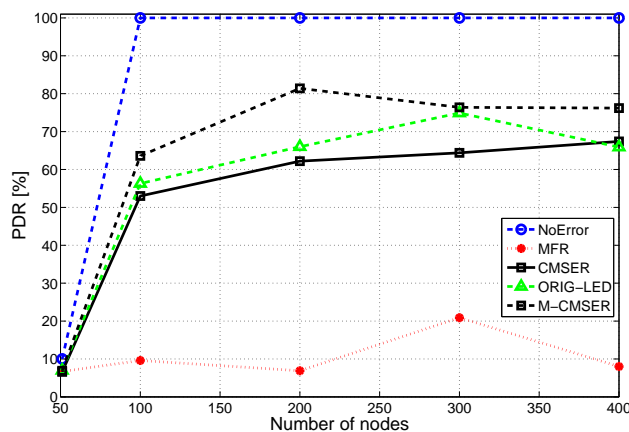


Figure 5.5: Routing performance for scenario 1, with M-CMSER

For Scenario 2, N and R are decreased and the location error is increased. The PDR decreases considerably for all algorithms, as in Figure 5.6. CMSER and M-CMSER have a similar behaviour, with a difference in PDR which shows the superiority of M-CMSER. When σ_{max} is below 30% of R , the PDR is above 60% for CMSER and above 70% for M-CMSER. So, if a tolerable amount of location error is associated with the case when σ_{max} is up to 10% of R , then M-CMSER is the most indicated choice for routing because it provides a PDR of 85%. Due to the reduced R in Scenario 2, LED maintains the PDR values under 60% and is constantly lower in delivery in comparison to CMSER and M-CMSER.

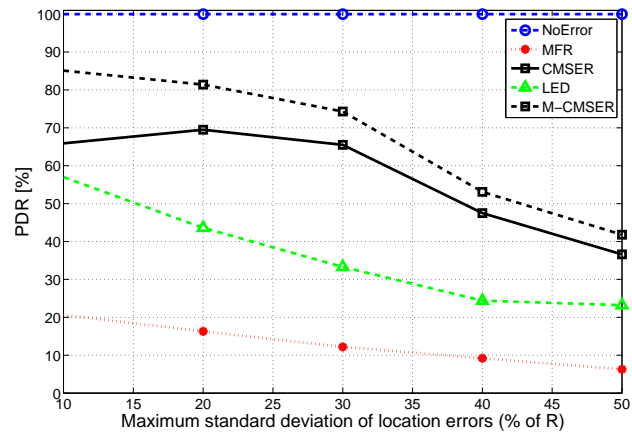


Figure 5.6: Routing performance for scenario 2, with M-CMSER

However, Figure 5.7 which considers an increase in R , while keeping the location error constant, reveals the change in behaviour for the LED algorithm. While LED performs worse than CMSEER for $R \leq 10$, its PDR is similar to M-CMSER for larger values, reaching 90% values for $R \geq 15$. Nevertheless, M-CMSER is preferred to LED because it performs better for small values of R making it more energy efficient.

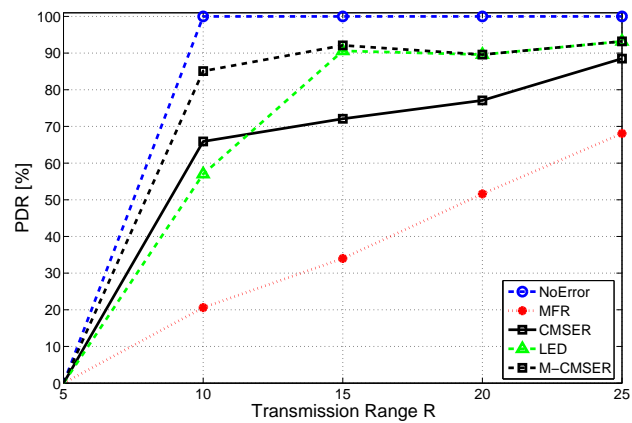


Figure 5.7: Routing performance for scenario 3, with M-CMSER

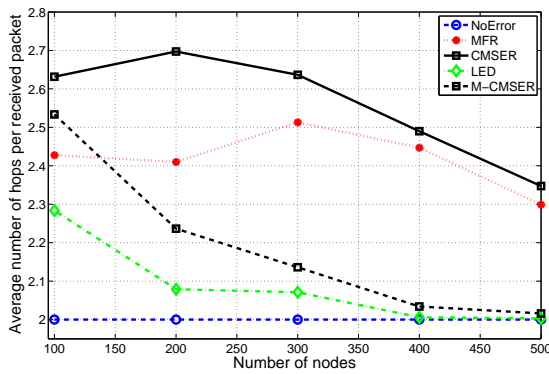
The following results are obtained for the networks where the routing benefits from packet acknowledgement. For the two scenarios in Figure 5.8, the hop count values are mainly influenced by the number and position of the sources in the network.

In scenario 4 the one source sending packets has its erroneous location varied for each iteration, but the distance between it and D does not change considerably, being limited by the error variance. For scenario 5, the 50 different sources affect the number of hops of the received packets severely because the sending nodes are located at different distances from D . An average hop count will vary on the average distance between them and D , which does not coincide with the one in scenario 4.

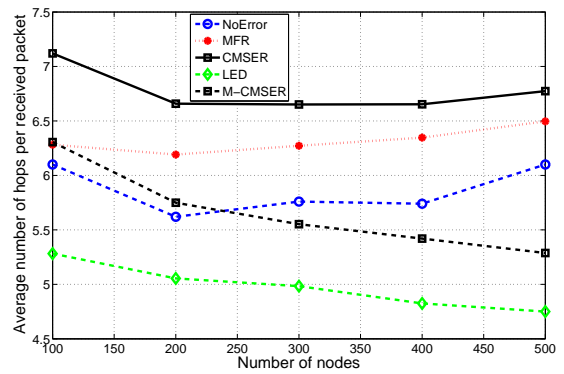
For scenario 4, the average number of hops for the received packets in the network does not vary much from one algorithm to the next (being approximately 2 or 3 hops). Also, as expected, LED provides shorter paths than CMSEER and M-CMSEER, but this does not mean it is more energy efficient (as can be seen in Figure 5.11). Naturally, the hop count decreases with the increase in node density which contributes to the increase of the forwarding options, but none of the networks chooses a shorter path than the network with no location error. Between CMSEER and M-CMSEER, the improved version of the algorithm provides visibly shorter routes.

For scenario 5, the figure reflects that M-CMSEER provides routing paths similar to the network with no location error, improving for the denser networks with more than 300 nodes. LED however chooses even shorter paths to guarantee the same PDR. Although this can be seen as an advantage, the trade-off is a higher number of retransmissions which consume energy and whose numbers rise for denser networks. An overall analysis indicates that LED is also more suitable for sparser networks.

The more ineffective the calculations of the routing algorithm are (of what the next forwarding node should be), the more transmissions will be necessary. It is thus estimated that when nodes are located accurately, there will be no need for retransmissions and, when in error, MFR and LED will make use of more retransmissions than CMSEER and M-CMSEER. This expectation is confirmed in Figure 5.9. The



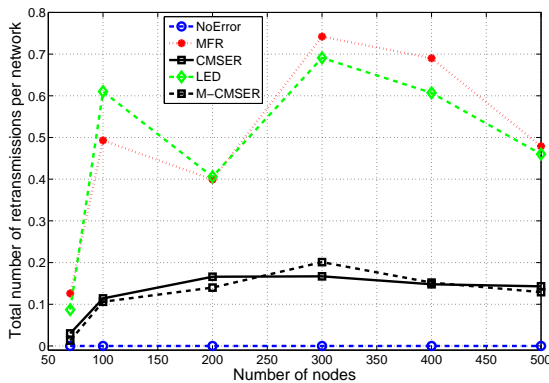
(a) Scenario 4



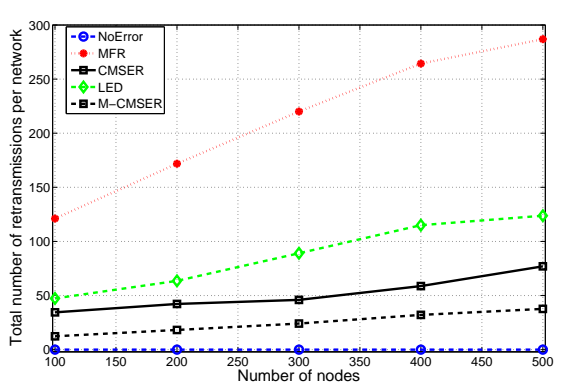
(b) Scenario 5

Figure 5.8: Average number of hops per received packet, in networks with ACK

number of total transmissions depends on the number of retransmissions and on the number of hops of the received packets. Because the routing paths of the received packets for the CM SER algorithm are longer than any other, but its number of retransmissions are fewer than that of MFR or LED, the total number of transmissions situate it above LED and under MFR, as it can be seen in Figure 5.10.



(a) Scenario 4



(b) Scenario 5

Figure 5.9: Total number of retransmissions in networks with ACK

The energy costs are presented in Figure 5.11. Simulations show that M-CM SER is energy efficient, while providing the same PDR as the rest of the algorithms.

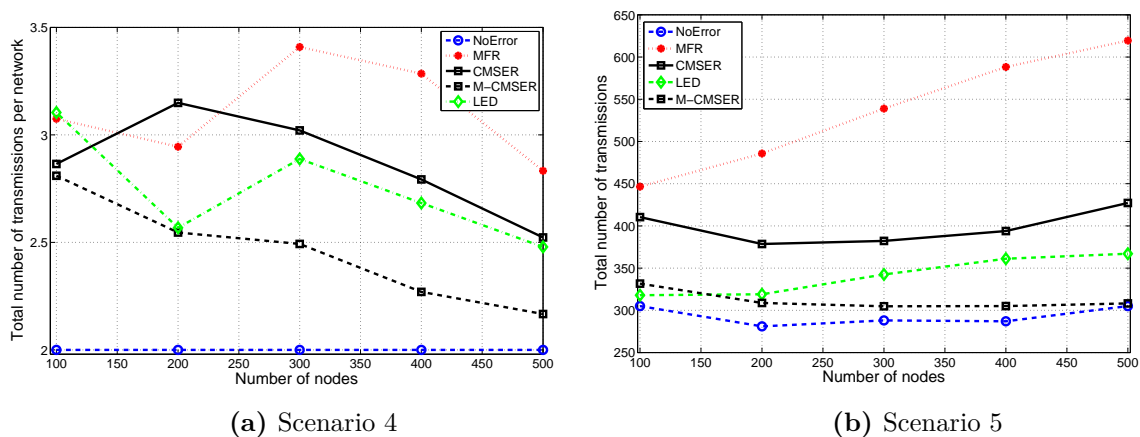


Figure 5.10: Total number of transmissions in networks with ACK

For Scenario 4, M-CMSEr is the most energy efficient being surpassed only by the network in which nodes benefit from exact location knowledge. In this case, LED is the second most energy efficient algorithm, followed by CMSEr whose longer routing paths cause more energy consumption. CMSEr is slightly more wasteful due to error-aware decisions based only on a distance metric, without consideration for energy-optimal forwarding choices. For all the algorithms, the energy expenditure is reduced by increasing the network density. For Scenario 5, M-CMSEr, LED and the network with no location error have a similar energy consumption level, with a slight decrease for M-CMSEr when increasing the number of nodes in the network.

5.5 Conclusions

Making geographic routing algorithms resilient to location error is imperative as this type of routing is energy efficient and very suitable to large scale networks. In subchapter 5.3, a novel routing algorithm, CMSEr, is proposed, whose performance in terms of throughput is considerably better when compared to other basic greedy routing techniques such as those employed of MFR, MSER, COND and MED. The

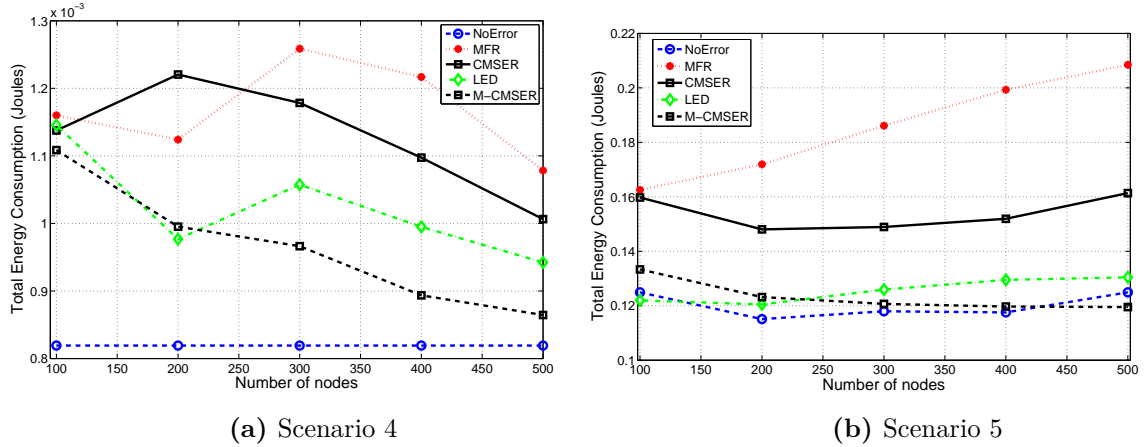


Figure 5.11: Total energy consumption in networks with ACK

PDR is analysed under different network sizes, error characteristics and communication ranges and all results confirm that CMSER outperforms other algorithms when the network objective is to increase the throughput. Overall energy costs are also kept down to a minimum. CMSER makes use of the notion of maximum advance to destination, but gives more importance to the probability of success when coordinates are affected by location error. As a consequence, the energy spent on lost routing packets is considerably decreased. While the paths of the received packets of CMSER may be longer, the routes of the lost packets are kept short, being surpassed only by MFR, which does not cope with location error at all.

Subchapter 5.4 presents a modified version of the CMSER algorithm, M-CMSER, whose focus is equally distributed between maximizing the throughput and minimizing energy consumption. The improved algorithm makes use of a neighbour selection technique which was previously employed by LED and provides the possibility to compare the novel proposal to LED, this time on a similar basis. All the simulated scenarios prove that M-CMSER performs better than LED in terms of both PDR and overall energy consumption. The behaviour of M-CMSER is conditioned by network node density, making it ideal for large scale networks. Under the same

location error and energy constraints as other algorithms, M-CMSER is an optimal routing candidate for WSN applications in need of efficient, location error-coping geographic routing. It is a robust solution when sensor devices use low transmission power and has been proven energy efficient because of the number of required retransmissions for a best-effort routing scenario with reception acknowledgement. Even with slightly longer paths than LED, it performs better in terms of throughput (as seen when no ACK is used) and energy savings alike.

Although geographic routing solutions resilient to location errors have been provided in this chapter, the current algorithms are not fully developed to the degree that a protocol or standard would be. Furthermore, the approaches of MSER, CMSER and M-CMSER are based on the simplifying assumption that the location errors of each node are the same for the x and y coordinates. This facilitates the statistical supposition that the distances between nodes are Ricianly distributed. Because the initial assumption is clearly not always true, it is believed to contribute to a less-realistic routing behaviour. The impact of this theoretical presumption on the proposed algorithms is explored in chapter 6.

6 On the Rician assumption for geographic routing design

Geographic routing algorithms for WSNs need to be resilient to location errors inherent with positioning algorithms. As seen from the previous chapters, proposed forwarding algorithms in the literature make use of statistical assumptions of Gaussianly distributed location coordinate estimates and Ricianly distributed distances between sensor nodes. However the validity of the Rician hypothesis is questionable when designing realistic geographic routing algorithms because it depends on simplified theoretical assumptions. To verify it and to check its impact on the routing performance, realistic localisation simulation is also necessary. Therefore, in this chapter, a realistic method of localisation is used, based on received signal strength (RSS) ranging using the linear least squares method (LLS) [12,13]. The RSS method of ranging is chosen over others because it is suitable for smaller networks and allows fast simulation processing. However, possible future work can make use of TW-ToA ranging or other methods of localisation, i.e. AoA.

Anchor nodes estimate the position of the target sensor nodes and their error characteristics. Location error values are random in reality and their variance for the x and y coordinates may or may not be the same. No physical environmental factors are considered that may affect their values (i.e. wind currents), but differences

may still exist because of the network geometry (number and position of the anchor nodes) [11, 29]. This is also shown via simulation in the following subchapters.

As mentioned before, geographic routing algorithms which cope with inaccurate position knowledge of the nodes are based on a chain of statistical assumptions, amongst which, one is that of equality of the location error variance for the x and y coordinates of the same node. When RSS ranging is used for the localisation, the error statistics for the x and y coordinates of each node are assumed to be the same in order for the Rician assumption of distance estimates to be valid. However if the theoretical calculations or the simulation results of these statistics are not the same (or not assumed to be the same) then node distances may also not be Ricianly distributed. Consequently, the routing algorithms using this assumption may not perform optimally either. Several tests are used to analyse this observation. Simulation results confirm that the Rician assumption is not true in most cases for practical localisation (be it RSS based or otherwise). To counter the negative impact of incorrect statistical assumption, two packet forwarding alternatives are proposed, with a statistically correct approach.

6.1 Problem statement

Efficient geographic routing algorithms for WSNs are designed to cope with inaccurate localisation [3, 7, 8]. The widely used mathematical error model considers location errors as random variables (RVs) Gaussianly distributed with $N(\mu, \sigma^2)$ (where the mean $\mu = 0$ and σ^2 is the finite variance) (see equation 3.4), which facilitates the assumption that the measured distance \hat{d}_{ij} between any two nodes i and j is Ricianly distributed with $R(\nu, \sigma_{ij})$ (ν is the non-centrality parameter and σ_{ij} is the scale parameter with the expression from equation 5.4). R has a Rice distribution

(see equation 5.1) if $R = \sqrt{X^2 + Y^2}$, where X and Y are statistically independent normal RVs distributed with $N(\nu \cos \theta, \sigma_{ij}^2)$ and $N(\nu \sin \theta, \sigma_{ij}^2)$, where $\theta \in R$. The RVs X and Y are represented by $(\hat{x}_i - \hat{x}_j)$ and $(\hat{y}_i - \hat{y}_j)$, where $\hat{x}_i, \hat{x}_j, \hat{y}_i, \hat{y}_j$ are themselves normally distributed RVs.

The distribution of the difference of two normally distributed variates, $(\hat{x}_i - \hat{x}_j)$ or $(\hat{y}_i - \hat{y}_j)$, is also Gaussian with mean $\mu = \mu_i - \mu_j$ and variance $\sigma_{ij}^2 = \sigma_i^2 + \sigma_j^2$. The distribution of R is Rician only if X and Y have the same variance σ_{ij}^2 . This is the equivalent of the variance in any node i or j being the same on the x and y axes: $\sigma_{ix}^2 = \sigma_{iy}^2$ (referred to as σ_i^2) and $\sigma_{jx}^2 = \sigma_{jy}^2$ (referred to as σ_j^2). Such a statistical presumption is a simplification of reality and can affect the forwarding algorithms based on Rician assumptions.

It is considered that N target sensor nodes are randomly distributed in the network having a location error model as described above. Received signal strength (RSS) ranging is used for localisation and simulated using the linear least square method (LLS) as in [12]. Following [12], the error variance associated with each node i is theoretically estimated using the trace of the covariance matrix:

$$MSE(\hat{\boldsymbol{\theta}}_i) = \text{Tr} \{ \text{Cov}(\hat{\boldsymbol{\theta}}_i) \}, \quad (6.1)$$

where $\hat{\boldsymbol{\theta}}_i = \begin{bmatrix} \hat{x}_i \\ \hat{y}_i \end{bmatrix}$ represents the estimated location via LLS, $\boldsymbol{\theta}_i = \begin{bmatrix} x_i \\ y_i \end{bmatrix}$ represents the true location coordinates and $\text{Cov}(\hat{\boldsymbol{\theta}}_i)$ is the covariance matrix:

$$\begin{aligned} \text{Cov}(\hat{\boldsymbol{\theta}}_i) &= E \left[(\hat{\boldsymbol{\theta}}_i - \boldsymbol{\theta}_i) (\hat{\boldsymbol{\theta}}_i - \boldsymbol{\theta}_i)^T \right] \\ &= E \left[\begin{bmatrix} \hat{x}_i - x_i \\ \hat{y}_i - y_i \end{bmatrix} \begin{bmatrix} \hat{x}_i - x_i & \hat{y}_i - y_i \end{bmatrix} \right] \end{aligned} \quad (6.2)$$

$$\begin{aligned}
 &= E \begin{bmatrix} (\hat{x}_i - x_i)^2 & (\hat{x}_i - x_i)(\hat{y}_i - y_i) \\ (\hat{y}_i - y_i)(\hat{x}_i - x_i) & (\hat{y}_i - y_i)^2 \end{bmatrix} \\
 &= \begin{bmatrix} E [(\hat{x}_i - x_i)^2] & E [(\hat{x}_i - x_i)(\hat{y}_i - y_i)] \\ E [(\hat{y}_i - y_i)(\hat{x}_i - x_i)] & E [(\hat{y}_i - y_i)^2] \end{bmatrix}.
 \end{aligned}$$

The main diagonal terms of the matrix in equation 6.2 represent the variance of the location error on the x and y axes. For x , the variance is:

$$\sigma_{ix}^2 = E [(\hat{x}_i - x_i)^2], \quad (6.3)$$

while for y coordinate it is:

$$\sigma_{iy}^2 = E [(\hat{y}_i - y_i)^2]. \quad (6.4)$$

The terms in the off-diagonal represent the covariance between the x and y location error and, if the RVs are independent,

$$E [(\hat{x}_i - x_i)(\hat{y}_i - y_i)] = E [(\hat{y}_i - y_i)(\hat{x}_i - x_i)] = 0.$$

The calculation of the theoretical MSE, from equation 6.1, as well as the theoretical variances σ_{ix-th}^2 and σ_{iy-th}^2 are presented in detail in [12]. The simulation of the LLS-RSS localisation takes place with a prescribed noise value s_{rss} (dB) reflected in the distance variance (m^2). The localisation simulation results in the erroneous coordinates \hat{x}_i and \hat{y}_i and the value of the variance for each target node i based on equation 6.1, $\sigma_{RSS}^2 = \sigma_{ix}^2 + \sigma_{iy}^2$. When the distances are assumed Ricianly distributed, then $\sigma_{ix}^2 = \sigma_{iy}^2 = \frac{\sigma_{RSS}^2}{2}$. However, they may not actually be equal in reality. The aim is to show that $\sigma_{ix}^2 \neq \sigma_{iy}^2$ and to analyse the impact of this inaccurate assumption on geographic routing performance. More accurate forwarding alternatives are needed.

6.1.1 Preliminary analysis

Three tests are used in this subchapter and their simulations benefit from similar assumptions. They are all proposed as methods of verification as to whether the RSS-resulted location variance confirms the theoretically calculated variance values of the x and y coordinates of i random nodes. The randomly deployed target nodes are localised through LLS-RSS by the anchors, placed at the edge of the square network (with side $l = 50$ [m], except for the first test where $l = 100$ [m] as well), in the corners, on the edges and in the centre [13]. The communication range R is kept the same in all the test, for all the target nodes ($R = 10$), while the transmission range of the anchors covers the entire network surface. The localisation process is simulated over η iterations.

The variance of the location error of the nodes is influenced only by the number and position of the anchors nodes. The number of target nodes is not relevant, but their position in regards to the anchor nodes is. For example, the coordinates of a centrally placed target node, which is equally far from all anchor nodes, will be estimated with more precision than a target node which is closer only to few anchor nodes. This has been discussed and presented in [11, 29].

Test 1: Comparison via simulation samples

A network of $N = 30$ and $M = 9$ is considered (anchors are placed on the edges, in the corners and in the center of the network) ($\alpha = 2.5$). Random nodes i are selected and a comparison is made between the average variance value resulting from the RSS localisation process, using $\frac{\sigma_{RSS}^2}{2}$ (averaged over $\eta = 100$), and the estimated values of σ_{ix}^2 and σ_{iy}^2 calculated in two ways: theoretically and through simulation.

The theoretical values of σ_{ix}^2 and σ_{iy}^2 (designated through σ_{ix-th}^2 and σ_{iy-th}^2) are calculated during the LLS-RSS localisation as the diagonal terms of the covariance

matrix (equations 6.3 and 6.4). The simulation-based values (designated σ_{ix-sm}^2 and σ_{iy-sm}^2) are calculated using $Var(X) = E[(X - E(X))^2]$, where X is represented by the erroneous coordinates of node i whose values are different for each iteration, $E(X)$ is the mean of X (the actual coordinates of node i).

The results of this initial test show $\sigma_{ix}^2 \neq \sigma_{iy}^2$ and that the RSS calculated variance is an approximation (an example is presented in Table 6.1). As the $\frac{\sigma_{RSS}^2}{2}$ value is an estimation, its accuracy depends on the target node position referenced to the anchor nodes and on the network size (RSS ranging is not suitable for large networks [11,13]). The values for σ_{ix}^2 and σ_{iy}^2 which are obtained through theoretical calculations are similar, but not equal.

TN	l	s_{rss}	$\frac{\sigma_{RSS}^2}{2}$	σ_{ix-sm}^2	σ_{iy-sm}^2	σ_{ix-th}^2	σ_{iy-th}^2
4	100	0.6	37.69	27.82	23.93	36.68	38.70
10	100	0.6	44.00	32.71	33.89	42.93	45.07
4	100	1	63.25	46.10	40.02	61.55	64.95
25	50	1	7.84	5.01	6.71	7.49	8.19
2	50	0.6	9.61	8.87	9.62	9.32	9.90
27	50	0.6	6.72	5.25	6.43	6.40	7.04
3	50	1.5	12.48	15.89	8.88	12.67	12.28
10	50	1.5	27.92	20.71	22.02	27.24	28.61

Table 6.1: Results for test 1

Test 2: Network visualisation comparison

This test aims to illustrate the location error of the nodes, when estimated with equal or different variance for the x and y coordinates. The simulations consider $N = 10$ and $\eta = 100$ and the employed scenarios are listed in Table 6.2. Using the LLS-RSS localisation, the variations are made for the PLE α , the number M and position of the anchor nodes and for the noise value s_{rss} .

The theoretical values σ_{ix}^2 and σ_{iy}^2 are calculated for each node i and compared with the values $\frac{\sigma_{RSS}^2}{2}$ obtained from the simulation.

Scenario	α	M	s_{RSS}
1	2	9	0.6
2	2.5	9	0.6
3	3	9	0.6
4	3.5	9	0.6
5	2.5	5	0.6
6	2.5	6	0.6
7	3	6	0.6
8	3	5	1

Table 6.2: Scenarios for test 2

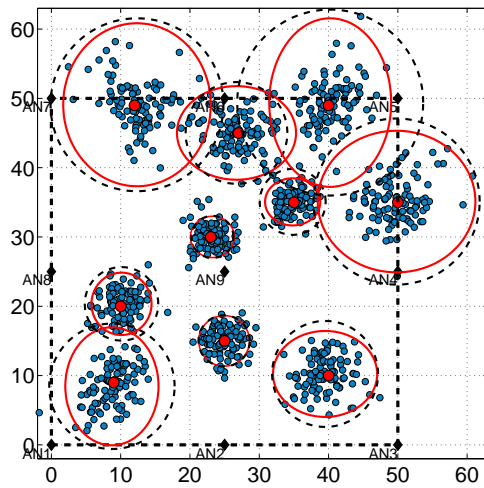
The black dashed circles represent the area where the estimated positions of the nodes are considered to be when $\sigma_{ix}^2 = \sigma_{iy}^2$ (centred is the accurate location of node i , of radius $\frac{\sigma_{RSS}^2}{2}$). The red ellipses represent the areas of the estimated positions when $\sigma_{ix}^2 \neq \sigma_{iy}^2$ (centred is accurate location of node i , with ellipse axes $\sigma_{ix}^2, \sigma_{iy}^2$).

Aside from facilitating the possibility to observe the difference in the area covered by the circles and that of the ellipses, the Scenarios 1, 2, 3 and 4 in Figure 6.1 illustrate how a larger α makes the location estimation more accurate (notice the decreased area of both the ellipses and the circles). Figure 6.2 shows the influence of the anchor positions on the localisation process. By reducing the number of the anchors and removing them from the middle of the edge (Scenarios 5 and 8), the localisation loses from its overall accuracy, but not as much as when eliminating anchors from key positions, such as all the ones on the north side of the network, affecting the localisation especially in this region (Scenarios 6 and 7). While all the error ellipses of the nodes in Scenarios 5 and 8 become larger and flatter, in Scenarios 6 and 7 it is mostly the nodes on the north side that are affected by the change and their error ellipses are particularly larger and more elongated.

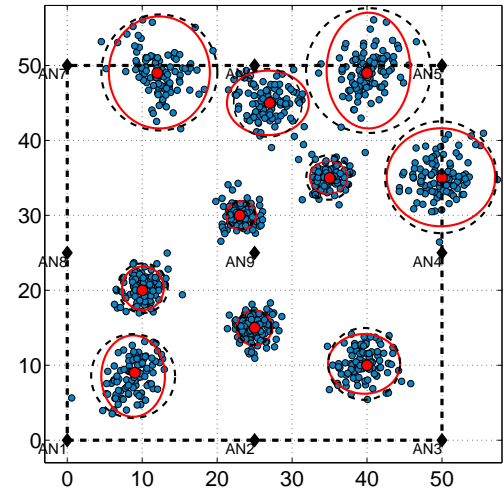
In this study, it has been assumed that the location errors on the x and y axes are independent and therefore uncorrelated. Consequently their covariance is zero and the minor and major axes of the error-ellipses are parallel to the x and y axes.

6.1 Problem statement

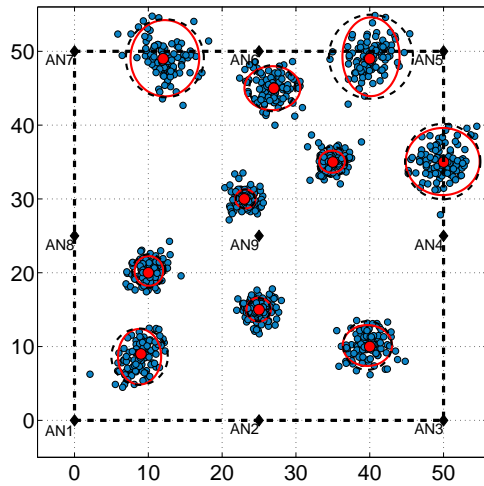
However, in reality, the error on the two axes may be correlated to a degree (as the LLS-RSS localisation process shows) and this would imply that the error ellipses are rotated according to an angle whose calculation is based on the correlation matrix. This case is not illustrated, but it is one more example of a simplifying assumption on which some routing algorithms are based.



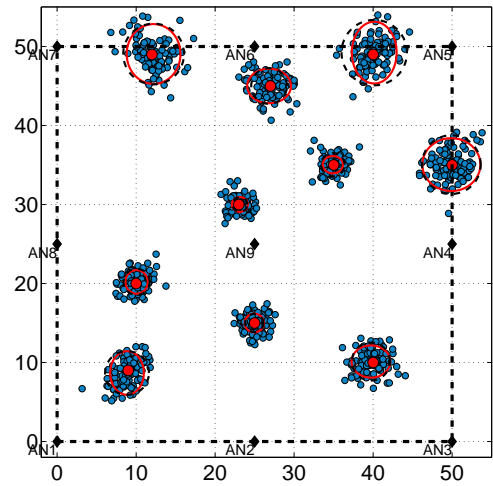
(a) Scenario 1



(b) Scenario 2



(c) Scenario 3



(d) Scenario 4

Figure 6.1: Varying α

Test 3: Cumulative distribution function comparison

In this test $N = 2$, $M = 9$ and $\alpha = 2.5$. As the distance between target nodes is a

6.1 Problem statement

multivariate random variable (depending on the σ^2 of both coordinates of two target nodes), the cumulative distribution function (CDF) is used to verify the non-Rician hypothesis for the LSS-RSS localisation resulted errors: $F_X(x) = 1 - Q_1\left(\frac{d_{ij}}{\sigma_{ij}}, \frac{\hat{d}_{ij}}{\sigma_{ij}}\right)$, where Q_1 is the Marcum Q-function.

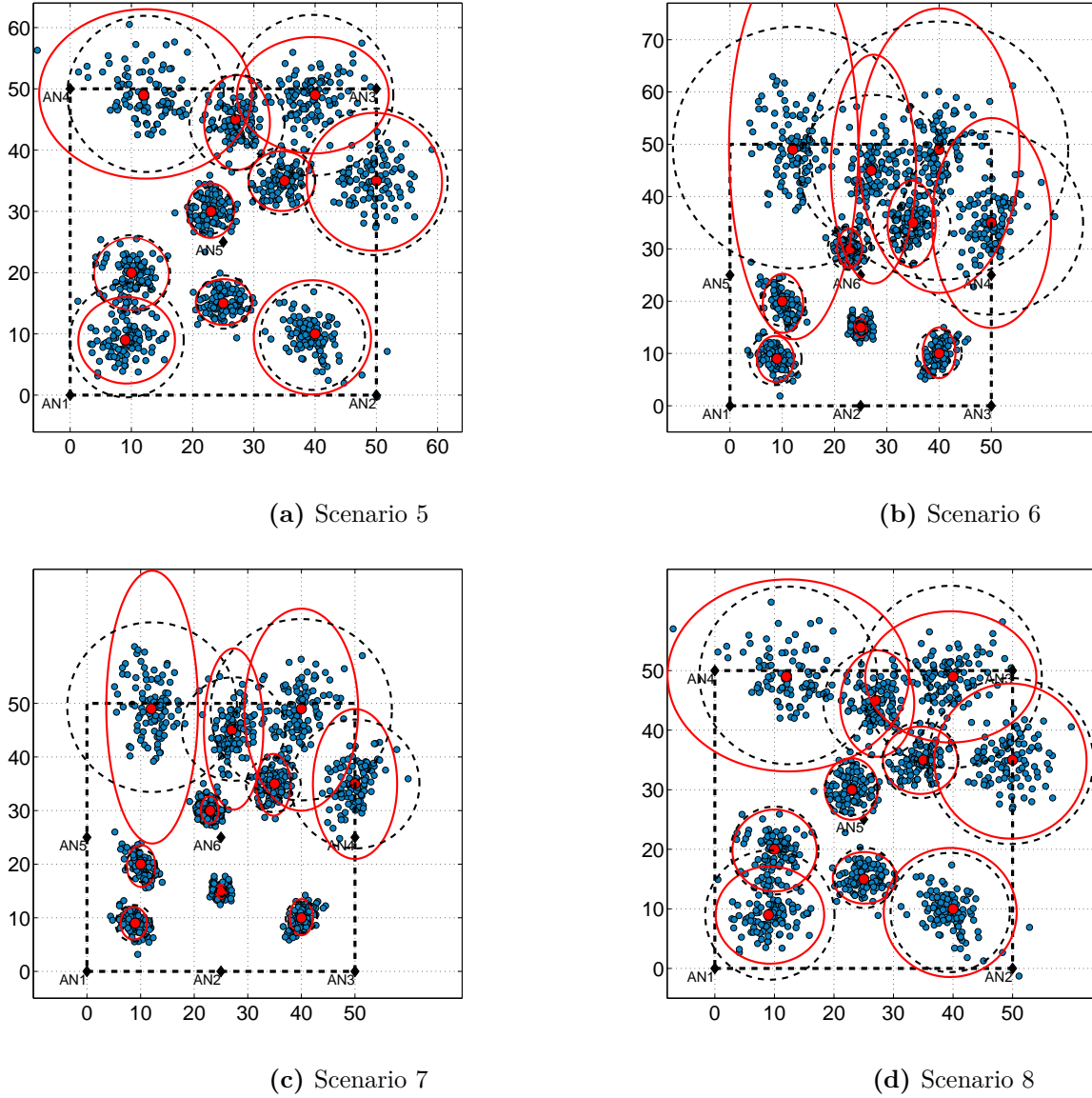


Figure 6.2: Varying the anchor node placement and the noise values

Firstly, the location error of two target nodes is considered Gaussianly distributed, so $\sigma_i^2 \neq \sigma_j^2$ and $\sigma_{ix}^2 = \sigma_{iy}^2$ and $\sigma_{jx}^2 = \sigma_{jy}^2$. Both the theoretical as well as the empirical

Rician CDFs are computed, the empirical CDF using simulation-obtained estimated distances \hat{d}_{ij} , for $\eta = 1000$. Secondly, the theoretical and empirical Rician CDFs are calculated for the same nodes, when these are located through LLS-RSS. The estimated \hat{d}_{ij} are taken from the anchors, which perform the ranging over the same η as before. To calculate the scale parameter σ_{ij} , the theoretical Rician CDF (for the RSS case) assumes $\sigma_{ix}^2 = \sigma_{iy}^2$ and $\sigma_{jx}^2 = \sigma_{jy}^2$. The CDFs can be seen in Figure 6.3.

For the target nodes with Gaussian errors and an equal variance on both x and y axes, the theoretical and empirical CDFs overlap as a confirmation that the distances are Ricianly distributed. For RSS estimated node coordinates and variances, it is not accurate to assume the error variance is equal on the x and y axes. The difference in the CDF curves shows that such an assumption would implicitly lead to a suboptimal routing performance when the forwarding decisions are based on Rician statistics.

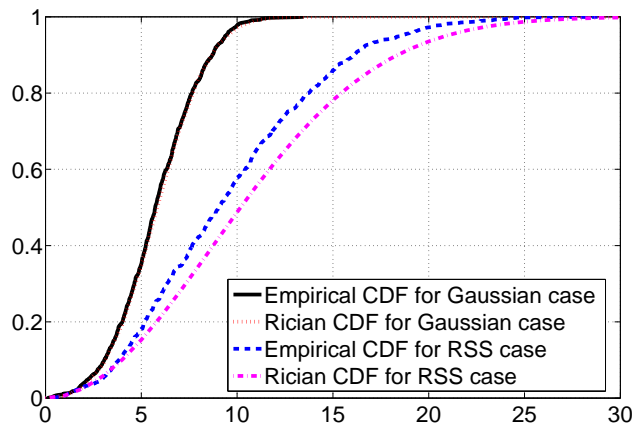


Figure 6.3: CDF analysis

6.2 Non-Rician geographic routing solution

Two new algorithms are proposed, non-rician mean square error ratio (NR-MSER) and non-rician conditioned mean square error ratio (NR-CMSER), adaptations of the propositions in chapter 5. The forwarding is made on the same principles as

before, but the algorithms are adapted to cope with the difference in the x and y location error. They no longer use the Rician expectation and variance in their calculations. By assuming the mean equal to the actual distance $E(\hat{d}_{ij}) = d_{ij}$, the mathematical expression of the mean square error from equation 5.9 changes into:

$$NR MSE_{ij} = E(\hat{d}_{ij}^2) - d_{ij}^2. \quad (6.5)$$

$E(\hat{d}_{ij}^2)$ is calculated as previously:

$$\begin{aligned} E(\hat{d}_{ij}^2) &= E(\hat{x}_i^2 - 2\hat{x}_i\hat{x}_j + \hat{x}_j^2 + \hat{y}_i^2 - 2\hat{y}_i\hat{y}_j + \hat{y}_j^2) \\ &= E(\hat{x}_i^2) + E(\hat{x}_j^2) + E(\hat{y}_i^2) + E(\hat{y}_j^2) - 2E(\hat{x}_i\hat{x}_j) - 2E(\hat{y}_i\hat{y}_j). \end{aligned}$$

And using the second moments, which are now different from those in chapter 5, $E(\hat{x}_i^2) = x_i^2 + \sigma_{ix}^2$, $E(\hat{y}_i^2) = y_i^2 + \sigma_{iy}^2$, $E(\hat{x}_j^2) = x_j^2 + \sigma_{jx}^2$ and $E(\hat{y}_j^2) = y_j^2 + \sigma_{jy}^2$, the equation 5.11 becomes:

$$E(\hat{d}_{ij}^2) = \sigma_{ix}^2 + \sigma_{iy}^2 + \sigma_{jx}^2 + \sigma_{jy}^2 + x_i^2 + x_j^2 + y_i^2 + y_j^2 - 2x_ix_j - 2y_iy_j. \quad (6.6)$$

Consequently the MSE of the new algorithm NR-CMSER has the following expression, where d_{ij} is not known, so in simulations \hat{d}_{ij} is used instead:

$$NR MSE_{ij} = \sigma_{ix}^2 + \sigma_{iy}^2 + \sigma_{jx}^2 + \sigma_{jy}^2 + x_i^2 + x_j^2 + y_i^2 + y_j^2 - 2x_ix_j - 2y_iy_j - d_{ij}^2, \quad (6.7)$$

The mean square error ratio (MSER) is calculated, for a balanced selection of the forwarding node and NR-MSER makes its decision by minimizing the MSE and maximizing the distance between i and j :

$$NR MSER_{ij} = NR MSE_{ij} / \hat{d}_{ij}. \quad (6.8)$$

Consequently, part of the routing decision is made using:

$$F_j = \arg \min (NRMSER_{ij}). \quad (6.9)$$

The NR-CMSER also makes use of an additional, modified condition where $Var(\hat{d}_{ij})$ is replaced with the sum of the average variance in the x and y coordinates of the two nodes i and j ,

$$(R - \hat{d}_{ij})^2 > \frac{\sigma_{ix}^2 + \sigma_{iy}^2}{2} + \frac{\sigma_{jx}^2 + \sigma_{jy}^2}{2}. \quad (6.10)$$

6.2.1 Simulations and results

Although the preliminary analysis already proved that the Rician assumption is not correct, it is still necessary to test the impact it has on the geographic routing performance using the algorithms discussed in this thesis and the solutions proposed in the previous subchapter: NR-MSER and NR-CMSER.

Firstly, the performance of the algorithms MFR, MED, LED, MSER, CMSER is studied in two cases: when the routing makes use of Gaussian location errors and the Rician distance assumptions are correct, and when the location error is no longer Gaussian and the Rician assumptions are erroneous.

Secondly, MFR, MSER, CMSER, NR-MSER and NR-CMSER are analysed to confirm the validity of the proposed solutions.

6.2.1.1 First method of simulation-based analysis

The simulations in this subchapter, consider two different assumptions on how nodes are informed about their location error. The first simulation uses Gaussian-generated location error (Ge), whose variance is user-prescribed, while the second

uses LLS-RSS localisation, which performs its own statistical calculations of the location error variance (RSSe). Both simulations make use of Rician assumptions for the distance estimates, but only the first is accurate in its assumptions. It is therefore expected that the performance of the simulated algorithms be better for the Gaussian-generated location error, than for the RSS based one. The performance is measured in terms of PDR versus the increase in location error.

The following paragraphs contain an explanation of how the two simulations are designed and how they differ in functionality. To be able to compare their results on a similar basis, an estimation of the standard deviation of the location error σ is needed, as a percent of R . For both simulations, the considered parameters are $\eta = 100$, $l = 50$ (m), $N = 200$, $\alpha = 3$, $R = 10$ (m), $SE = 10$, $pkts = 1$. The level of accuracy in the estimation of σ as a percent of R is debatable, so it will not be the only measure of how the Rician assumption impacts the routing performance.

1. Simulation with Gaussian-generated location error: In this case a maximum variance value ($max \sigma^2$) is prescribed by the user. With this input, the program generates a number of random integer values representing the variances (σ^2) of the target nodes (each for one node, equal in value for the x and y coordinate and kept the same during each iteration η). The location error itself is different for each node (and during each iteration), being a normally distributed RV with zero mean and standard deviation (σ) whose value is obtained from the previously generated random variances σ^2 .

To estimate the average σ as a percent of R , because $R = 10$ an approximate σ should be respectively equal to 1-5(m), representing 10-50% of R . This means that σ^2 should be equal to 1-25(m²). These are the values prescribed as $max \sigma^2$.

2. Simulation based on LLS-RSS localisation: In this case the location error variance of each node is calculated to be $\sigma_{ix}^2 = \sigma_{iy}^2 = \frac{\sigma_{RSS}^2}{2}$. The simulator uses the prescribed

σ	1	2	3	4	5
σ (% of R)	10	20	30	40	50
$max \sigma^2$	1	4	9	16	25

Table 6.3: Correspondance table for Ge simulation

noise value s_{rss} (dB), which affects the estimated positions of the nodes and their estimated variances, $\sigma^2 = \frac{\sigma_{RSS}^2}{2}$ (m), and standard deviations, σ (m). So in this case σ^2 is not prescribed as previously; it is calculated in the RSS localisation stage. It will therefore be necessary to detect which value of s_{rss} results in a σ representing a percentage of R .

To estimate the average σ as a percent of R , η iterations are simulated and, for each iteration, the variances σ^2 of all the nodes are saved. With this information, either the average is calculated $mean \sigma^2$ or the maximum value is extracted, $max \sigma^2$. The results are then averaged over η iterations to then calculate σ as a percentage.

s_{rss} for $max \sigma^2$	s_{rss} for $mean \sigma^2$	σ (% of R)
0.08	0.2	10
0.3	0.7	20
0.6	1.5	30
1	2.6	40
1.5	4	50

Table 6.4: Correspondance table for RSSe simulation

Because in the LLS-RSS case there are two possibilities for the calculations of σ^2 , simulations were performed for both. However, observing that the simulation with Gaussian-generated location error makes use of a “maximum” variance ($max \sigma^2$), the estimations made for the RSS case seems to be more accurate when using the maximum σ^2 (Figure 6.5), instead of an average σ^2 (Figure 6.4). Figure 6.4 and Figure 6.5 illustrate the performance of the algorithms for the simulations with Gaussian-generated location error (Ge) in coloured bars and for the simulation based on LLS-RSS-measured location error (RSSe) in black bars. The legend of the figures

shows the use of the algorithms MFR, MED, MSER, LED, CMSER, together with the type of simulation used for that particular algorithm (Ge or RSSe).

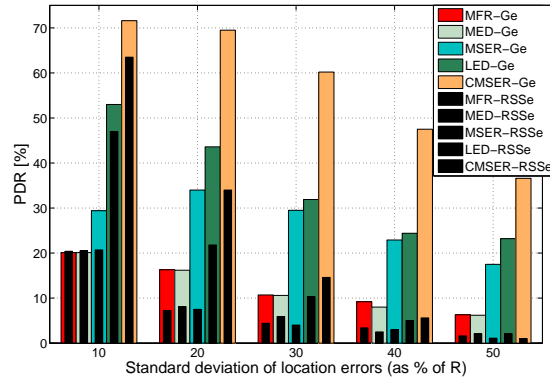


Figure 6.4: Routing performance (average σ^2 case)

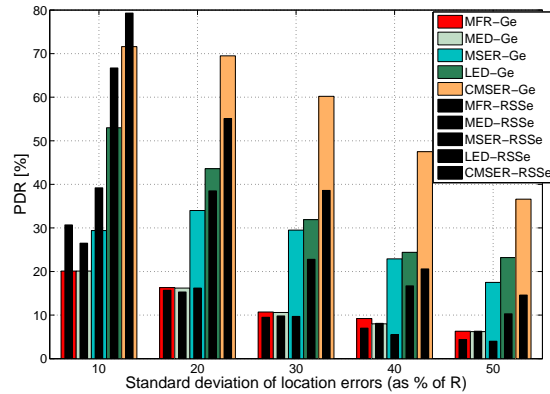


Figure 6.5: Routing performance (maximum σ^2 case)

For both cases, the PDR naturally decreases with the standard deviation of location errors, calculated as a percent of the R increase. The figures confirm that the CMSER outperforms MFR, MED, MSER and even LED. LED is outperformed because of the assumed R ; for larger values of R , LED could outperform CMSER, but would not outperform M-CMSER, as it can be seen in Figure 5.7).

According to the expectations, in both Figure 6.4 and Figure 6.5 the Ge case (seen in coloured bars) provides better results for all algorithms because of their correct assumption that the inter-nodal distances are Rician RVs. In the RSSe case,

because the Rician assumption is not necessarily true, the routing performance degrades. The PDR difference in performance between the Ge and RSSe simulations is noticeably higher in Figure 6.4 than in Figure 6.5. However, the results which are considered more accurate, in Figure 6.5, do suffer a change in performance when standard deviation $\sigma = 10\%$ of R , leading to better results for the RSSe case. This is explained by the small location error and small difference between the error in the x and y coordinates, thus making the RSS localisation process more accurate.

Although the two graphs show a difference between the two cases (Ge and RSSe), further simulations are needed because the comparison is based on presumptions of a similitude in location error (the quantity is estimated and possibly in error).

6.2.1.2 Second method of simulation-based analysis

In this subchapter, the performance study is dedicated to the proposed solutions NR-MSER and NR-CMSER, which are compared with their Rician-based algorithmic counterparts. The simulation is based on LLS-RSS localisation. MSER and CMSER make use of inaccurate Rician assumptions and, unaware of a difference between the x and y error of node i , use $\sigma_{ix}^2 = \sigma_{iy}^2 = \frac{\sigma_{RSS}^2}{2}$ in their decisions. The provided solutions, NR-MSER and NR-CMSER, are designed to cope with $\sigma_{ix}^2 \neq \sigma_{iy}^2$ and are expected to perform the same or better than MSER and CMSER. The PDR is analysed for $\eta = 1000$, $l = 50$, $N = 200$, $M = 5$ (placed in the corners and centre of the network), $\alpha = 3$, $R = 10$, $SE = 10$, $p_kts = 1$ and increasing values of the s_{rss} .

For the smallest values of $s_{rss} = 0.1$, the highest PDR is reached, 54% for MSER and NR-MSER and 85% for CMSER and NR-CMSER. As s_{rss} is increased, reaching the value of 1, the routing performance for all algorithms degrades to such a level that the PDR becomes 15% for MSER and NR-MSER or 30% for CMSER and NR-CMSER. In Figure 6.6 the PDR of the non-Rician algorithms remains approximately

the same as that of the Rician ones. Because one would expect a bigger difference in routing performance, it is considered that the routing performance may be affected only by a large difference in σ_{ix}^2 and σ_{iy}^2 . Such a scenario may exist and the large difference in the x and y variance may be undetected by the localisation system, depending on its method of estimation, accuracy, number of anchors and network area. This possibility is tested in Figure 6.7.

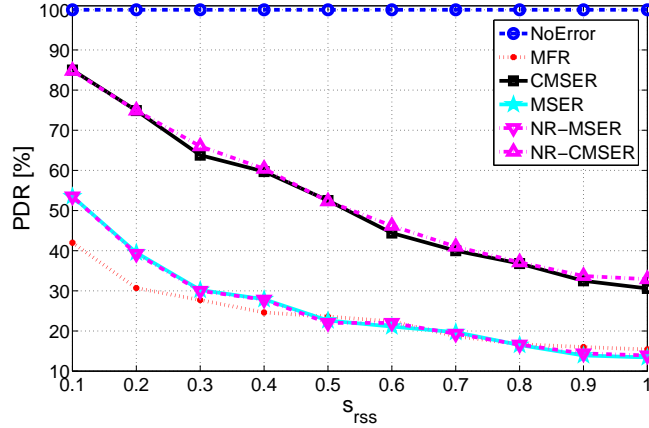


Figure 6.6: Performance based on RSS localisation

The difference in the x and y error is increased “artificially” by considering $\sigma_{ix}^2 = \frac{\sigma_{RSS}^2}{2}$ as obtained from the LLS-RSS localisation process and $\sigma_{iy}^2 = 3\sigma_{ix}^2$. MSER and CMSEr are unaware of this difference (all according to the hypothesis that the localisation method does not reflect accurately the difference in the actual error on the x and y axes) and still use $\sigma_{ix}^2 = \sigma_{iy}^2 = \frac{\sigma_{RSS}^2}{2}$. In this new scenario (Figure 6.7), although the PDR for all algorithms is smaller, the NR-CMSEr algorithm performs better. The test illustrates that only large differences in σ_{ix}^2 and σ_{iy}^2 reveal the improvement of the new algorithms.

Overall, the performance of the new algorithms is either the same or better than the un-adjusted counterparts and most importantly, NR-MSEr and NR-CMSEr are formulated correctly and cope with realistic location error differences.

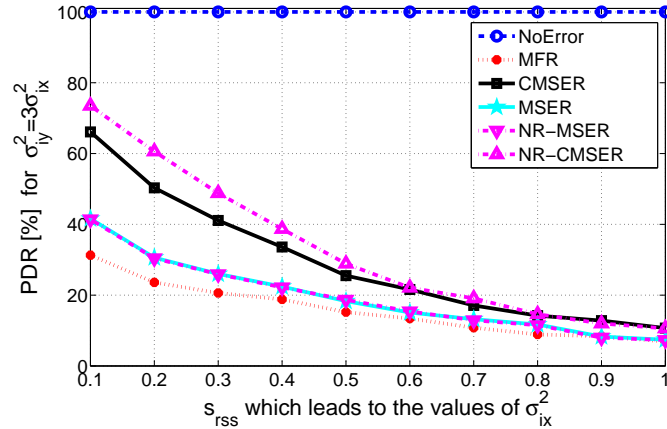


Figure 6.7: Performance based on RSS resulted σ_{ix}^2 , but with large σ_{iy}^2

6.3 Conclusions

Analysis through the above described methods proves the Rician assumption is not valid when nodes are located through realistic localisation methods (RSS or otherwise) because the error variance in the x and y coordinates of a node may not be the same (as the Rician assumption implies). The main contribution of chapter 6 is the analysis made for the RSS localisation and, although there are differences in the error variance of the x and y coordinates, they are not considerable. Similar studies can be made for TW-ToA ranging or for other methods of localisation and it is anticipated that in some cases, the process will result in more considerable differences in the error variance. However, due to time constraints such simulations have not been included in this thesis. While Rician-based algorithms can perform well in simulations, their results are not realistic and the performance can be affected by a large difference in the x and y error. The proposed geographic routing algorithms NR-MSER and NR-CMSER realistically forward data, while coping with location error, without using the Rician assumption. The contribution of these algorithmic solutions is necessary, especially for those cases where the location variance differences are greater, but also for the correct functionality of geographic routing.

7 Conclusions and future work

7.1 Conclusions

The need to design efficient, scalable protocols makes position-based routing and especially geographic routing attractive solutions for efficient packet forwarding. The latter facilitates stateless, energy efficient data forwarding which both ad-hoc and the more demanding WSNs can make use of. The number of applications that can benefit from geographic routing is impressive and, as a consequence, numerous position based protocols have been developed to better accomplish the packet forwarding process according to the application demands [4]. Some protocols propose different solutions and trade-offs and their design successfully answers only some of the requirements of volatile, demanding WSNs. Thus they are suitable for certain applications only, where chosen characteristics are valued above others. Current work has made possible a list of application suggestions for geographic routing, according to the relevant features of each application category [4].

While some geographic routing protocols have been implemented already, a great number of position-based routing methods have been disregarded for practical use due to certain disadvantages. Although some routing solutions guarantee delivery, have excellent throughput, are adaptive to mobility or seem satisfactory in terms of memory usage, improvement is still needed where unrealistic design assumptions

are made. Some of the issues which affect the realistic performance of geographic routing have been analysed in this thesis and solutions were proposed to deal with the stated problems.

By investigating network design issues and by surveying the existent literature, a better understanding of the packet forwarding possibilities provided by previous research has been achieved. The study of WSN application principles and requirements has paved the way for the in-depth study and realistic simulation of geographic routing algorithms for practical and highly demanding scenarios. Therefore, when considering the simulation tools for the presented analysis, the particular characteristics of the application area need to be looked at. Once the size of the desired network and the environment where it should be set up is established, the focus can move to the most stringent demands of the application and on the desired QoS. Regarding the forwarding method, there are some generic characteristics a position-based routing algorithm must have to be WSN suitable, and some particular ones, more application-dependent. Taking as an example dynamic networks, one can consider either static or mobile nodes. In the static case, the routing protocol will not suffer from delays or latency, since there are no updates to be made, and the resources should therefore be focused in the direction of efficient packet delivery or real time communication. Because mobility results in extra energy consumption spent on updates and processing of location information, a reliable mobile protocol should focus more on energy consumption issues, without ignoring communication speed or delivery efficiency. However, in most cases there is a trade-off between these factors. Designing a position-based routing protocol ultimately results in making a compromise between certain stringent features and others with lower priority. Without an efficient protocol for the specific application, the communication goal of the network may not be fully accomplished. The short lifetime of sensor nodes and the failure to

deliver the minimum targeted amount of transmitted packets in a desired amount of time can be translated into a design failure and a waste of resources.

The initial assumptions in the design of a position-based protocol must be carefully considered. Assumptions made about network placement and node density, which is sometimes considered high enough to prevent the existence of communication voids, can lead to a faulty routing behaviour in a sparse network. Also, increasing the density above a certain threshold may not be beneficial to the localisation process as shown in [130]. When designing a network routing protocol, assumptions about precise localisation or the employment of expensive GPS devices in all nodes can lead to either packet failure or increased routing costs. Also, lack of connectivity or insufficient consideration of weak links can severely affect real-time network communication through congestion, end-to-end delay and packet loss. Energy efficiency is directly related to all this aspects.

To demonstrate the importance of the initial assumptions for realistic network design, a first step was to simulate network behaviour in MATLAB and to analyse the geographic routing performance (in terms of energy consumption and PDR) for different node distributions: Grid, Gaussian, Uniform Random, Pareto, Stensor, StensorX. Looking at a fire prevention application over a large forest area (because most WSNs are large scale), it was concluded that the best results are obtained when nodes have a Gaussian distribution (this refers to throughput, hop count, energy consumption and MAC delay). However, when the destination was not centrally placed, other node distributions had a better performance (Uniform Random, Stensor, StensorX), while some were found to be completely inefficient (Pareto), unless superimposed for a better area coverage. While for a fire prevention application high throughput values are critical, for other application scenarios the PDR can be of secondary importance, in the detriment of communication speed or network

lifetime. Each application quantifies the QoS in different terms. The interest of the current research was mainly for throughput and energy efficiency, considered here as primary WSN concerns.

A second step for the analysis of the impact of unrealistic assumptions on geographic routing referred to localisation issues. As previously mentioned, network performance analysis is related to location accuracy. Basic geographic routing behaviour is considerably influenced by the positioning information nodes have and the magnitude of the location errors. Therefore, two cases were analysed: one in which the localisation process is not simulated and the location error is given by a statistical error model (Gaussian), and one in which the positioning is performed using specific localisation techniques (received signal strength (RSS) and time of arrival (ToA)).

When the localisation process was not simulated, the degree to which the network throughput was affected by location error indicated that, regardless of the node density, a standard deviation of 10% of R or more reduces the PDR to less than 50%. The research here was based on considerations of a random, uniform node placement as a worst-case scenario of stochastic node distribution. While for the networks with accurate location information, packet failure took place due to the network topology, sparsity or traffic congestion, for the case of inaccurate localisation the main cause was location error. It influenced the percentage of failures and the energy consumption values. Inaccurate coordinates led to more energy being spent on both received and lost packets alike. The paths of the successful packets were therefore longer, while the number of lost packets was higher. Node density also influenced the results; sparse networks led to a quick packet loss due mostly to localisation or lack of forwarding options, while dense networks provided more routing options, longer paths and failed mostly when there were no forwarding options with progress

to destination.

When the localisation process was simulated, the analysis reflected different results for the two employed ranging methods, even if the assumed network traffic was not high or the node density was acceptable. The magnitude of the estimated errors differed for ToA and RSS and consequently so did the network response. Because the study was interested in large scale networks, the comparison between the two methods was biased against RSS ranging. (ToA ranging is favoured by large networks, unlike RSS ranging.) The PDR for RSS was less than 20%, even when density was optimal. The number of anchors used in the study also led to subjective results and more anchors could have improved the network performance when RSS localisation was employed. Sparse networks had a low PDR for both positioning techniques, reaching a loss rate of 80-90%. Dense networks had an improved throughput for ToA, but also consumed more energy. The energy efficiency evaluation was made for both the positioning stage as well as the routing and networks based on ToA ranging consumed almost three times more on localisation than on routing. The denser the networks, the more energy was spent.

The investigations confirmed the need for geographic routing algorithms to be designed in a location-error resilient way, without compromising on energy efficiency. Consequently, a novel routing algorithm has been proposed to solution this acute problem. The conditioned mean square error ratio algorithm (CMSER), is intended as a simple greedy routing approach, one that considers location errors and chooses forwarding nodes based on distance estimations and knowledge of standard deviation of location error. Its performance was tested in comparison with that of other routing algorithms, which have been modified for an evaluation under the same initial assumptions. The throughput of CMSER has been analysed for networks with different network sizes, error characteristics and communication ranges. All re-

sults confirmed that CMSEER outperforms other basic forwarding techniques (MFR, MSER, COND and MED) in terms of PDR, while energy expenses are kept down to a minimum. The trade-off for the obtained PDR values consists in slightly longer paths for the received packets, but this does not affect the efficiency of the algorithm. Overall energy consumption figures were kept down to a minimum through few packet losses occurring close to the sources.

As CMSEER is based on a distance metric and LED, another resilient to location error algorithm proposed in the literature, uses a hybrid distance-energy metric, these two algorithms could not be initially compared on similar grounds. This is why CMSEER was compared with MED, an adaptation of LED, which is based only on distance instead. However, because LED is a power-efficient algorithm, the CMSEER algorithm was later improved so that it too could make use of the same hybrid metric as LED. This novel geographic routing solution, the M-CMSEER, showed the same performance improvements over LED, as CMSEER had over MED. M-CMSEER outperformed all other algorithms if an optimal node density was ensured and was particularly efficient for a small R and LED fell behind.

The novel forwarding method was analysed further using a different, more realistic scenario: a network in which nodes benefit from packet reception acknowledgement messages. With this new simulation feature, the performance of CMSEER, M-CMSEER and LED was analysed again and the results reconfirmed previous findings: M-CMSEER provides the highest throughput and, although it chooses longer packet routes, its overall energy consumption is the smallest due to the reduced number of retransmissions necessary to reach the same 100% PDR as the rest of the algorithms. It is followed by LED and CMSEER.

LED, CMSEER and M-CMSEER are based on the same statistical assumption: that the distances between nodes are random variables which follow the Rice distribution.

This assumption is founded on an oversimplification which states that the location errors of the x and y coordinates of each node are equal. Because in reality this is not always true, tests were necessary to identify how the algorithms cope with a different location error for the x and y coordinates and what is the impact of the Rician assumption on the routing performance. The considered network scenarios were small scale, to allow faster simulation. This allowed the realistic localisation simulation to successfully make use of RSS ranging. Test results showed a difference between the real location error in the x and y coordinates and the error assumed by the positioning process. In terms of network performance, while the proposed geographic routing algorithms could still function well, even with the simplifications assumed by the Rician hypothesis, the performance was found inaccurate. The forwarding solutions proposed in this thesis were therefore modified to be aware of the difference in the error of the x and y coordinates and to route packets in a more correct, but still efficient manner.

Statement

Noticeably, some of the graphs in this thesis contain irregular curves. It is a situation which has been observed as more obvious for specific analysed parameters (such as those related to congestion and low-connectivity packet failures) and as less obvious for others, where only mild fluctuations can be seen for specific node densities. A likely-cause of this irregular behaviour is in the author's opinion related to the targeted level of realism of the simulator and to the MATLAB programming limitations.

The MATLAB simulator used in the current research has been developed to allow a very large number of parameters to be random variables, as they would be in

reality (both the x and y coordinates of nodes, the location error variance for each node, the location error itself, the position of the traffic-generating sources, the busy/idle channel, the channel shadowing) making the simulation complex and the results difficult to analyse. The degree of complexity also comes from the fact that the simulations employ a large number of nodes, multiple sources, multiple packet transmissions per source, multiple node distributions, multiple routing algorithms and multiple localisation methods. All results are processed and collected during the same simulation, in which multiple trials take place. This is done by using concentric loops, switching cases and testing all the algorithms in multiple trials.

For example, to evaluate the behaviour of 2 routing algorithms (A1 and A2) with 2 node distributions (Distrib1 and Distrib2) for 2 network sizes of N1 and N2 nodes, averaging the results for 10 trials, the following take place:

-Distrib1 is set with N1 nodes. A1 and then A2 are run 10 times (each trial has a different seed so results are different). Averages are calculated.

-Distrib1 is set with N2 nodes. A1 and then A2 are run 10 times (each trial has a different seed so results are different). Averages are calculated.

-Distrib2 is set with N1 nodes. A1 and then A2 are run 10 times (each trial has a different seed so results are different). Averages are calculated.

-Distrib2 is set with N2 nodes. A1 and then A2 are run 10 times (each trial has a different seed so results are different). Averages are calculated.

If more distributions, nodes, algorithms or trials are used, the simulation becomes more complex and takes longer. (Omitted: localisation methods or number of traffic connections simulated in each algorithm, which can also increase complexity and slow the process down further).

In addition to this, the MATLAB library functions which allow the user to model the

random variables are actually pseudo-random and require a lot of attention when used in concentric loops. Random numbers are generated in streams in MATLAB, each stream starting from a particular seed. If the seed is not the same for all compared algorithms, then the comparison is not made on similar terms. It is this particular aspect that has been given a lot of care to, especially when using loops and resetting other parameters as well. The seed is reset in such a way that algorithms are compared on similar terms, but each trial has a different stream of random numbers. Also, although increasing the number of trials normally leads to smoother curves because of better estimated average values; it is not a single random parameter which is evaluated during these trials. The presented graphs were intended to be as smooth as possible and this is why a higher number of trials was used, higher than by other sources in the literature (who have used values of 20 [3,95], 50 [5,8]. Most references used 100 trials [7,53,83,112]. It is believed that the combination of the random parameters in the simulations is the one leading to the results in discussion.

In support of the statement that it is the combination of many random factors influencing the average final results which causes the irregular behaviour, comes the fact that the mild irregular behaviour remains constant throughout the thesis. Although the simulations are changed to accommodate the desired parameter evaluation, the structure of the simulator and the methods of encoding the simulated network operations are kept the same.

The correct behaviour of the simulator has been analysed at each stage of the work. Also, it has been tested that if the input of the simulations is not random in nature, then the results have smooth curves. In the development stage of the functions, tests were made on simple scenarios, using a grid and as few random variables as possible (no location error, no MAC assumptions) and the results visualised graphically and

analysed for correct behaviour (in terms of chosen routing paths and number of hops for various network sizes). The final versions of the employed functions performed optimally and as expected.

However, because this is only an estimate of a likely cause for the irregularities and they may be produced by other factors, these aspects would have been investigated further if time had allowed.

7.2 Future work

Geographic routing investigations revealed that this type of forwarding requires further research and improvement, mainly because of its indisputable and promising benefits. Although the solutions proposed in this thesis addressed a part of the issues ignored until now, this forwarding technique can be made more practical. The present work explored problems related to unrealistic localisation assumptions, which can influence the design and behaviour of the routing protocols in real-life applications. However, the novel algorithms focused only to the basic greedy forwarding component and can be developed further into protocols, which being more complex tackle typical problems for geographic routing, such as network voids and backwards progress. Geographic routing recovery methods also need to be resilient to localisation. Furthermore, localisation investigations can be extended to cover other assumptions which have not been entirely addressed.

A part of the research here was limited to the use of nine anchor nodes. Localisation accuracy depends on the number and placement of the anchor nodes which perform ranging and this also influences the behaviour of the routing component. It is thus necessary to analyse the relationship between these aspects and to perform simulations with a higher number of anchors involved in the positioning process, while

changing their placement as well. This, in collaboration with the node distribution can modify the routing results altogether. Furthermore, while the current studies are made for ToA and RSS ranging, there are other localisation techniques which may impact geographic routing in a different way. ToA is more recommended for larger, outdoor networks and RSS for small, indoor ones, but a hybrid process may be more useful for distributed WSNs and localised routing [131, 132]. Cooperative localisation is also of interest for WSNs and should be considered for the study of geographic routing performance. It implies only few nodes know their location with accuracy, but others can act as pseudo-anchors [133, 134]. Localising in a cooperative way will affect energy consumption and network lifetime in an undetermined way.

Further work can also be done to explore more congested networks and other more practical issues, such as clock synchronization for localisation, the introduction of the ARQ protocol, the possibility to have more than one routing destination as well as node mobility considerations. All these aspects have not been properly addressed and they can impact the energy consumption severely. Dynamic networks need to be investigated as a separate category and appropriate geographic routing solutions need to be found for highly dynamic cases. The algorithms developed in this thesis address static networks and while they can be adapted for mobility, they may not perform similarly. Their energy consumption can be negatively affected by mobility, but it can also be improved by considering nodes with energy harvesting capabilities. Power replenishment can increase the battery capacity of either dynamic or key-positioned nodes which can then cope with excess energy consumption. In such a case, relay nodes or anchor nodes without unlimited power supply may be able to continue functioning for longer periods of time, avoiding network sparsity. Also, while assuming that the higher the energy consumption, the shorter the network

lifetime, more simulations are necessary to reveal the relationship between the two. While studying node distribution, localisation and routing for WSNs, the present work entirely focused on conventional 2D scenarios. Because the aim is to design practical geographic routing algorithms, the algorithms need to be evaluated in 3D scenarios. Although their behaviour is assumed similar in 3D, it may bring forward sophisticated issues which have not been foreseen. As underlined in [135], open research in 3D scenarios is motivated by the interest in WSN applications for space exploration, underwater surveillance, air and oceanic studies. Unconventional spaces require innovative solutions to answer more stringent needs for coverage and connectivity. Sometimes networks cannot benefit from high node density or devices with more resources, so intelligent routing protocols are needed to effectively cope with such issues, with obstacles and communication interferences. Several 3D geographic routing techniques have already been proposed in recent years [6, 136–138], some even considering multidimensional spaces. However, these propositions are not focused on localisation inaccuracies having different approaches from those proposed in this thesis. Therefore, future work is needed in the extension of CMSER, M-CMSER and NR-CMSER for efficient routing in 3D. It is also vital that their performance be explored considering 3D node placement and 3D localisation.

Bibliography

- [1] Y. Kim, J.-J. Lee, and A. Helmy, “Modeling and analyzing the impact of location inconsistencies on geographic routing in wireless networks,” *SIGMOBILE Mob. Comput. Commun. Rev.*, vol. 8, no. 1, pp. 48–60, January 2004. [Online]. Available: <http://doi.acm.org/10.1145/980159.980168>
- [2] E. Kolega, V. Vescoukis, and D. Voutos, “Assessment of network simulators for real world wsns in forest environments,” in *IEEE International Conference on Networking, Sensing and Control (ICNSC)*, 2011, pp. 427–432.
- [3] S. Kwon and N. B. Shroff, “Geographic routing in the presence of location errors,” *Computer Networks*, vol. 50, no. 15, pp. 2902–2917, October 2006. [Online]. Available: <http://dx.doi.org/10.1016/j.comnet.2005.11.008>
- [4] A. M. Popescu, I. G. Tudorache, and A. H. Kemp, “Surveying position based routing protocols for wireless sensor and ad-hoc networks,” *International Journal of Communication Networks and Information Security (IJCNIS)*, vol. 4, no. 1, pp. 41–66, April 2012, iISSN: 2076-0930 (Print); ISSN: 2073-607X (Online). [Online]. Available: <http://ijcnis.org/index.php/ijcnis/issue/view/10>
- [5] Y.-J. Kim, R. Govindan, B. Karp, and S. Shenker, “Geographic routing made practical,” in *Proceedings of the 2nd conference on Symposium on Networked*

- Systems Design & Implementation - Volume 2*, ser. NSDI'05. Berkeley, CA, USA: USENIX Association, 2005, pp. 217–230. [Online]. Available: <http://dl.acm.org/citation.cfm?id=1251203.1251219>
- [6] J. Zhou, Y. Chen, B. Leong, and P. S. Sundaramoorthy, “Practical 3d geographic routing for wireless sensor networks,” in *Proceedings of the 8th ACM Conference on Embedded Networked Sensor Systems*, ser. SenSys '10. New York, NY, USA: ACM, 2010, pp. 337–350. [Online]. Available: <http://doi.acm.org/10.1145/1869983.1870016>
- [7] B. Peng and A. H. Kemp, “Energy-efficient geographic routing in the presence of localization errors,” *Computer Networks (Elsevier)*, vol. 55, no. 3, pp. 856 – 872, 2011. [Online]. Available: <http://www.sciencedirect.com/science/article/pii/S1389128610003415>
- [8] R. Marin-Perez and P. M. Ruiz, “Effective geographic routing in wireless sensor networks with inaccurate location information,” in *Proceedings of the 10th international conference on Ad-hoc, mobile, and wireless networks*, ser. ADHOC-NOW'11. Berlin, Heidelberg: Springer-Verlag, 2011, pp. 1–14. [Online]. Available: <http://dl.acm.org/citation.cfm?id=2032462.2032464>
- [9] A. M. Popescu, G. I. Tudorache, and A. Kemp, “Performance study of node placement for geographic routing in wsns,” in *Communication Technologies Workshop (Swe-CTW), 2011 IEEE Swedish*, 2011, pp. 13–18.
- [10] A. M. Popescu, N. Salman, and A. H. Kemp, “Energy consumption analysis of geographic routing in wsns with location error,” in *European Wireless, 2012. EW. 18th European Wireless Conference*, 2012, pp. 1–8.
- [11] N. Salman, H. K. Maheshwari, A. H. Kemp, and M. Ghogho, “Effects of anchor placement on mean-crb for localization,” in *The 10th IFIP Annual*

- Mediterranean Ad Hoc Networking Workshop (Med-Hoc-Net)*, June 2011, pp. 115–118.
- [12] N. Salman, M. Ghogho, and A. H. Kemp, “Optimized low complexity sensor node positioning in wireless sensor networks,” *Accepted for publication in IEEE Sensors Journal*, 2013.
- [13] A. M. Popescu, N. Salman, and A. Kemp, “Energy consumption of geographic routing with realistic localisation,” *Networks, IET*, vol. 1, no. 3, pp. 126–135, 2012.
- [14] A. Popescu, N. Salman, and A. Kemp, “Geographic routing resilient to location errors,” *Wireless Communications Letters, IEEE*, vol. 2, no. 2, pp. 203–206, 2013.
- [15] Jennic, “www.jennic.com/support/index.php,” Online, accessed February 2011.
- [16] G. Ács and L. Buttyán, “A taxonomy of routing protocols for wireless sensor networks,” 2007. [Online]. Available: <http://citeseerx.ist.psu.edu/viewdoc/summary?doi=10.1.1.75.525>
- [17] K. Akkaya and M. Younis, “A survey on routing protocols for wireless sensor networks,” *Ad Hoc Networks*, vol. 3, pp. 325–349, May 2005.
- [18] Rajashree.V.Biradar, V. .Patil, S. Sawant, and R. Mudholkar, “Classification and comparison of routing protocols in wireless sensor networks,” *Special Issue on Ubiquitous Computing Security Systems*, vol. 4, July 2009.
- [19] A. Boukerche, M. Z. Ahmad, B. Turgut, and D. Turgut, “Algorithms and protocols for wireless sensor networks,” *Wiley Series on Parallel and Distributed Computing - online publication*, pp. 129–160, 2008.
- [20] S. Giordano, I. Stojmenovic, and L. Blazevic, “Position based routing algo-

- rithms for ad hoc networks: A taxonomy,” in *Ad Hoc Wireless Networking*. Kluwer, 2001, pp. 103–136.
- [21] A. Papadopoulos and J. A. McCann, “Towards the design of an energy-efficient, location-aware routing protocol for mobile, ad-hoc sensor networks,” in *Proceedings of the Database and Expert Systems Applications, 15th International Workshop*, ser. DEXA '04. Washington, DC, USA: IEEE Computer Society, 2004, pp. 705–709. [Online]. Available: <http://dx.doi.org/10.1109/DEXA.2004.168>
- [22] L. K. Qabajeh, L. M. Kiah, and M. M. Qabajeh, “A qualitative comparison of position-based routing protocols for ad-hoc networks,” *IJCSNS International Journal of Computer Science and Network Security*, vol. 9, no. 2, February 2009.
- [23] I. Stojmenovic, “Position-based routing in ad hoc networks,” *Communications Magazine, IEEE*, vol. 40, no. 7, pp. 128–134, July 2002.
- [24] K. Seada and A. A. Helmy, “An overview of geographic protocols in ad hoc and sensor networks,” in *The 3rd ACS/IEEE International Conference on Computer Systems and Applications*, 2005, p. 62.
- [25] M. Mauve, J. Widmer, and H. Hartenstein, “A survey on position-based routing in mobile ad hoc networks,” *Network, IEEE*, vol. 15, no. 6, pp. 30–39, Nov.-Dec. 2001.
- [26] C. J. Lemmon, S. M. Lui, and I. Lee, “Geographic forwarding and routing for ad-hoc wireless network: A survey,” in *Fifth International Joint Conference on INC, IMS and IDC, 2009. NCM '09*, August 2009, pp. 188–195.
- [27] S. Basagni, I. Chlamtac, V. R. Syrotiuk, and B. A. Woodward, “A distance routing effect algorithm for mobility (dream),” in *Proceedings of the*

- 4th annual ACM/IEEE international conference on Mobile computing and networking, MobiCom '98*. New York, NY, USA: ACM, 1998, pp. 76–84. [Online]. Available: <http://doi.acm.org/10.1145/288235.288254>
- [28] G. Mao, B. Fidan, and B. D. Anderson, “Wireless sensor network localization techniques,” *Computer Networks*, vol. 51, no. 10, pp. 2529 – 2553, 2007. [Online]. Available: <http://www.sciencedirect.com/science/article/pii/S1389128606003227>
- [29] B. Peng, R. Mautz, A. H. Kemp, W. Ochieng, and Q. Zeng, “On the effect of localization errors on geographic routing in sensor networks,” in *IEEE International Conference on Communications, 2008. ICC '08.*, 2008, pp. 3136–3140.
- [30] K. Seada, A. Helmy, and R. Govindan, “On the effect of localization errors on geographic face routing in sensor networks,” in *Proceedings of the 3rd international symposium on Information processing in sensor networks*, ser. IPSN '04. New York, NY, USA: ACM, 2004, pp. 71–80. [Online]. Available: <http://doi.acm.org/10.1145/984622.984633>
- [31] B. Peng and A. H. Kemp, “Impact of location errors on geographic routing in realistic wsns,” in *2010 International Conference on Indoor Positioning and Indoor Navigation (IPIN)*, September 2010, pp. 1–7.
- [32] S. Slijepcevic, S. Megerian, and M. Potkonjak, “Location errors in wireless embedded sensor networks: Sources, models, and effects on applications,” *ACM SIGMOBILE Mobile Computing and Communications Review*, vol. 6, pp. 67–78, 2002.
- [33] J. P. Macker and M. S. Corson, “Mobile ad hoc networking and the ietf,” pp. 9–14, 1998.
- [34] H. Takagi and L. Kleinrock, “Optimal transmission ranges for randomly dis-

- tributed packet radio terminals,” *IEEE Transactions on Communications*, vol. 32, no. 3, pp. 246–257, 1984.
- [35] E. Kranakis, H. Singh, and J. Urrutia, “Compass routing on geometric networks,” in *In Proceedings 11th Canadian Conference on Computational Geometry*, 1999, pp. 51–54.
- [36] Y.-B. Ko and N. H. Vaidya, “Location-aided routing (lar) in mobile ad hoc networks,” *Wireless Networks (ACM)*, vol. 6, no. 4, pp. 307–321, July 2000. [Online]. Available: <http://dx.doi.org/10.1023/A:1019106118419>
- [37] I. Stojmenovic and X. Lin, “Loop-free hybrid single-path/flooding routing algorithms with guaranteed delivery for wireless networks,” *IEEE Transactions on Parallel and Distributed Systems*, vol. 12, no. 10, pp. 1023–1032, October 2001.
- [38] B. Chen, K. Jamieson, H. Balakrishnan, and R. Morris, “Span: an energy-efficient coordination algorithm for topology maintenance in ad hoc wireless networks,” *ACM Wireless Networks Journal*, vol. 8, no. 5, pp. 481–494, September 2002. [Online]. Available: <http://dx.doi.org/10.1023/A:1016542229220>
- [39] T. He, J. A. Stankovic, C. Lu, and T. Abdelzaher, “Speed: A real-time routing protocol for sensor networks,” 2002.
- [40] H. Fussler, J. Widmer, M. Mauve, and H. Hartenstein, “A novel forwarding paradigm for position-based routing (with implicit addressing),” in *Proceedings. 2003 IEEE 18th Annual Workshop on Computer Communications, CCW 2003*, October 2003, pp. 194–200.
- [41] A. Rao, S. Ratnasamy, C. Papadimitriou, S. Shenker, and I. Stoica, “Geographic routing without location information,” in *Proceedings of the 9th*

- annual international conference on Mobile computing and networking*, ser. MobiCom '03. New York, NY, USA: ACM, 2003, pp. 96–108. [Online]. Available: <http://doi.acm.org/10.1145/938985.938996>
- [42] Y. Cao and S. Xie, “A position based beaconless routing algorithm for mobile ad hoc networks,” in *Proceedings. 2005 International Conference on Communications, Circuits and Systems*, vol. 1, May 2005, pp. 303–307.
- [43] C. Liu and J. Wu, “Swing: Small world iterative navigation greedy routing protocol in manets,” in *Proceedings 49th IEEE Globe Telecommunications (GLOBECOM)*, 2006.
- [44] Y. Yu, R. Govindan, and D. Estrin, “Geographical and energy aware routing: a recursive data dissemination protocol for wireless sensor networks,” Tech. Rep., 2001.
- [45] S. Carter and A. Yasinsac, “Secure position aided ad-hoc routing,” in *Proceedings of the IASTED International Conference on Communications and Computer Networks (CCN02)*, 2002, pp. 329–334.
- [46] J. Boleng and T. Camp, “Adaptive location aided mobile ad hoc network routing,” in *Performance, Computing, and Communications, 2004 IEEE International Conference on*, pp. 423–432.
- [47] S. M. M. Rahman, M. Mambo, A. Inomata, and E. Okamoto, “An anonymous on-demand position-based routing in mobile ad hoc networks,” in *International Symposium on Applications and the Internet*, January 2006, pp. 300–306.
- [48] J. Li, J. Jannotti, D. S. J. D. Couto, D. R. Karger, and R. Morris, “A scalable location service for geographic ad hoc routing,” in *Proceedings of the 6th annual international conference on mobile computing and networking*, 2000, pp. 120–130.

- [49] P. Bose, P. Morin, I. Stojmenović, and J. Urrutia, “Routing with guaranteed delivery in ad hoc wireless networks,” in *Proceedings of the 3rd international workshop on Discrete algorithms and methods for mobile computing and communications, DIALM '99*. New York, NY, USA: ACM, 1999, pp. 48–55. [Online]. Available: <http://doi.acm.org/10.1145/313239.313282>
- [50] L. Blazevic, S. Giordano, and J.-Y. L. Boudec, “Self organized terminode routing,” *Cluster Computing*, vol. 5, pp. 215–218, 2002.
- [51] B. M. Blum, T. He, S. Son, and J. A. Stankovic, “Igf: A state-free robust communication protocol for wireless sensor networks,” Tech. Rep., 2003.
- [52] D. Niculescu and B. Nath, “Trajectory based forwarding and its applications,” in *Proceedings of the 9th annual international conference on Mobile computing and networking, MobiCom '03*. New York, NY, USA: ACM, 2003, pp. 260–272. [Online]. Available: <http://doi.acm.org/10.1145/938985.939012>
- [53] K. Seada, M. Zuniga, A. Helmy, and B. Krishnamachari, “Energy-efficient forwarding strategies for geographic routing in lossy wireless sensor networks,” in *Proceedings of the 2nd international conference on Embedded networked sensor systems (SenSys '04)*. Baltimore, MD, USA: ACM, 2004, pp. 108–121, isbn = 1-58113-879-2.
- [54] K. Zeng, K. Ren, W. Lou, and P. J. Moran, “Energy aware efficient geographic routing in lossy wireless sensor networks with environmental energy supply,” *Wireless Networks*, vol. 15, no. 1, pp. 39–51, January 2009. [Online]. Available: <http://dx.doi.org/10.1007/s11276-007-0022-0>
- [55] B. Karp and H. T. Kung, “Gpsr: greedy perimeter stateless routing for wireless networks,” in *Proceedings of the 6th annual international conference on Mobile*

- computing and networking (MobiCom '00)*, New York, NY, USA, 2000, pp. 243–254, isbn=1-58113-197-6.
- [56] H. Frey and I. Stojmenovic, “On delivery guarantees of face and combined greedy-face routing in ad hoc and sensor networks,” in *Proceedings of the 12th annual international conference on Mobile computing and networking, MobiCom '06*. New York, NY, USA: ACM, 2006, pp. 390–401. [Online]. Available: <http://doi.acm.org/10.1145/1161089.1161133>
- [57] J. A. Sanchez and P. M. Ruiz, “Locally optimal source routing for energy-efficient geographic routing,” *Wireless Networks*, vol. 15, no. 4, pp. 513–523, May 2009. [Online]. Available: <http://dx.doi.org/10.1007/s11276-007-0066-1>
- [58] R. Jain, A. Puri, and R. Sengupta, “Geographical routing using partial information for wireless ad hoc networks,” *Personal Communications, IEEE*, vol. 8, no. 1, pp. 48–57, January 2001.
- [59] M. Heissenbüttel, T. Braun, T. Bernoulli, and M. Wälchli, “Blr: beacon-less routing algorithm for mobile ad hoc networks,” *Elsevier's Computer Communications (ECC)*, vol. 27, no. 11, pp. 1076 – 1086, 2004. [Online]. Available: <http://www.sciencedirect.com/science/article/pii/S0140366404000271>
- [60] H. Luo, F. Ye, J. Cheng, S. Lu, and L. Zhang, “Ttdd: Two-tier data dissemination in large-scale wireless sensor networks,” *Wireless Networks*, vol. 11, pp. 161–175, January 2005.
- [61] R. Baumann, S. Heimlicher, M. Strasser, and A. Weibel, “A survey on routing metrics,” TIK-Report, Tech. Rep., 2007.
- [62] C.-C. Shen, C. Srisathapornphat, and C. Jaikaeo, “Sensor information net-

- working architecture and applications,," *IEEE Personal Communications*, pp. 52–59, 2001.
- [63] C. D. Kidd and R. J. Orr, "The aware home: A living laboratory for ubiquitous computing research," in *Proceedings Of the International Workshop on cooperative Building*, 1999.
- [64] J. A. Gutierrez, M. Naeve, E. Callaway, M. B. V. Mitter, and B. Heile, "Ieee 802.15.4: A developing standard for low-power low-cost wireless personal area networks," *IEEE Network*, pp. 12–19, 2001.
- [65] S. El-Haddad, M. G. Genet, and B. El-Hassan, "Mobile wireless sensor networks using mdsap, model for a hospital application," in *4th International Conference on Wireless Communications, Networking and Mobile Computing, WiCOM '08*, October 2008, pp. 1–6.
- [66] E. Lawrence, K. F. Navarro, D. Hoang, and Y. Y. Lim, "Data collection, correlation and dissemination of medical sensor information in a wsn," in *Fifth International Conference on Networking and Services, 2009. ICNS '09*, April 2009, pp. 402–408.
- [67] A. Mainwaring, J. Polastre, R. Szewczyk, and D. Culler, "Wireless sensor networks for habitat monitoring," Intel Corporation, Intel Research Berkeley, 2002.
- [68] V. Rodoplu and T. H.-Y. Meng, "Minimum energy mobile wireless networks," in *IEEE Journal Selected Areas in Communications*, vol. 17, no. 8, August 1999, pp. 1333–1344.
- [69] L. Li and J. Halpern, "Minimum-energy mobile wireless networks revisited," in *IEEE International Conference on Communications, 2001. ICC 2001*, vol. 1, June 2001, pp. 278–283.

- [70] E. Shi and A. Perrig, "Designing secure sensor networks," *IEEE Wireless Communications*, pp. 38–43, 2004.
- [71] C. Lochert, M. Mauve, H. Fussler, and H. Hartenstein, "Geographic routing in city scenarios," *ACM SIGMOBILE Mobile Computing and Communications Review*, vol. 9, no. 1, pp. 69–72, January 2005. [Online]. Available: <http://doi.acm.org/10.1145/1055959.1055970>
- [72] K. Peters, A. Jabbar, E. K. Cetinkaya, and J. P. G. Sterbenz, "A geographical routing protocol for highly-dynamic aeronautical networks," in *In proceeding of: 2011 IEEE Wireless Communications and Networking Conference, WCNC 2011*, Cancun, Mexico, January 2011.
- [73] M. Ayaida, H. Fouchal, L. Afilal, and Y. Ghamri-Doudane, "A comparison of reactive, grid and hierarchical location-based services for vanets," in *Vehicular Technology Conference (VTC Fall), 2012 IEEE*, 2012, pp. 1–5.
- [74] A. Beach, "Gls (grid location system) - performance observations and summary," technical report, Northwestern University, Northwestern University, June 2005, technical report, Northwestern University.
- [75] E. Amir and H. Balakrishnan, "An evaluation of the metricom ricochet wireless network," CS 294-7 Class Project for the Department of Electrical Engineering and Computer Science, University of California at Berkeley, 1996.
- [76] Nokia, "Nokia rooftop availability expands to meet wireless broadband demand in canada," Nokia Online Press Release, June 2002.
- [77] Simulator, "www.isi.edu/nsnam/ns/," Online.
- [78] OPNET, "<http://www.riverbed.com/products-solutions/products/network-performance-management/network-planning-simulation/network-simulation.html>," Online, accessed in 2010.

- [79] QualNet, “<http://web.scalable-networks.com/content/qualnet/>,” Online, accessed in 2010.
- [80] MATLAB, “<http://www.mathworks.co.uk/products/matlab/>,” Online, accessed in 2010.
- [81] Sourceforge, “<http://wireless-matlab.sourceforge.net/>,” Online, accessed in 2010.
- [82] L. Moraru, P. Leone, S. Nikoletseas, and J. Rolim, “Path quality detection algorithms for near optimal geographic routing in sensor networks with obstacles,” *Wireless Communications and Mobile Computing*, vol. 00, pp. 1–13, 2008.
- [83] M. Z. Zamalloa, K. Seada, B. Krishnamachari, and A. Helmy, “Efficient geographic routing over lossy links in wireless sensor networks,” *ACM Transactions on Sensor Networks*, vol. 4, no. 3, pp. 12:1–12:33, June 2008. [Online]. Available: <http://doi.acm.org/10.1145/1362542.1362543>
- [84] C. Lochert, H. Hartenstein, J. Tian, H. Fussler, D. Hermann, and M. Mauve, “A routing strategy for vehicular ad hoc networks in city environments,” in *Intelligent Vehicles Symposium, 2003. Proceedings. IEEE*, June 2003, pp. 156–161.
- [85] P. Peng, A. H. Kemp, and H. Maheshwari, “Power-saving geographic routing in the presence of location errors,” in *IEEE International Conference on Communications, ICC '09*, June 2009, pp. 1–5.
- [86] IEEEStandards, “<http://standards.ieee.org/getieee802/download/802.15.4-2006.pdf>,” Online, accessed in 2014.
- [87] N. Salman, I. Rasool, and A. H. Kemp, “Overview of the ieee 802.15.4 stan-

- dards family for low rate wireless personal area networks,” in *7th International Symposium on Wireless Communication Systems (ISWCS)*, 2010, pp. 701–705.
- [88] T. S. Rappaport, *Wireless Communications. Principles and Practice*. Prentice Hall PTR, 1996.
- [89] I. Ramachandran and S. Roy, “Clear channel assessment in energyconstrained wideband wireless networks,” *IEEE Wireless Communications*, vol. 14, no. 3, pp. 70–78, 2007.
- [90] B. Peng and A. H. Kemp, “Impact of location errors on geographic routing in realistic wsns,” in *2010 International Conference on Indoor Positioning and Indoor Navigation (IPIN)*, 2010, pp. 1–7.
- [91] D. Cerotti, M. Gribaudo, A. Bobbio, C. T. Calafate, and P. Manzoni, “A markovian agent model for fire propagation in outdoor environments,” in *Proceedings of the 7th European performance engineering conference on Computer performance engineering*, ser. EPEW’10. Berlin, Heidelberg: Springer-Verlag, 2010, pp. 131–146.
- [92] J. Azevedo and F. Santos, “An empirical propagation model for forest environments at tree trunk level,” *IEEE Transactions on Antennas and Propagation*, vol. 59, no. 6, pp. 2357–2367, June 2011.
- [93] C. Lozano and O. Rodríguez, “Design of forest fire early detection system using wireless sensor networks,” in *The World Congress on Electronics and Electrical Engineering (WCEEENG’10)*, Egypt, 2010.
- [94] S. Nix, “<http://forestry.about.com/od/forestfire/a/causes-of-forest-fires.htm>,” Online, accessed in 2011.
- [95] C. Sergiou and V. Vassiliou, “Energy utilization of htap under specific node

- placements in wireless sensor networks,” in *European Wireless Conference*, April 2010, pp. 482–487.
- [96] M. Ishizuka and M. Aida, “Stochastic node placement improving fault tolerance in wireless sensor networks,” *Electronics and Communication in Japan*, vol. 90, pp. 42–53, 2006.
- [97] Y. Liu, H. Ngan, and L. M. Ni, “Power-aware node deployment in wireless sensor networks,” in *International Journal of Distributed Sensor Networks (IJDSN)*, vol. 3, no. 2, 2007, pp. 225–241.
- [98] X. Wu, G. Chen, I. C. Society, and S. K. Das, “Avoiding energy holes in wireless sensor networks with nonuniform node distribution,” *IEEE Transaction on Parallel and Distributed Systems*, vol. 19, no. 5, pp. 710–720, 2008.
- [99] M. Fayed and H. T. Mouftah, “Characterizing the impact of routing holes on geographic routing,” in *In Proceedings of the 2005 Systems Communications (ICW '05)*, Washington, DC, USA, 2005, pp. 401–406.
- [100] D. fang Wang and X. gang Qi, “An estimation approach for uniformity of node-distribution in wireless sensor networks,” in *Proceedings of the 5th International Conference on Wireless communications, networking and mobile computing (WiCOM'09)*. Piscataway, NJ, USA: IEEE Press, 2009, pp. 3552–3555.
- [101] A. Sinha and B. Pal, “Stensor: A novel stochastic algorithm for placement of sensors in a rectangular grid,” Awarded 1st position in paper-presentation competition Eureka in Kshitij, IIT Kharagpur, 2007.
- [102] V. Vassiliou and C. Sergiou, “Performance study of node placement for congestion control in wireless sensor networks,” in *3rd International Conference on New Technologies, Mobility and Security (NTMS)*, 2009, pp. 1–8.

- [103] MATLAB, “<http://www.mathworks.co.uk/help/stats/generalized-pareto-distribution.html>,” Online, accessed in 2010.
- [104] NaturalEngland, “<http://www.naturalengland.org.uk/>,” Online, accessed 2014.
- [105] C. S. Chen, Y. Liyz, and Y.-Q. Songz, “An exploration of geographic routing with k-hop based searching in wireless sensor networks,” 2008, pp. 376–381.
- [106] J. Champ and C. Saad, “An energy-efficient geographic routing with location errors in wireless sensor networks,” in *International Symposium on Parallel Architectures, Algorithms, and Networks, I-SPAN 2008*, May 2008, pp. 105–110.
- [107] B. K. Szymanski and B. Yener, *Advances in pervasive computing and networking*. Springer, 2006.
- [108] G. Chen, J. Branch, and B. Szymanski, “Self-selective routing for wireless ad hoc networks,” in *Wireless And Mobile Computing, Networking And Communications, 2005. (WiMob'2005), IEEE International Conference on*, vol. 3, Aug 2005, pp. 57–64 Vol. 3.
- [109] A. K. Sidhik, W. Feng, and J. M. Elmirghani, “Energy-efficient geographic routing in ad-hoc wireless networks,” in *London Communications Symposium*, 2009.
- [110] R. Shah, A. Wolisz, and J. Rabaey, “On the performance of geographical routing in the presence of localization errors [ad hoc network applications],” in *2005 IEEE International Conference on Communications, 2005. ICC 2005.*, vol. 5. IEEE, 2005, pp. 2979–2985.
- [111] S. Basagni, M. Nati, and C. Petrioli, “Localization error-resilient geographic

- routing for wireless sensor networks,” in *Global Telecommunications Conference, IEEE GLOBECOM 2008*, 2008, pp. 1–6.
- [112] G. Fan, R. Wang, H. Huang, L. Sun, and C. Sha, “Coverage-guaranteed sensor node deployment strategies for wireless sensor networks,” *Sensors (Basel)*, vol. 10(3), pp. 2064–2087, 2010.
- [113] T. He, C. Huang, B. M. Blum, J. A. Stankovic, and T. Abdelzaher, “Range-free localization schemes for large scale sensor networks,” in *Proceedings of the 9th annual international conference on Mobile computing and networking (MobiCom '03)*. San Diego, CA, USA: ACM, 2003, pp. 81–95.
- [114] M. Witt and V. Turau, “The impact of location errors on geographic routing in sensor networks,” in *Proceedings of the International Multi-Conference on Computing in the Global Information Technology ICCGI '06*. Washington, DC, USA: IEEE Computer Society, 2006.
- [115] S. Basagni, M. Nati, and C. Petrioli, “Demonstrating the resilience of geographical routing to localization errors,” in *IEEE International Conference on Mobile Adhoc and Sensor Systems, MASS 2007*, October 2007, pp. 1–4.
- [116] B. Peng and A. H. Kemp, “Impact of location errors on geographic routing in realistic wsns,” in *International Conference on Indoor Positioning and Indoor Navigation (IPIN)*, September 2010, pp. 1–7.
- [117] Y. Kong, Y. Kwon, J. Shin, and G. Park, “Localization and dynamic link detection for geographic routing in non-line-of-sight (nlos) environments,” *EURASIP Journal on Wireless Communications and Networking*, 2011.
- [118] B. Peng, R. Mautz, A. H. Kemp, W. Ochieng, and Q. Zeng, “On the effect of localization errors on geographic routing in sensor networks,” in *IEEE In-*

- ternational Conference on Communications, ICC 2008*, Beijing, China, May 2008.
- [119] N. Patwari., A. Hero, M. Perkins, N. Correal, and R. J. O’Dea, “Relative location estimation in wireless sensor networks,” *IEEE Transactions on Signal Processing*, vol. 51, no. 8, pp. 2137–2148, August 2003.
- [120] J. Sanchez, P. Ruiz, and R. Marin-Perez, “Beacon-less geographic routing made practical: challenges, design guidelines, and protocols,” *IEEE Communications Magazine*, vol. 47, no. 8, pp. 85–91, August 2009.
- [121] K. Islam, “Energy aware techniques for certain problems in wireless sensor networks,” Ph.D. dissertation, School of Computing, Queen’s University, Kingston, Ontario, Canada, 2010.
- [122] Jennic, “www.jennic.com/products/modules/,” Online, accessed February 2011.
- [123] A. Boukerche, *Algorithms and Protocols for Wireless Sensor Networks*. John Wiley & Sons, 2008.
- [124] J. Luo, C. Pan, R. Li, and F. Ge2, “Power control in distributed wireless sensor networks based on noncooperative game theory,” *International Journal of Distributed Sensor Networks*, vol. 2012, p. 10, 2012.
- [125] G. A. F. Seber and C. J. Wild, *Nonlinear Regression*. Wiley-Interscience, 2003.
- [126] J. J. Caffery, “A new approach to the geometry of toa location,” in *Proceedings IEEE Vehicle Technologies Conference (VTC)*, vol. 4, Boston, MA, September 2000, pp. 1943–1949.
- [127] S. M. Kay, *Fundamentals of Statistical Signal Processing: Estimation Theory*. Upper Saddle River, NJ: Prentice Hall, Inc., 1993.

- [128] A. R. Eckler, "A survey of coverage problems associated with point and area targets," *Technometrics*, vol. 11, no. 3, pp. 561–589, Aug. 1969.
- [129] I. Stojmenovic and X. Lin, "Power-aware localized routing in wireless networks," *IEEE Trans. Parallel Distrib. Syst.*, vol. 12, no. 10, pp. 1122–1133, Oct. 2001. [Online]. Available: <http://dx.doi.org/10.1109/71.969123>
- [130] A. Savvides, W. L. Garber, R. L. Moses, and M. B. Srivastava, "An analysis of error inducing parameters in multihop sensor node localization," *IEEE Transactions on Mobile Computing*, vol. 4, no. 6, pp. 567–577, 2005.
- [131] D. Niculescu and B. Nath, "Ad hoc positioning system (aps)," in *Global Telecommunications Conference, 2001. GLOBECOM '01. IEEE*, vol. 5, 2001, pp. 2926–2931 vol.5.
- [132] Y. Hu and Y. Li, "Research on heterogeneous wireless sensor networks localization algorithms," in *Progress in Informatics and Computing (PIC), 2010 IEEE International Conference on*, vol. 2, 2010, pp. 1122–1125.
- [133] X. Sun, T. Chen, W. Li, and M. Zheng, "Performance research of improved mds-map algorithm in wireless sensor networks localization," in *Computer Science and Electronics Engineering (ICCSEE), 2012 International Conference on*, vol. 2, 2012, pp. 587–590.
- [134] F. Engel and M. Hedley, "A comparison of cooperative localisation techniques for wireless mobile sensor networks," in *Communications and Information Technologies, 2007. ISCIT '07. International Symposium on*, 2007, pp. 887–892.
- [135] M. Younis and K. Akkaya, "Strategies and techniques for node placement in wireless sensor networks: A survey," *Elsevier Ad Hoc Networks*, vol. 6, pp. 621–655, 2008.

- [136] R. Flury and R. Wattenhofer, "Randomized 3d geographic routing," in *INFOCOM 2008. The 27th Conference on Computer Communications. IEEE*, 2008.
- [137] S. Lam and C. Qian, "Geographic routing in d -dimensional spaces with guaranteed delivery and low stretch," *Networking, IEEE/ACM Transactions on*, vol. 21, no. 2, pp. 663–677, 2013.
- [138] M. Witt and V. Turau, "Geographic routing in 3d," in *Proceedings of the 6th GI/ITG KuVS Fachgespräch "Drahtlose Sensornetze" (FGSN'07)*, July 2007, pp. 75–78. [Online]. Available: <http://www.ti5.tuhh.de/staff/witt/>